# Papers presented to the

# SEVENTH SYMPOSIUM

# ON ANTARCTIC METEORITES

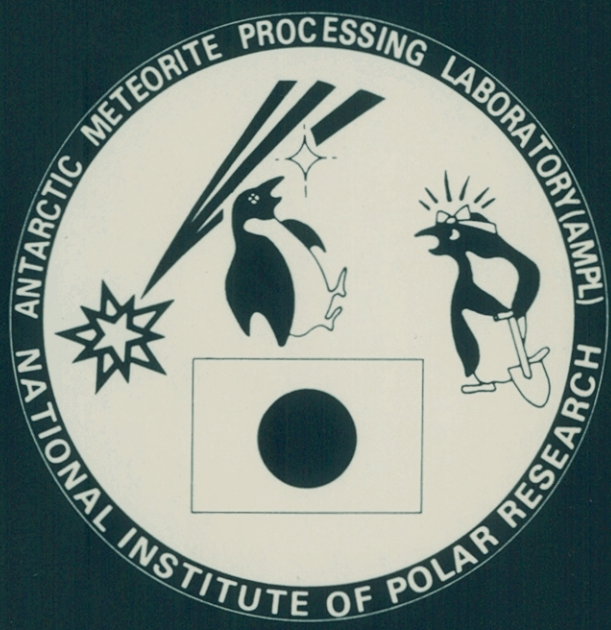


19-20 February 1982

NATIONAL INSTITUTE OF POLAR RESEARCH,
TOKYO

国立極地研究所
南極隕石処理室

# The Seventh Symposium on Antarctic Meteorites

## Programme

19 - 20 February 1982

National Institute of Polar Research, Tokyo

## Friday, February 19, 1982

0900-1200 Registration Auditorium (6th Floor)

* - Speaker

1000 - 1005 Takesi Nagata : Opening address

Chairmen: Ichiro Sunagawa and Ikuo Kushiro

1 1005 - 1020 Yanai K.* Kojima H. Antarctic Meteorites Preliminary Examination Team
Preliminary Examination of the Yamato-79 Meteorites.

2 1020 - 1035 Takeda H.* Antarctic Meteorites Preliminary Examination Team
Consortium Studies of Yamato and Victoria Land Meteorites

3 1035 - 1050 Taylor L.*
NASA-Supported Meteorite Research: Past, Present and Future

4 1050 - 1105 Matsumoto Y.* Miura Y.
Classification of Several Yamato-75 Chondrite (IV)

5 paper only Ohta Y. Griffin W. L.
Preliminary Studies of 3 Yamato Meteorites

6 1105 - 1120 Ohta T.* Duke M. B. Sato G.
Computer Aided Classification of Chondrites Based on EPMA Data and Its Application to Yamato-79 Collection.

7 1120 - 1155 Mason B.* Clarke Jr. R. S.
Characterization of the 1980-81 Victoria Land Meteorite Collections

1155 - 1300 Lunch Time

Chairmen: Nobuo Morimoto and Ken-ichiro Aoki

8 1300 - 1315 Sato G.* Takeda H. Yanai K. Kojima H.
Impact-Melted LL-Chondrites of Yamato 79-Collection

9 1315 - 1330 Ikeda Y.* Onuma N.
Petrochemical Study of the ALH-77003 Chondrite (C30)

10 1330 - 1345 Nagahara H.* Kushiro I.
Petrology of ALH-77307 (C03) Chondrite

11 1345 - 1400 Kimura M.*
Petrology of Lithic Fragments in Unequilibrated Ordinary Chondrites

12 1400 - 1415 Clarke Jr. R. S. Mason B.* Jarosewich E.
A New Metal-Rich Mesosiderite from Antarctica, RKPA79015

13 1415 - 1430 Nagahara H.*
Ni-Fe Metals in the Unequilibrated Chondrites

14 1430 - 1445 Takeda H.* Yanai K.
Mineralogical Examination of the Yamato-79 Achondrites, Preliminary View

15 1445 - 1515 McSween H. Y.*
Igneous Layering and Shock Metamorphism in a New Antarctic Achondrite

1515 - 1530 Tea Time

Chairmen: Hiroshi Takeda and Yukio Ikeda

16 1530 - 1545 Mori H.* Takeda H.
Analytical Electron Microscopic Studies of Pigeonites in Eucrites

17 1545 - 1605 Duke M. B.*
A Major and Trace Element Comparison of Antarctic Polymict Eucrites and Common Eucrites

18 1605 - Miura Y.* Matsumoto Y.
Compositional Variations of Plagioclase, Apatite and Chromite in Yamato-75135,93 Chondrite

19 Miura Y.* Matsumoto Y.
First Description of Whitlockite in Yamato-75 Chondrites

20 - 1645 Miura Y.*
Exsolution Texture of Plagioclase in Meteorite

21 1645 - 1700 Akai J.*
High Resolution Electron Microscopic Investigation on Matrix Phyllosilicate of Yamato-74662 (CM2)

22 1700 - 1720 Fredriksson K.*
Elemental Correlation Anomalies in Individual Chondrules from Chondrites of Different Types

23 1720 - 1735 Morimoto N.* Yasuda M. Kitamura M.
Study of the Radial Pyroxene Chondrule in Yamato-74191 (L3) by Analytical Electron Microscopy

24 1735 - 1800 Fukuoka T.* Ishida H.
Chemical Compositions of the ALH-765 and -77302 Polymict Eucrites

Naoki Onuma
1800-1930 Reception (Lecture Room, 2nd Floor in Research Building)

## Saturday, February 20, 1982

Chairmen: Akira Shimoyama and Nobuo Takaoka

25 1000 - 1015 Haramura H.* Kushiro I.
Major Element Chemistry of Antarctic Meteorites (I)

1015 - 1030 Aoki K* (Commentator)
Bulk Chemical Analysis of the Antarctic Chondrites

26 1030 - 1045 Onuma N.*
SB Systematics on Meteorites

27 1045 - 1100 Nakamura N.* Komi H. Nishikawa Y. Pellas P.
REE Abundances in the Chassigny Meteorite

28 1100 - 1115 Masuda A.* Makoshi Y. Shimizu H. Takahashi K.
A Howardite Model Based on Rare Earth and Major Elements in the Kapotea Meteorite and It's Mineral Separate

29 1115 - 1130 Nishiizumi K. Arnold J. R. Imamura M.* Inoue T. Honda M.
Cosmogenic Radionuclides in Antarctic Meteorites

30 1130 - 1145 Takaoka N.* Saito K.
Isotopic Measurement of Rare Gases in Antarctic Meteorites

31 1145 - 1200 Yagi K.* Kuroda Y. Koshimizu S.
Chemical Composition and F. T. Age of Some Muong Nong-Type Tektites

1200 - 1300 Lunch Time

Chairmen: Akimasa Masuda and Naoki Onuma

32 1300 - 1315 Nishimura H.* Okano J.
SIMS Measurement of Magnesium Isotopic Ratios in Yamato-74662 and 74191 Meteorites

33 1315 - 1330 Komura K.* Tsukamoto M. Sakanoue M.
Cosmogenic Al of Yamato Meteorites

34 1330 - 1345 Miono S.* Yoshida M. Takaoka N. Ninagawa K.
Measurement of Terrestrial Age of Meteorites by Thermoluminescence Technique

35 1345 - 1400 McFadden L. A. Gaffey M. J. Takeda H.*
Reflectance Spectroscopy and Mineralogy of a Crystalline LL Chondrite

36 1400 - Nagata T.*
Magnetic Classification of Meteorites
- Iron Meteorites -

37 Nagata T.*
High Coercive Magnetic Properties of Meteorites Containing Ordered FeNi (Tetrataenite)

38 - 1440 Nagata T.* Funaki M.
Peizo-Remanent Magnetization of Antarctic Meteorites

39 1440 - 1505 Hamano Y.* Yomogida K.
Magnetic Susceptibility Anisotropies of Some Antarctic Chondrites

1505 - 1530 Tea Time

Chairmen: Hiroichi Hasegawa and Jun Okano

40 1530 - 1545 Miyamoto M.* Mito A. Takano Y.
The Spectral Reflectance of Black Meteorites

41 1545 - 1600 Hasegawa H.*
Destruction of Meteorites

42 1600 - 1615 Yomogida K.* Matsui T.
Physical Properties of Antarctic Chondrites, II

43 1615 - 1630 Fujii N.* Miyamoto M. Kobayashi Y. Ito K.
On the Shape of Fe-Ni Grains among Ordinary Chondrites

44 1630 - 1645 Miyamoto M.* Fujii N. Ito K. Kobayashi Y.
The Vibrational Fracturing Rate of Shock-Melted Chondrites

45 1645 - Sugiura N. Strangway D. W.*
Magnetic and Thermal History of the Brecciated Chondrite Abee

46 Sugiura N. Strangway D. W.*
Magnetic Properties of Primitive Non-Carbonaceous Chondrites

47 - 1730 Strangway D. W.* Sugiura N.
Lunar Magnetism

# CLASSIFICATION OF SEVERAL YAMATO-75 CHONDRITES (IV)

Matsumoto, Y. and Miura, Y.

Department of Mineralogical Sciences and Geology, Faculty of Science, Yamaguchi University, Yamaguchi 753, Japan

Among one hundred-fifty meteorites (*i.e.* from Yamato-75108 to -75257 chondrites), six specimens of Yamato-75119,91, -75124,91, -75125,91, -75126, 91, -75128,92 and -75133,93 chondritic meteorites were analyzed by using a JXA-50A electron microprobe analyzer at the Department of Mineralogical Sciences, Yamaguchi University by one of the authors, Miura.

Analytical data of six chondrites (*i.e.* Yamato-75119, -75124, -75125, -75126, -75128 and -75133) which weighed 41.9, 46.9, 62.9, 63.1 and 40.0 g, respectively, are shown in Tables 1 to 4.

Table 1 shows frequency distribution of iron contents of olivines and orthopyroxenes in the analyzed Yamato-75 chondrites. It is found in Table 1 that the five chondrites, Yamato-75119,91, -75124,91, -75125,91, -75126,91 and -75128,92, belong to L-group same as the previous eighteen Yamato-75 chondrites reported by Matsumoto *et al.* (1979), Matsumoto and Hayashi (1980) and Miura and Matsumoto (1981). However, an unclassified Yamato-75133,93 chondrites is determined to be of LL group.

Tables 2 and 3 show mean compositions of the olivines and orthopyroxenes, mean deviations (M.D.) and percent mean deviations (% M.D.) of their iron contents in the analyzed Yamato-75 chondrites. Five chondrites, Yamato-75119, 91, -75124,91, -75125,91, -75128,92 and -75133,93, have 2-3 % M.D. for olivine and orthopyroxene, but Yamato-75126,91 contains less than 2 % M.D. for olivine and more than 4 % M.D. for orthopyroxene.

The chemical compositions of plagioclases in these six chondrites show oligoclase as shown in Table 4.

EPMA analytical data and microscopical observation show that Yamato--75119,91 and -75124,91 chondrites correspond to L4 type; Yamato-75125,91 and -75126,91 chondrites, L4-5 type; Yamato-75128,92 chondrite, L4 type; Yamato--75133,93 chondrite, LL4 type.

Therefore, the Yamato-65133,93 chondrite (LL4) might be different body from another twenty-three Yamato-75 chondrites (L4-5) which are considered to be originally one single body of meteorite broken into many fragments during its passage through the atmosphere.

Table 1. Frequency distribution of iron contents of olivines and orthopyroxenes in six Yamato-75 chondritic meteorites.

| | Olivine | | | | | | | | Orthopyroxene | | | | | | | | |
|---|---|---|---|---|---|---|---|---|---|---|---|---|---|---|---|---|---|
| Atomic % Fe | 21 | 22 | 23 | 24 | 25 | 26 | 27 | 28 | 18 | 19 | 20 | 21 | 22 | 23 | 24 | 25 | 26 |
| Sample No. | Percent of measurements | | | | | | | | Percent of measurements | | | | | | | | |
| Yamato-75119,91 | 6.7 | 13.3 | 60.0 | 20.0 | - | - | - | - | 6.7 | 20.0 | 66.6 | - | - | - | - | - | 6.7 |
| -75124,91 | - | - | 20.0 | 53.3 | 26.7 | - | - | - | - | 20.0 | 66.6 | 6.7 | 6.7 | - | - | - | - |
| -75125,91 | - | 12.5 | - | 56.3 | 25.0 | 6.2 | - | - | 6.7 | 20.0 | 33.3 | 40.0 | - | - | - | - | - |
| -75126,91 | - | - | 12.5 | 75.0 | 6.3 | 6.2 | - | - | - | 20.0 | 33.3 | 26.7 | 13.3 | 6.7 | - | - | - |
| -75128,92 | - | - | - | 6.7 | 46.6 | 26.7 | 20.0 | - | - | - | 6.7 | 6.7 | 66.6 | 20.0 | - | - | - |
| -75133,93 | - | - | - | 6.7 | 6.7 | 66.6 | 13.3 | 6.7 | - | - | - | 20.0 | 20.0 | 40.0 | 13.3 | 6.7 | - |

Table 2. Mean compositions of olivines and percent mean deviations of their iron contents in the analyzed Yamato-75 chondrites.

| Sample No. | Mean composition (%) Ca | Mg | Fe | No. of measure-ments | Mean deviation | Percent mean deviation | Remarks |
|---|---|---|---|---|---|---|---|
| Yamato-75119,91 | 0.01 | 76.61 | 23.38 | 15 | 0.509 | 2.18 | L5 |
| -75124,91 | 0.01 | 75.55 | 24.44 | 15 | 0.622 | 2.55 | L5 |
| -75125,91 | 0.01 | 75.40 | 24.59 | 16 | 0.714 | 2.91 | L4-5 |
| -75126,91 | 0.03 | 75.50 | 24.47 | 16 | 0.437 | 1.79 | L4-5 |
| -75128,92 | 0.02 | 73.91 | 26.07 | 15 | 0.710 | 2.72 | L4 |
| -75133,93 | 0.01 | 73.37 | 26.62 | 15 | 0.654 | 2.46 | LL4 |

Table 3. Mean compositions of orthopyroxenes and percent mean deviations of their iron contents in the analyzed Yamato-75 chondrites.

| Sample No. | Mean composition (%) Ca | Mg | Fe | No. of measure-ments | M.D. | % M.D. | Remarks |
|---|---|---|---|---|---|---|---|
| Yamato-75119,91 | 1.11 | 78.31 | 20.58 | 15 | 0.681 | 3.31 | L5 |
| -75124,91 | 1.10 | 78.20 | 20.70 | 15 | 0.615 | 2.97 | L5 |
| -75125,91 | 1.13 | 78.29 | 20.58 | 15 | 0.703 | 3.42 | L4-5 |
| -75126,91 | 1.15 | 77.94 | 20.91 | 15 | 0.888 | 4.25 | L4-5 |
| -75128,92 | 1.52 | 76.09 | 22.39 | 15 | 0.541 | 2.42 | L4 |
| -75133,93 | 1.40 | 75.36 | 23.24 | 15 | 0.811 | 3.49 | LL4 |

Table 4. Chemical compositions of plagioclases in the analyzed Yamato-75 chondrites.

| Sample No. | Or | Ab | An(mol.%) | Or | Ab | An(mol.%) |
|---|---|---|---|---|---|---|
| Yamato-75119,91 | 7.8 | 81.2 | 11.0 | | | |
| -75124,91 | 0.4 | 89.5 | 10.1 | | | |
| -75125,91 | 3.7 | 72.7 | 23.6 ; | 7.7 | 67.7 | 24.6 |
| -75126,91 | 0.5 | 87.9 | 11.6 | | | |
| -75128,92 | 5.1 | 79.2 | 15.7 ; | 7.5 | 63.4 | 29.1 |
| -75133,93 | 8.5 | 76.8 | 14.7 | | | |

# PRELIMINARY STUDIES OF 3 YAMATO METEORITES

Y. Ohta W.L. Griffin

Norsk Polarinstitutt, Geol. Museum, Univ. of Oslo

Y794039 (wt. 41.52 gm) is a diogenite, consisting of fine-grained opx and scattered chromite grains up to 3mm diameter. It has a glossy surface, but no fusion crust. The opx forms a polygonal mosaic with grain size about 0.3mm. Larger (0.5mm) grains occur next to large idiomorphic chromites and in areas with many small allomorphic chromites and troilite grains. The opx is chemically homogenous (Fe/Fe+Mg=25.6, $\sigma n-1=0.918$). Large idiomorphic chromites have lower Al/Cr (0.20) than small allomorphic grains (0.32) or chromite in irregular seams (0.46), while Fe/Mg varies little (2.3-2.8). Troilite is often intergrown with small chromites and included as irregular grains in the large chronites. Y794039 is petrographically similar to Y6902, Y74013, Y74136 etc., but the variation in chromite composition reported here covers most of the range previously reported from similar stones. No olivine or plagioclase were observed.

B80010629-S (47.55 gm) has a red-brown glassy surface similar to that on many achondrites, but small (<1mm) well defined chondrules make up ½ of the stone. The matrix consists of medium-grained olivine and opx, stained brown along cracks. Many large broken olivine grains in the matrix appears to be derived from crushed chondrules, if so, the rock is >70% chondrule material. Chondrule types include porphyritic (34%), blocky (16%), barred (13%), ophetic (13%), radial (12%) and granular (12%). Despite textural differences and low degree of recrystallization, olivine and opx are chemically homogeneous. Some radial chondrules consist of cpx, locally associated with small oligoclase grains. Taenite and kamacite from discrete grains, and troilite is the most abundant opaque phase. The stone is classified as H4, possibly H5.

B80010629-L (2203.8 gm) has a partial black fusion crust and represents ca. 3/4 of the original stone. Chondrules (<2mm) and oxidized iron and troilite grains are scattered in a pale grey matrix. Chondrule outlines are mostly obliterated, often rimmed by coarse-grained olivine. The matrix consists mostly of coarse-grained olivine, grains are fractured but not strained. Several chondrule types can be recognized, but the blocky, granular and porphyritic types are difficult to distinguish from matrix. Olivine, opx and chromite are homogeneous throughout a thin section. Clear intersitial grains of andesine are found both in matrix and in chondrules; those in matrix have inclusions of apatite. Chromite, taenite and kamacite grains form irregular aggregates in the matrix, and may outline recrystallized chondrules. The stone is classified as L6, possibly L5.

# 5 — 2

Chromites

| | Yamato 794039 (diogenite) | | | | | | B-80010629-L. (L·6 chond.) | | |
|---|---|---|---|---|---|---|---|---|---|
| | Idiomorphic large | | Xenomorph. small | | grains along cracks | | Inside chond. | Matrix | |
| | $\bar{x}$ | $\sigma_{n-1}$ | $\bar{x}$ | $\sigma_{n-1}$ | $\bar{x}$ | $\sigma_{n-1}$ | | $\bar{x}$ | $\sigma_{n-1}$ |
| $SiO_2$ | 0.20 | 0.159 | 0.33 | 0.041 | 0.25 | 0.354 | — | 0.30 | 0.028 |
| $TiO_2$ | 0.86 | 0.058 | 0.71 | 0.068 | 0.76 | 0.076 | 3.27 | 2.96 | 0.219 |
| $Al_3O_3$ | 8.10 | 0.608 | 11.59 | 0.421 | 15.56 | 0.338 | 5.33 | 5.77 | 0.127 |
| $Cr_2O_3$ | 59.25 | 0.902 | 55.02 | 1.113 | 50.58 | 0.622 | 54.91 | 55.76 | 0.106 |
| FeO | 24.61 | 0.493 | 25.85 | 0.827 | 25.05 | 0.612 | 32.02 | 31.53 | 0.078 |
| MnO | 0.46 | 0.352 | 0.72 | 0.133 | 0.31 | 0.353 | 1.13 | 1.07 | 0.198 |
| MgO | 5.95 | 0.253 | 5.48 | 0.653 | 6.13 | 0.141 | 2.15 | 2.48 | 0.156 |
| total | 99.43 | | 99.70 | | 98.64 | | 98.81 | 99.87 | |
| n | 9 | | 4 | | 4 | | 1 | 2 | |

Opx

| Yamato 794039 (diogenite) | | |
|---|---|---|
| $n = 15$ | $\bar{x}$ | $\sigma_{n-1}$ |
| | 53.84 | 0.524 |
| | — | — |
| | 0.64 | 0.358 |
| | 0.89 | 0.134 |
| | 16.13 | 0.509 |
| | 0.53 | 0.107 |
| | 26.34 | 0.606 |
| CaO | 1.30 | 0.198 |
| total | 99.67 | |
| Fe/Fe+Mg | 25.57 | 0.918 |

B-80010629-S; H·5 chondrite

Olivine

| | Matrix | | Granular·Blocky chondrules | | Ophitic·Radial chondrules | | Total average | |
|---|---|---|---|---|---|---|---|---|
| | n = 11 | | n = 5 | | n = 4 | | n = 20 | |
| | $\bar{x}$ | $\sigma_{n-1}$ | $\bar{x}$ | $\sigma_{n-1}$ | $\bar{x}$ | $\sigma_{n-1}$ | $\bar{x}$ | $\sigma_{n-1}$ |
| SiO2 | 39.03 | 0.220 | 39.16 | 0.251 | 38.82 | 0.335 | 39.02 | 0.264 |
| FeO | 18.31 | 0.466 | 18.17 | 0.337 | 18.14 | 0.479 | 18.24 | 0.425 |
| MnO | 0.50 | 0.063 | 0.48 | 0.147 | 0.49 | 0.145 | 0.49 | 0.100 |
| MgO | 42.77 | 0.308 | 42.55 | 0.501 | 42.48 | 0.291 | 42.66 | 0.365 |
| total | 100.61 | | 100.36 | | 99.93 | | 100.41 | |
| Fe/Fe+Mg | 19.36 | 0.433 | 19.33 | 0.440 | 19.43 | 0.597 | 19.36 | 0.442 |

Opx

| | n = 7 | | n = 5 | | n = 4 | | n = 16 | |
|---|---|---|---|---|---|---|---|---|
| SiO2 | 55.87 | 0.566 | 55.92 | 0.476 | 56.43 | 0.672 | 56.03 | 0.569 |
| TiO2 | — | — | 0.09 | 0.115 | 0.13 | 0.151 | 0.07 | 0.112 |
| $Al_2O_3$ | — | — | — | — | 0.24 | 0.277 | 0.06 | 0.163 |
| FeO | 11.50 | 0.527 | 11.52 | 0.398 | 11.37 | 0.436 | 11.48 | 0.424 |
| MnO | 0.52 | 0.054 | 0.42 | 0.219 | 0.55 | 0.037 | 0.48 | 0.153 |
| MgO | 30.97 | 0.480 | 31.09 | 0.316 | 31.11 | 0.147 | 31.06 | 0.331 |
| CaO | 0.60 | 0.034 | 0.65 | 0.102 | 0.64 | 0.079 | 0.63 | 0.080 |
| total | 99.46 | | 99.69 | | 100.47 | | 99.81 | |
| F3/Fe+Mg | 17.24 | 0.769 | 17.18 | 0.541 | 17.01 | 0.492 | 17.16 | 0.575 |

Cpx

| | n = 3 | |
|---|---|---|
| | $\bar{x}$ | $\sigma_{n-1}$ |
| | 54.64 | 0.384 |
| | 0.11 | 0.191 |
| | 0.54 | 0.935 |
| | 5.70 | 0.692 |
| | 0.15 | 0.260 |
| | 20.69 | 1.059 |
| | 15.67 | 1.947 |
| $Cr_2O_3$ | 0.52 | 0.032 |
| $Na_2O$ | 0.65 | 0.221 |
| total | 98.67 | |

B-80010629-L; L·5-6 chondrite

| Olivine | In-side chondrules | | Edge of chondrules | | Matrix, clear grains | | Matrix, turbid grains | | Total average | |
|---|---|---|---|---|---|---|---|---|---|---|
| | n = 7 | | n = 11 | | n = 6 | | n = 3 | | n = 24 | |
| | $\bar{x}$ | $\sigma_{n-1}$ | $\bar{x}$ | $\sigma_{n-1}$ | $\bar{x}$ | $\sigma_{n-1}$ | $\bar{x}$ | $\sigma_{n-1}$ | $\bar{x}$ | $\sigma_{n-1}$ |
| SiO2 | 37.77 | 0.397 | 37.99 | 0.234 | 37.88 | 0.146 | 37.76 | 0.382 | 37.88 | 0.301 |
| FeO | 23.26 | 0.927 | 23.59 | 0.265 | 23.09 | 1.137 | 23.80 | 0.180 | 23.46 | 0.651 |
| MnO | 0.50 | 0.064 | 0.43 | 0.226 | 0.49 | 0.107 | 0.35 | 0.312 | 0.45 | 0.187 |
| MgO | 38.59 | 0.466 | 38.77 | 0.349 | 38.97 | 0.405 | 38.33 | 0.463 | 38.69 | 0.419 |
| total | 100.12 | | 100.78 | | 100.43 | | 100.24 | | 100.48 | |
| Fe/Fe+Mg | 25.26 | 0.554 | 25.45 | 0.353 | 24.95 | 1.053 | 25.84 | 0.148 | 25.38 | 0.539 |
| Opx. | n = 3 | | n = 3 | | n = 6 | | n = 3 | | n = 15 | |
| SiO2 | 54.98 | 0.064 | 54.39 | 0.180 | 54.82 | 0.422 | 54.48 | 0.566 | 54.70 | 0.412 |
| FeO2 | 0.09 | 0.150 | 0.11 | 0.095 | 0.03 | 0.069 | 0.20 | 0.107 | 0.09 | 0.109 |
| Cr2O3 | — | — | 0.05 | 0.087 | 0.03 | 0.082 | — | — | 0.02 | 0.062 |
| FeO | 14.42 | 0.105 | 14.64 | 0.245 | 14.63 | 0.267 | 14.53 | 0.222 | 14.57 | 0.225 |
| MnO | 0.48 | 0.074 | 0.49 | 0.107 | 0.48 | 0.088 | 0.56 | 0.045 | 0.50 | 0.081 |
| MgO | 28.74 | 0.183 | 28.44 | 0.159 | 28.45 | 0.325 | 28.20 | 0.384 | 28.46 | 0.313 |
| CaO | 0.68 | 0.168 | 0.85 | 0.270 | 0.97 | 0.144 | 0.98 | 0.032 | 0.89 | 0.189 |
| total | 99.39 | | 98.97 | | 99.41 | | 99.12 | | 99.23 | |
| Fe/Fe+Mg | 21.90 | 0.089 | 22.41 | 0.215 | 22.39 | 0.194 | 22.43 | 0.227 | 22.31 | 0.270 |

6 — 1

# COMPUTER AIDED CLASSIFICATION OF CHONDRITES BASED ON EPMA DATA AND ITS APPLICATION TO YAMATO-79 COLLECTION

Tsutomu Ohta*, Michael B. Duke** and Gen Sato***
* Mineralogical Inst., Faculty of Science, University of Tokyo
** Planetary and Earth Sciences Division, NASA-Johnson Space Center
*** Dept. of Earth Sciences, Faculty of Science, Chiba University

In order to classify a large number of meteorites with relatively good accuracy, it appears to be necessary to develop a standardized rapid procedure for meteorite classification. It usually takes a considrable time not only to analyze chemical compositions of metorites but also to get pertinent information out of the analyses. This problem could be resolved by establishing a standardized analytical method and by developing a computer program which yields summarized quantitative information of an analysis soon after each analysis of a meteorite.

In the present study, a computation program which systematically processes electron microprobe data has been developed to help classify ordinary chondrites rapidly. The program gives pertinent data of chemical compositions for classification of a chondrite under study. Figure 1 shows the scheme of the program.

Data are read from a file on a tape or other physical devices in the routine DAT. Since computer-controlled electron microanalyzers have been used in this study, the data have already been corrected and reduced to oxide concentration. All the data read in DAT are tabulated in TABLE. This routine will be also used later for printing a table for each mineral species. EDIT routine allow spurious analysis points to be discarded or mineral names to be reassigned to analysis points. This routine is not often used because the routine GRP essentially has the functions of assigning mineral names and discarding questionable points automatically. In GRP, grains at analysis points are identified and given mineral names of olivine, pyroxene or feldspar based on oxide wt% and cation ratios. Any point which is not considered to be one of the three minerals is classified as an unknown. Data are also screened for spurious measurements.

At the next step, CALC is called. Mean molecular percent, percent mean deviation (%MD) and range of chemical compositions for each mineral species are calculated. The computed results are printed out in OUT. Histograms of iron concentrations of olivine and pyroxene are made in FIG. After the hardcopies of summary of calculated results, tables and figures are made, those results may be examined. If any spurious data, in some reasons, are considered to have been included for the calculation, those data can be rejected by calling the routine EDIT, and then the edited data set will be called in the successive routines CALC, OUT, TABLE and FIG.

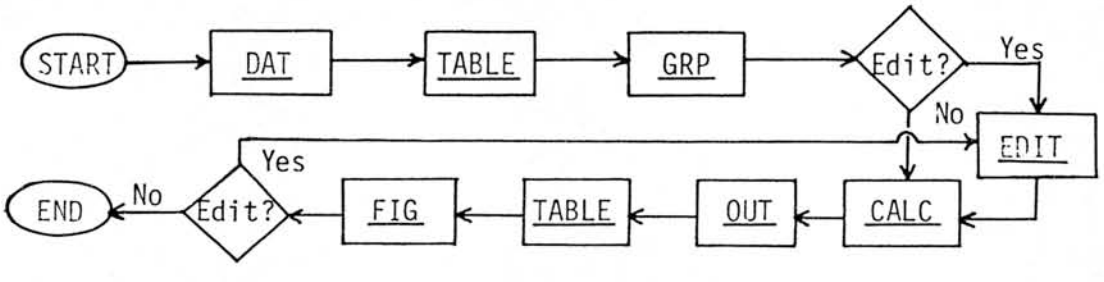


Figure 1. Program scheme to process EPMA data for the classification of chondritic meteorites.

Yanai et al. (1978) determined petrologic types of chondrites based on the position of prominent peak and the range of compositional variation of olivine and pyroxene on histograms. This method can be easily applied to chondrite classification with a great help of the histograms produced by our program. On the other hand, percent mean deviation of olivine or pyroxene composition is one of the criteria to determine petrologic types of chondritic meteorites (Van Schmus and Wood, 1967). However the criterion has not been really quantitative. Once the quantitative criteria for each meteorite type vs. compositional variation have been established, the criteria my be feeded back into the computation program, so that a chondrite is automatically classified based on its chemistry.

The combination of the computation program with the program which controls a computer-automated electron microprobe would make it possible to give preliminary results of classification anytime during microprobe analyses. If no compositional variation is observed on olivine and pyroxene for a possibly equilibrated chondrite on a halfway of a measurement, then one can stop the measurement. If there is an implication of a wide range of compositional variation, considerable number of grains of olivine and pyroxene should be analyzed.

The present study has been aimed to develop an efficient way to classify chondrites primarily based on their chemistry. However we do not intend to ignore textural and mineralogical observations under an optical microscope. Since the current classification of chondrites (Van Schmus and Wood, 1967) is chemical and petrographic, microscopic observations are obviously necessary. In addition there may be the case where chemical information alone is not conclusive for determining a meteorite type.

Electron microprobe data of twelve equilibrated chondrites from Yamato-79 Collection have been processed with the aid of the computation program. About 20% of total nalysis points were assigned to be spurious measurements or unknown minerals. This ratio should be decreased so that sound statistical results of chemical compositions of olivine and pyroxene for a chondrite under study are obtained on the basis of less number of measurements.

The twelve equilibrated chondrites resulted in six H chondrites, five L, and one LL. The mean composition of olivine for each chemical-group of chondrites ranges from 17.6 to 18.5 Fa mole % for H, 23.8 to 24.7 for L, and 30.1 for LL. The mean composition of pyroxene ranges from 15.5 to 16.1 Fs mole % for H, 19.9 to 20.5 for L, and 24.2 for LL. These mean compositions of olivine and pyroxene are comparable with those for common H, L and LL group chondrites from Antarctica.

The computation program developed here is planed to be used for the classification of chondrites in the Japanese Collection of Antarctic Meteorites, with the cooperation of Dr. K. Yanai, National Institute of Polar Research, whom we thank for his interest in this study.

References

Van Schmus, W. R. and Wood, J. A. (1967) A chemical-petrologic classification for the chondritic meteorites. Geochim. Cosmochim. Acta, 31, 747-765.

Yanai, K, Miyamoto, M, and Takeda, H. (1978) A classification for the Yamato-74 chondrites based on the chemical compositions of their olivines and pyroxenes. Mem. Natl. Inst. Polar Res., Spec. Issue, 8, 110-120.

7

CHARACTERIZATION OF THE 1980-81 VICTORIA LAND METEORITE COLLECTIONS

Mason, Brian and Clarke, Roy S., Jr.
Smithsonian Institution, Washington, DC 20560

In the 1980-81 field season a U.S. party collected 32 meteorite specimens in the Allan Hills (ALH) area, 67 near Reckling Peak (RKP), and 1 from the Outpost (OTT) area. These specimens have been classified as follows: irons, 2; ureilite, 1; eucrites, 2; mesosiderites, 4; chondrites, 91. The chondrites belong to the following classes and types: C3, 2; H3, 2; H4, 7; H5, 25; H6, 18; L3, 2; L4, 2; L5, 3; L6, 22; LL5, 2; LL6, 4; E5, 1. The mesosiderites are paired with RKPA79015 (originally classified as an iron with silicate inclusions); 15 L6 chondrites from the Allan Hills appear to be pieces of a single meteorite; several of the L6 chondrites from Reckling Peak are paired with RKPA78001; 13 H6 chondrites from Reckling Peak appear to be pieces of a single meteorite. Additional pairings are possible on further examination.

# IMPACT-MELTED LL-CHONDRITES OF YAMATO 79-COLLECTION

Gen Sato*, Hiroshi Takeda**, Keizo Yanai***, Hideyasu Kojima****

* Dept. of Earth Sciences, Faculty of Science, Chiba University
** Mineralogical Institute, Faculty of Science, University of Tokyo
*** National Institute of Polar Research
**** Institute of Mining Geology, Mining College, Akita University

In the course of preliminary examination of YAMATO-79 collection, we found dark colored stones, having fine-grained glassy texture and full of vesicles. They are visibly distinct from other ordinary chondrites. The bulk chemical composition of both Y-790519 and Y-790964 of this type (analysis by H. Haramura) indicates that they are LL-group chondrites. The microscopic examination of polished thin sections and the electron microprobe analyses of selected specimens revealed that these chondrites are similar to some lithic fragments known in LL-group chondrites described by Fodor and Keil (1978). The electron microprobe analyses were performed in Y-790143, Y-790345, Y-790519, Y-790536, Y-790964. Fayalite contents of olivines in these specimens fall within the range observed in LL-group chondrites (Keil and Fredriksson, 1964) exept a compact and fine-grained portion of Y-790519, with fayalite content classified as L-group chondrite.

The presence of vesicles is the characteristic feature of these chondrites. The amount of vesicles observed in thin sections increases in following order: Y-790345 / Y-790519, Y-790536 / Y-790964 / Y-790143. Y-790143 is full of irregular vesicles, occupying about 20% area in the polished thin section and usually surrounded by brown glass. In other chondrites of this type, the glass is also observed near vesicles in many cases. In a matrix, the brown glass and fine-grained glassy materials fill interstices of lath of euhedral pyroxene crystals and fragments of minerals, including coarse remnant olivines. Most of larger olivine and pyroxene grains show undulating extinction. Numerous closely spaced fractures in some mineral grains are also apparent. Margines of these minerals are fractured into fragments and integrated with glass. Euhedral pyroxene crystals are embedded in extreamely comminuted and vitreous matrix.

In Y-790964, lath of euhedral pyroxenes show chemical zoning with Ca-enrichment at the rim ( $EN_{67}FS_{25}WO_{08}$ at the core, $EN_{50}FS_{18}WO_{32}$ at the rim ). Slight enrichment of Al-content toward the rim is also observed ( 0.7 wt. % at the core, 1.8 wt. % at the rim ). Small euhedral olivine crystals with sub-micron in size are scattered in the glass.
In Y-790143, the same chemical zorning of euhedral pyroxenes is recognized but not so obvious as Y-790964. Euhedral pyroxene and olivine crystals may have been formed by rapid crystallization from an impact melt.

Y-790519 has unusual features. It can be distinguished into two parts with the naked eye. The larger one is similar to LL-chondrites mentioned above. The bulk chemical composition and the fayalite component of olivine indicate that this specimen is LL-chondrite. Coarse remnant olivines are set in comminuted and vitreous matrix. Euhedral pyroxenes are scattered in the brown glass. Irregular vesicles are also present in the matrix. Chondritic textures are still preserved. The smaller part has different features from the other chondrites studied here, concerning the texture

and the fayalite content. The bulk chemical composition shows this portion is LL-chondrite but it can also be classified as L-chondrite on the base of the fayalite content. This portion is very dense and composed of fine grained fragments of olivine. Althogh Y-790519 has the unusual portion, the mechanism producing the vesicular glassy texture may be the same with the other chondrites studied here.

These chondrites are genetically related each other and even transitional. A shock heating may have yielded glasses and vesicles, from which euhedral pyroxene and olivine crystals have grown throuh rapid crystallization producing the chemical zoning. From the petrographic features, shock-melted recrystallization may be advanced in following order: Y-790345 / Y-790519, Y-790536 / Y-790964 / Y-790143. Characteristic textures of this type are often seen within one chondrite such as Y-790964. (Fig. 1) These chondrites are large samples of lithic fragments common in the brecciated LL-chondrites, and are interpreted as surface regolith materials of the LL-parent body.

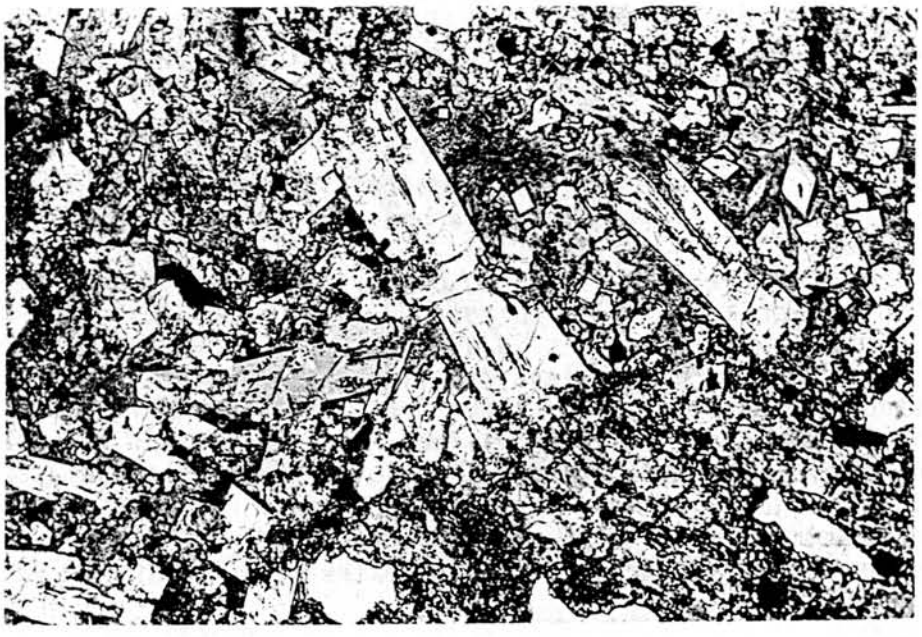

Fig. 1 Photomicrograph of Y-790964. Euhedral pyroxene crystals are embedded in an extremely comminuted mineral fragments and the brown-colored glass. These pyroxenes show Ca-enrichment at the rim. Width: 0.8mm

Reference:
Fodor, R. V. and K. Keil, (1978) Catalog of lithic fragments in LL-group chondrites: Univ. New Mexico Inst. of Meteoritics Sp. Pub. 19, 38pp
Keil, K. and K. Fredriksson, (1964) The iron, magnesium and calsium distribution in coexisting olivines and rhombic pyroxenes of chondrites. Jour. Geophys. Res. 69, 3487-3515

PETROCHEMICAL STUDY OF THE ALH-77003 CHONDRITE (C3O)

Ikeda, Y. and Onuma, N.
Earth Sciences, Ibaraki University, Mito 310.

The ALH-77003 chondrite (C3O) consists of a massive aggregate mainly of fine-grained CAI inclusions, amoeboidal olivine inclusions, botrioidal inclusions and chondrules with brown matrix filling interstitial spaces between them. Following discussion mainly depends upon the petrochemical study of the ALH-77003 chondrite.

Fine-grained CAI occurs as irregular-shaped black to gray aggregates of fine-grained materials and often has thin rims of micron-size width of olivine or aluminous Ca-rich pyroxene. The CAI inclusions show a wide variation of chemical compositions; $Al_2O_3$ 20-50 wt%, $SiO_2$ 12-48%, CaO 2-16%, MgO 3-13%, FeO 2-16%, and $Na_2O$ 0-11%. Their chemical compositions are represented by various mixtures of the normative spinel and fassaitic pyroxene components with variable amounts of the normative nepheline and anorthite components. Amoeboidal olivine inclusions are irregular-shaped aggregates mainly of fine olivine grains. Their chemical compositions are; $SiO_2$ 33-41%, MgO 19-38%, FeO 15-38%, $Al_2O_3$ 1-8%, CaO 1-8%, and $Na_2O$ 0-3%. These compositions are represented by the normative olivine component with variable amounts of the normative Ca-rich pyroxene, anorthite and nepheline components. Botrioidal inclusions consist of nodules,about several tens to hundred microns in diameter, and interstitial materials, the former corresponding to the fine-grained CAI in chemical composition and the latter the amoeboidal olivine inclusions respectively. The chondrules show a variety of texture, the commonest being porphyritic to granular olivine chondrules. The chemical compositions of the chondrules are; $SiO_2$ 35-60%, MgO 8-50%, FeO 2-33%, $Al_2O_3$ 0-13%, CaO 0-15%, and $Na_2O$ 0-3%, being represented by the mixtures of the normative olivine and pyroxene components with relatively constant normative plagioclase component. The chondrules are subdivided on the basis of the normative plagioclase component

into two types, SP and IP. The former has a sodic plagioclase as the normative component and the latter is characterized by the intermediate plagioclase normative component. The matrix is defined here to be an aggregate of materials finer than micron size and the compositions are ; $SiO_2$ 27-36%, MgO 22-30%, ΣFeO 30-40%, $Al_2O_3$ 0.5-3%, CaO 0-2%, and $Na_2O$ 0-1%; being the mixtures of the normative ferrous olivine, Ca-rich pyroxene, plagioclase, nepheline and Fe-oxide components.

As above-stated, each constituent unit in the chondrite shows a wide range of chemical composition, which is explained by the various ratios of mixture of the constituent minerals in the each unit. In spite of the wide variation of the chemical compositions of the each unit, they all together form a continuous major chemical trend from the fine-grained CAI to the matrix via the botrioidal inclusions, amoeboidal olivine inclusions, IP and SP chondrules in this order. The major trend can be explained by the condensation theory (Larimer and Anders,1967; Grossman,1974) with several additional effects as follow. 1: Separation of metal condesates occured during or prior to the formation of chondrule-precursor materials. 2: Contamination of FeO to fine-grained CAI, amoeboidal inclusions and chondrules took place probably at temperatures lower than 700°K after their formation and prior to the accretion. 3: High alkali contents of the fine-grained CAI may be due to a reaction with the gas which was in equilibrium with the dust resulting finally to the matrix of the chondrite. 4: The depletion of alkali and CaO contents in the matric is also characteristic nature of the chondrite.

# PETROLOGY OF ALH-77307 (CO3) CHONDRITE

Hiroko Nagahara and Ikuo Kushiro
Geological Institute, University of Tokyo, Hongo, Tokyo, 113

ALH-77307 chondrite is a typical CO3 chondrite, which consists of inclusions, chondrules and isolated olivine graines set in the dark matrix. The inclusions are irregular in shape and show various textures with size of crystals ranging from submicron to a few 100 μm. The textural variation among the inclusions appears to be continuous; with increasing crystallinity of olivine and pyroxene, the outer shape becomes smooth and rounded and the dispersed irregular magnetite (some may be originally metallic iron) becomes large and rounded (Fig. 1). The coarsest ones are texturally similar to some chondrules except their outer shape; the inner portion is occupied by anhedral olivines and clinoenstatite surrounds them along the outer shape. The bulk chemical compositions of the inclusions and the chondrules were determined by moving- broad beam microprobe analysis. The compositions of both the inclusions and the chondrules fall in the same region in the system MgO-FeO-SiO2 (Fig. 2). There is no distinct correlation between the bulk chemical composition and the texture, although coarse-grained ones are slightly more magnesian than the fine-grained ones. These results suggest that the textural difference of the inclusions is not due to the difference in chemical composition, but is due to the difference in the condition of their formation. We interpret that the textural variation described above is due to the difference in temperature; the temperature of heating of the inclusions was lower for the fine-grained inclusions and higher for the coarse-grained ones. It is likely that little or no liquid was present in the fine-grained ones, whereas a significant amount of liquid was present in the coarse-grained ones, although even the coarsest ones were probably not totally melted.

The chondrules (0.3-0.6 mm in diameter) include two different types; Mg-rich type and Fe-rich type. The former is rich in subhedral-anhedral magnesian olivine (Fo99.8-98.0) with smaller amounts of clinoenstatite (En98.5-96.0), and the latter consists of strongly zoned euhedral olivine in dark groundmass, similar to those in the UOC.

The isolated olivines show two different compositional ranges (Fig. 3). One is magnesian and show a narrow compositional range (Fo99.8-98.0) and reverse zoning of CaO, and the other is relatively iron-rich and strongly zoned (to Fo48) and shows normal zoning of CaO. The former and latter types are similar to those in the chondrules of Mg-rich and Fe-rich types, respectively. Exceptionally, two olivine crystals show a compositional range Fo99-60. Most of these isolated olivines are the same as those in the chondrules and

some inclusions. It is suggested that the isolated olivines are fragments of olivines in the chodnrules and inclusions, and may not be the products of direct condensation from the gas.

For the purpose of reproducing the textural variations of the inclusions, heating experiments are being conducted on the average composition of the inclusions. Preliminary results indicate that heating to 1500°-1630°C and cooling with rates 120-50°/min produced the textures with euhedral to subhedral olivine crystals with glass inclusions similar to those found in olivine crystals in some inclusions and isolated grians. The size of olivine crystals changes greatly with temperature of heating, but changes litlle with the duration of heating.

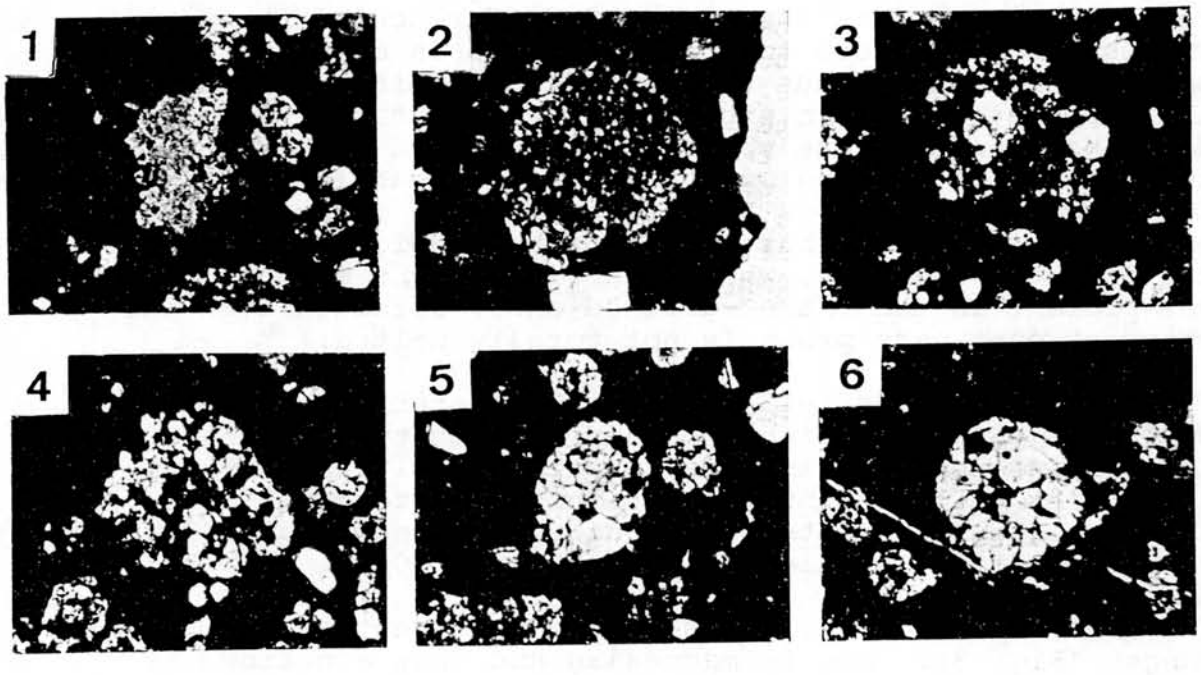


Fig.1 Textural variation of inclusions and chondrules. As the increase of crystallinity, sizes of silicate and opaque minerals become large and the outer shape becomes smooth and rounded (1 → 6).

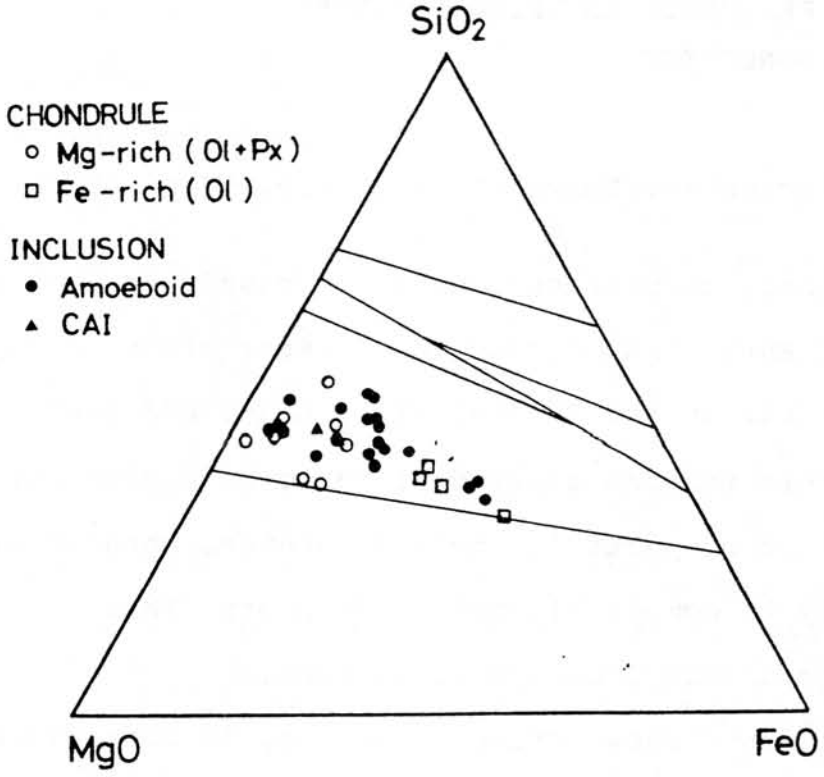


Fig.2 Chemical composition of chondrules and inclusions in ALH-77307 chondrite.

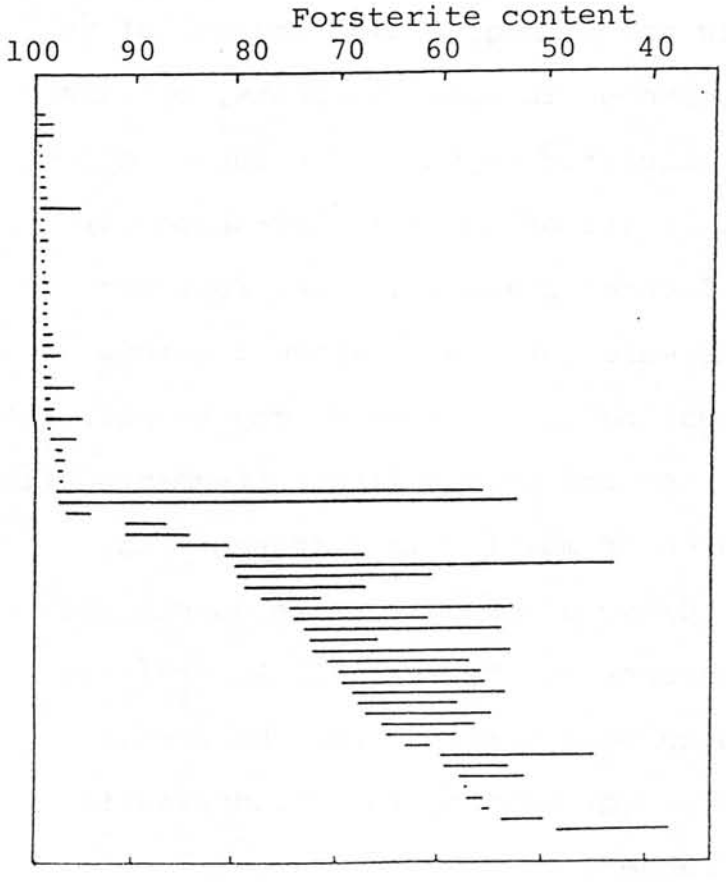


Fig.3 Zoning range of isolated olivines.
One bar represents compositional range of one grain.

11

# PETROLOGY OF LITHIC FRAGMENTS IN UNEQUILIBRATED ORDINARY CHONDRITES

Kimura, M.

Department of Earth Sciences, Ibaraki University, Mito 310

Unequilibrated ordinary chondrites consist of chondrules, lithic and mineral fragments, and matrix. The present study deals with lithic fragments in the Y-74191 (L3), ALH-77033 (LL3), and ALH-77249 (L3). Lithic fragments are defined to be aggregates of minerals which were not or partially melted, whereas chondrules were derived from nearly to completely molten droplets. Thus most of lithic fragments do not show spherical-form.

Although lithic fragments show various textures, in comparison with the features of chondrules they show generally the following features: 1)Anhedral crystals are common, 2)Distribution of relic minerals and glass is heterogeneous in some fragments, 3)Glasses are often devitrified and spherulitic crystals are observed in such glasses, 4)opaque minerals are often irregular-shaped,5) Minerals show various shock-induced features. These features reflect that lithic fragments were not heated above liquidus temperature. Shock-induced heating melted some fragments partially.

Constituent minerals and texture relate lithic fragments with chondrules, although the degree of melting is different. In addition, the variation of FeO/MgO of chondrules is consistent with that of minerals in fragments in the Y-74191. Accordingly, chondrules and lithic fragments were derived from the common precursor materials. Temperature of heating for chondrules is higher than that of lithic fragments.

# A NEW METAL-RICH MESOSIDERITE FROM ANTARCTICA, RKPA79015

Clarke, Roy S., Jr., Mason, Brian, and Jarosewich, Eugene
Smithsonian Institution, Washington, D.C. 20560

A 10.0 kg metal-rich silicate-containing meteorite was found in the area of Reckling Peak, Victoria Land, in 1979. On the basis of preliminary examination it was classified as an iron meteorite containing silicate inclusions. Four other silicate-rich specimens found the following year appear to be part of the same fall: RKPA80229, 80246, 80258, and 80263.

Half of the original specimen has been transferred to the Smithsonian Institution where a slice was removed for study. Samples from the slice are now under investigation in several laboratories. Half has been retained in the more protective environment at the Johnson Space Center.

The surface of RKPA79015 has been strongly weathered in most areas to a flaky iron oxide crust several millimeters deep. No fusion crust remains. Weathering has penetrated along silicate-metal boundaries into the interior.

Silicates make up about 30 weight percent of the specimen. They are found both in silicate-rich areas that contain only minor amounts of metal and troilite, and also dispersed into more metal-rich areas. They consist almost entirely of orthopyroxene; a little calcium-rich plagioclase of somewhat variable composition ($An_{86}$-$An_{94}$) was analyzed in one section. The orthopyroxene is essentially uniform in composition, $Wo_2En_{74}Fs_{24}$, except in one apparently heat-altered specimen in which the Fs content is 17-21; it contains small amounts of $Al_2O_3$ (0.4-1.4%), MnO (0.6-0.7%), $Cr_2O_3$ (0.2-0.8%), and $TiO_2$ (0.1-0.2%). Accessory minerals analyzed were chromite ($Al_2O_3$ 7.0%, MgO 1.8%, MnO 1.6%, and $TiO_2$ 0.5%) and merrillite.

A large metal-rich area essentially free of silicates consists predominantly of millimeter-size kamacite grains containing globular troilite at the grain centers. Kamacite grain boundries are heavily populated with cloudy taenite bordered by wide bands of tetrataenite, and this association is also observed within kamacite grains. The kamacite also contains Neumann bands and schreibersite. A sample from this area gave the following composition: Ni 9.87%, Co 0.52%, P 0.15%, and FeS 2.14%.

Approximately half of the surface area available for examination is gradational between the two types of areas described above. Also present is a comparatively small troilite-rich area that contains small amounts of kamacite in association with tetrataenite-cloudy taenite.

Classification of RKPA79015 and related specimens as mesosiderites seems required both by the observed silicate mineralogy and the distinctive metallography. The main mass is a metal-rich portion of this apparently plagioclase-poor mesosiderite, bearing similarities to the Chinguetti, Mauretania, meteorite.

13－1

# NI-FE METALS IN THE UNEQUILIBRATED CHONDRITES

Hiroko Nagahara
Geological Institute, University of Tokyo, Hongo, Tokyo, 113

Ni-Fe metals in some unequilibrated chondrites have been petrographically studied, and their cooling history was considered in relation to chemical and textural variations of the chondrules. Studied samples are ALH-77015 (L-3), - 77033 (LL- 3), -77278(LL-3), -77299(H-3) and -77304 (L-3).

Metal grains are isolated kamacite, isolated taenite, intergrowth of taenite and kamacite, and coexistence of troilite with each of the former three. Most of them occur as irregular shaped grains in the matrix and on the surface of the chodnrules, and some as large rounded grains usually with troilite and as small globules within chondrules. The latter is generally kamacite and occurs in the glassy part or the goundmass, indicating their formation from melt at the time of chondrule formation under reducing condition.

Mode of occurrence of metals in these UOCs is different from that in the equilibrated chondrites (Fig. 1); metals in an H-chondrite are large amounts of isolated kamacite, moderate amounts of associating kamacite and taenite, and small amount of isolated taenite. In L-chondrites, there are isolated kamacite, isolated taenite and grains of associating taenite and kamacite are present in the order of decreasing amount. Combining the Ni- Fe phase diagram and the mode of occurrence of metals in the equilibrated chodnrites which should have been once heated up to the "solvus" temperatures, it is inferred that (1)the UOCs have not been heated up to 600°C, (2) they should have cooled more rapidly than the equilibrated chodnrites below 600°C, and (3)kamacite and taenitte should have been originally contained in the chondrites.

Both taenite and kamacite show copmpositional zoning similar to those in the equilibrated chondrites. However, the range of zoning of kamacite is wider in the UOCs than in the equilibrated chodnrites. This also suggests rapid cooling of UOCs below 500°C. Because, the diffusion coefficient for Ni is larger in kamacite than in taenite, so kamacite in slowly cooled equilibrated chondrites nearly reached equilibrium, while taenite preserved compositional zoning formed during its cooling. On the contrary, even kamacite has not reached equilibrium and preserved zoning in relatively rapidly cooled UOCs.

Degree of equilibration of metals reflects that of silicate minerals. In the figure of Ni concentration in the core vs. apparent distance to edge (Wood's plot), some chondrites show approximately aligned relation along certain

cooling line, though others show no systematic relations on the figure(Fig. 2). The latter chondrites are highly unequilibrated and the chondrules in them show various textures and their bulk XMg varies widely, and constituent minerals show large heterogeneity. On the other hand, bulk XMg is fairly uniform and minerals show much less heterogeneity in the former chodnrites in spite of similar appearrance. The aligned and non-aligned relations would indicate heating up to 500 C°or not, respectively.

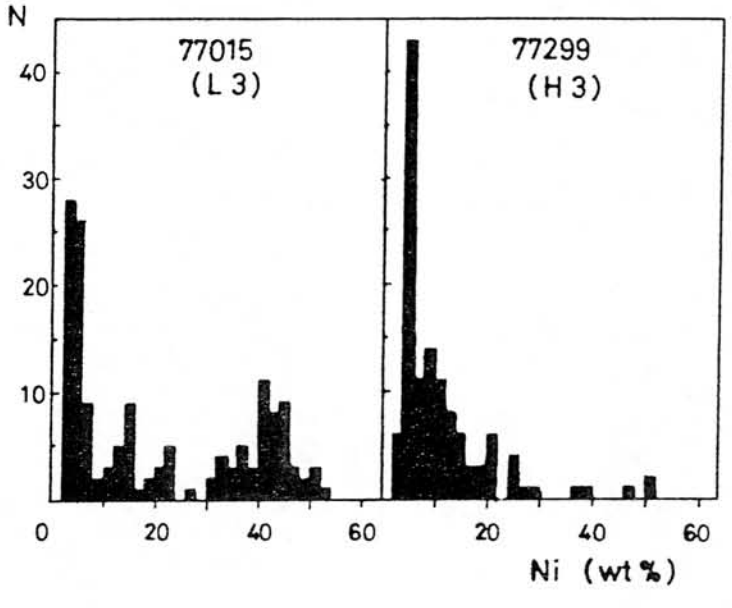


Fig.1 Mode of Ni-Fe metals. One point represents one grain on the thin section where the grain associated taenite and kamacite is shown as intermediate composition.

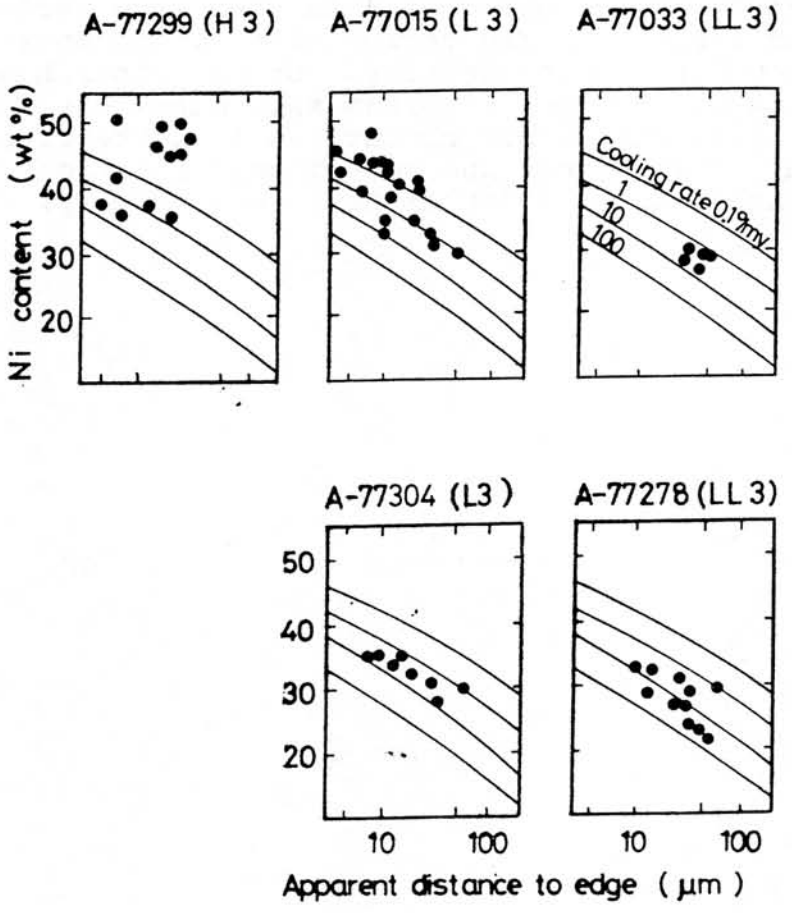


Fig.2 Relation between Ni concentration of core of a taenite grain and apparent distance to edge (Wood's plot) for five UOCs.

# MINERALOGICAL EXAMINATION OF THE YAMATO-79 ACHONDRITES, PRELIMINARY VIEW

Takeda, H.[1,2], and Yanai, K.[2]
[1] Mineralogical Institute, Faculty of Science, University of Tokyo, Hongo, Tokyo 113
[2] National Institute of Polar Research, 9-10 Kaga 1 chome, Itabashi-ku, Tokyo 173

A brief physical description of the Yamato-79 achondrites recovered by JARE in 1979 (Yanai and Kojima, priv. com.) has been carried out at the National Institute of Polar Research by the Preliminary Examination Team up to sample No. 791491. We report mineralogical studies on seven polymict eucrites, one howardite, and one ureilite, and physical observation on a few diogenites similar to Yamato-75032. A part of the study on a large lithic clast in Yamato 790266 has been carried out as a part of the Polymict Eucrite Consortium Study.

Polymict eucrite

New findings of many polymict eucrites have been one of the contributions of the recoveries of a large number of meteorites from the Yamato Mountains, Antarctica, by Japanese (JARE) teams in 1974 and 1975 (Miyamoto et al., 1978; Takeda et al., 1978). The Yamato eucrites (except Y74356) are unlike previously described eucrites and howardites in that they contain a series of fragments covering a range of eucrites types and are thus polymict but they do not appear to contain a diogenitic component as in typical howardites. Thus, the name polymict eucrite has been proposed by us. It is a polymict breccia of eucritic composition or howardites without diogenitic components. In spite of the variety of eucritic components, their bulk chemistries are essentially those of eucrites. The polymict eucrites have been interpreted to be lithified regoliths produced by impacts of various-sized meteorites, that is, various depths of excavation of the layered crust on their parent body (Takeda, 1979). Because comparison of lists of Antarctic and non-Antarctic achondrite (Mason et al., 1979) shows that polymict eucrites are more abundant in the Antarctic region, the new findings of many polymict eucrites from Antarctica, cast doubt on that they could be pieces from a single fall. To give better understanding of this problem, and their origin and evolution, we will report the characteristics of the Yamato-79 polymict eucrites.

Among nine polymict eucrites processed to date in the Yamato-79 collection, and listed in Table 1, Y790006, 790020, 790113, 790114 and 790260 are all polymict eucrites similar to those of the previous collections. Y790007 contains abundant inverted pigeonites from cumulate eucrites. Y790266 (208 g) is richest in lithic clasts, exhibiting ranges of textures, from coarse-grained Juvinas type to Pasamonte-like variolitic one. It is rather difficult to find matrix portions.

The largest clast in Y790266, which may occupy more than a half of the meteorite, is a medium-grained equigranular basalt with pyroxene crystals ranging from 0.2 to 0.5mm in diameter. The chemical variation from core to rim (Fig. 1) simulate the tie-line trend from the host pigeonite to exsolved augite of ordinary eucrites such as Y74356. One crystal has a Mg-rich core 0.08mm in diameter and show small enrichment of $Al_2O_3$. Our new finding of the Y790266 trend cast some doubt on an idea that the uniform pyroxene compositions of many ordinary (or equilibrated) eucrites were produced by extended subsolidus annealing and homogenization of the Pasamonte-type pyroxenes. Because the matrix of porphyritic clast in ALHA77302 and the final trend of the Pasamonte-type show the same trend as that of Y790266, the Fe-Ca trend is not entire unlikely trend for eucrite.

The bulk chemical composition of the Y790266 clast (Analysis by H. Haramura) is poorer in plagioclase component than that of Y790260 which is similar to the matrix portion of Y790266. $Na_2O$ (0.61 wt. %)vs. Mg / (Fe+Mg) (=0.41) plot of Y790266 is in the region of clasts in other Antarctic polymict eucrites (Wooden et al., 1981), and is more Na-rich than that of Y790260 ($Na_2O$ 0.50 wt. %). The plagioclase in the Y790266 clast is Na-rich ($An_{80}$). A thin section of Y790260 examined contains large pyroxene fragment (4mm) with a uniform core and chemically zoned rims, and fine-grained aggregates of pyroxene with chemical compositions of the ordinary eucrites.

Y790122 is rich in clasts, and one thin section examined consists of four different clasts (A-D) joined with small amounts of matrices between them. (A) The largest lithic clast is a medium grained ophitic basalt rich in mesostasis and with chemically zoned pyroxenes. (B) Very fine-grained ophitic basalt (Fig. 2) contains pyroxenes with nearly uniform compositions. (C) A coarse-grained equigranular clast has pyroxenes with uniform composition but with little Mg-rich than those in ordinary eucrites. (D) An angular aphanite-like clast with dark glassy matrix contains pyroxenes not different from those in B. Their plagioclase is most calcic (An 93).

Y790007 is different from the above three polymict eucrites in that it has abundant fragments of inverted pigeonites with blebby exsolved augites from cumulate eucrites. Their compositions ($Ca_3Mg_{64}Fe_{33}$) are close to those in Binda. In spite of the predominance of the slowly cooled eucrite components, this breccia contains round glassy clast with fethery phenocrysts. Clasts with glassy matrix were also found in Y790006. Inverted pigeonites have been detected also in Y790020 and Y790113. ALH78006, polymict eucrite is also rich in cumulate eucrites, but contained a small fragments of diogenites.

The Yamato-79 polymict eucrites revealed many similarity to the previously described Antarctic polymict eucrites, but some are rich in clasts of different types, and a few breccias are rich in cumulate eucrites. Presence of only one howardite in a thousand meteorites processed to date confirms the statement that polymict eucrites are predominant over howardites in Antarctic meteorites. Y790727 (120.4g) previously described as a polymict eucrite turned out to be howardite richer in eucritic components than Y7308. It contains a diogenite fragment partly molten and recrystallized.

Ureilite

Only one new Antarctic ureilite, Y790981 (213g, 0.3x5.5x4.0cm) was found. Y790981 exhibits many petrographic features characteristic of ureilite. It is predominantly composed of anhedral to euhedral olivine(88%) and pigeonite (7%) and dark carbonaceous (C) matrix(4%). Average olivine core composition is Fa21, and where in contact with C matrix, the composition is enriched in Mg by reduction. The olivine crystals display unduratory extinction and subgrain boundaries. The pigeonite compositions are similar to those of Kenna and Y74123, and contain small inclusions of diopside more Fe-poor than that expected from the tie-line. The most notable textures of the pigeonite is the presence of unmixed augite. ATEM examination by H. Mori revealed that the thickness of the exsolved augite lamellae is a few hundreds A, and that Al-rich spherical augite inclusions coexist with glass.

Diogenite

There are found a number of achondrites similar to Y75032 in hand specimen. Y791199 are rich in a crystalline portion which is 4x3 cm in size and contains light yellowish gray pyroxene crystals up to a few cm in diameter. Y791200 contains a lithic clast 1.5x2.0x0.3cm in size with plagioclase up to 3mm long. The pyroxenes in the clast is dark olive in color, and are similar to those in cumulate eucrite Moama. An apparent interface is

transitional. The fact givesa strong support for the close genetic link between diogenites and cumulate eucrites.

In summary, varieties of clast types found in the Yamato-79 polymict eucrites can be still explained by impact processes in various scales into a layered crust of the parent body. Basaltic clasts derived from the near surface is more dominant in size. Because the total number of the Yamato-79 collection is comparable to that of the world meteorite collection, it was expected that frequencies of different meteorite types may be similar to the know collection. However, our statistics revealed that the Yamato meteorites may represent meteorite falls during a certain period on some restricted areas of the Antarctic continent.

We thank members of the field party of the JARE in 1979, and of the Preliminary Examination Team at the NIPR. We are indebted to the Ministry of Education for the financial support for the meteorite processing. We thank Mr. H. Haramura for the wet chemical analysis.

References

Mason B., E. Jarosewich and J. A. Nelen (1979) Smithsonian Contrib. to Earth Sci. No. 22, p. 27-45, Fudali, ed.

Miyamoto M., H. Takeda, and K. Yanai (1978) Memoirs of the National Inst. of Polar Res., Special Issue No. 8 (T. Nagata, ed.), p. 185-197.

Takeda H. (1979) Icarus 40, 455-470.

Wooden J., A. M. Reid, R. Brown, B. Bansal, H. Wiesmann, and L. Nyquist (1981) Lunar and Planetary Science XII, p. 1203-1205, Lunar and Planetary Institute, Houston.

Table 1. Yamato-79 Polymict Eucrites (Y-790001-790990)

| Sample No. | Dimensions(cm) | Weights(g) |
|---|---|---|
| Y-790006 | 3.8x3.0x2.2 | 29.4 |
| Y-790007 | 5.6x5.0x2.6 | 80.4 |
| Y-790020 | 7.1x4.6x3.4 | 86.3 |
| Y-790113 | 3.3x2.6x1.6 | 19.0 |
| Y-790114 | 2.0x1.6x1.4 | 23.9 |
| Y-790122 | 5.7x5.0x3.1 | 109.5 |
| Y-790260 | 9.2x6.7x5.0 | 433.9 |
| Y-790266 | 7.4x5.0x5.9 | 208.0 |

Fig. 2. Photomicrograph of fine-grained clast B in Y790122. Width is 0.9mm. The composition is given Fig.3.

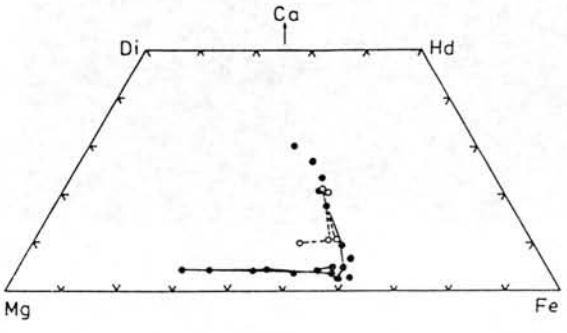


Fig. 1. Pyroxene chemical zoning trends in Y790266 medium grained basalt clast.

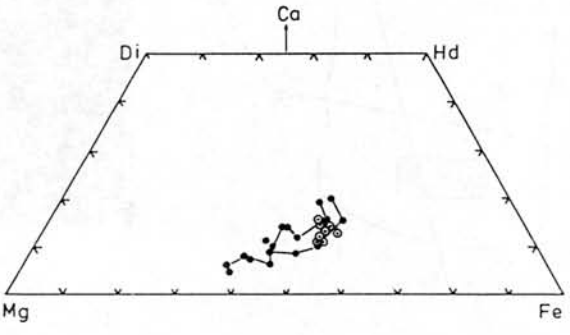


Fig. 3. Pyroxene compositions in clasts of Y790122. Dots-line: clast A, open circle with dots: clast B in Fig.2

15－1

# IGNEOUS LAYERING AND SHOCK METAMORPHISM IN A NEW ANTARCTIC ANCHONDRITE

Harry Y. McSween, Department of Geological Sciences, University of Tennessee, Knoxville, TN 37996, USA

Elephant Moraine A79001, a large (7.94 kg) shergottite from Victoria Land, contains the first extraterrestrial example of an unbrecciated contact between two distinct but related lithologies (Fig. 1). The contact is gradational in terms of modal variations (Fig. 2), suggesting that this sample formed by igneous layering processes. Lithology A is composed of phenocrysts of olivine, orthopyroxene, and chromite in a fine-grained groundmass of pigeonite, augite, maskelynite, and minor ilmenite, titanomagnetite, whitlockite, and pyrrhotite. Lithology B is coarser-grained than A and consists of zoned pigeonite, augite, maskelynite, and accessory ilmenite, titanomagnetite, pyrrhotite, and a silica polymorph. Petrologic mixing calculations using bulk chemical analyses of the two lithologies indicate that B could be formed from A by extraction of the phenocryst minerals in A. However, the relative proportions of phenocrysts required in the calculation are not the same as observed, and zoning and reaction rims in phenocrysts indicate that they are not in equilibrium with the enclosing groundmass. A more likely model is that both lithologies formed by fractionation of these phases from a common parental magma.

Pervasive shock metamorphism is indicated by the development of maskelynite from plagioclase and mosaicism and planar structures in olivine and pyroxene. Pockets of vesicular impact melt glass occur throughout both lithologies. Microfaults with recognizable offset are lined with glass. These features suggest peak shock pressures of 30-45 GPa.

This meteorite is an important find and provides significant new information on the petrogenesis of the shergottite parent body.

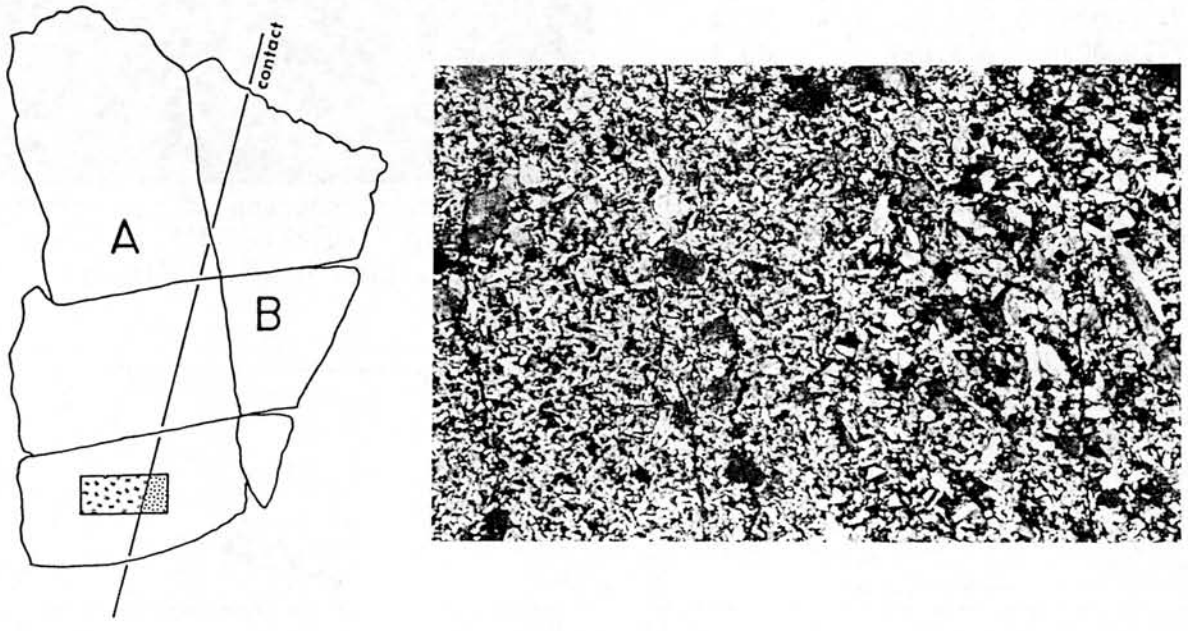


Fig. 1. Sketch of sawed slab of A79001 showing approximate contact between lithogies A and B and location of 1 x 2 inch thin section pictured.

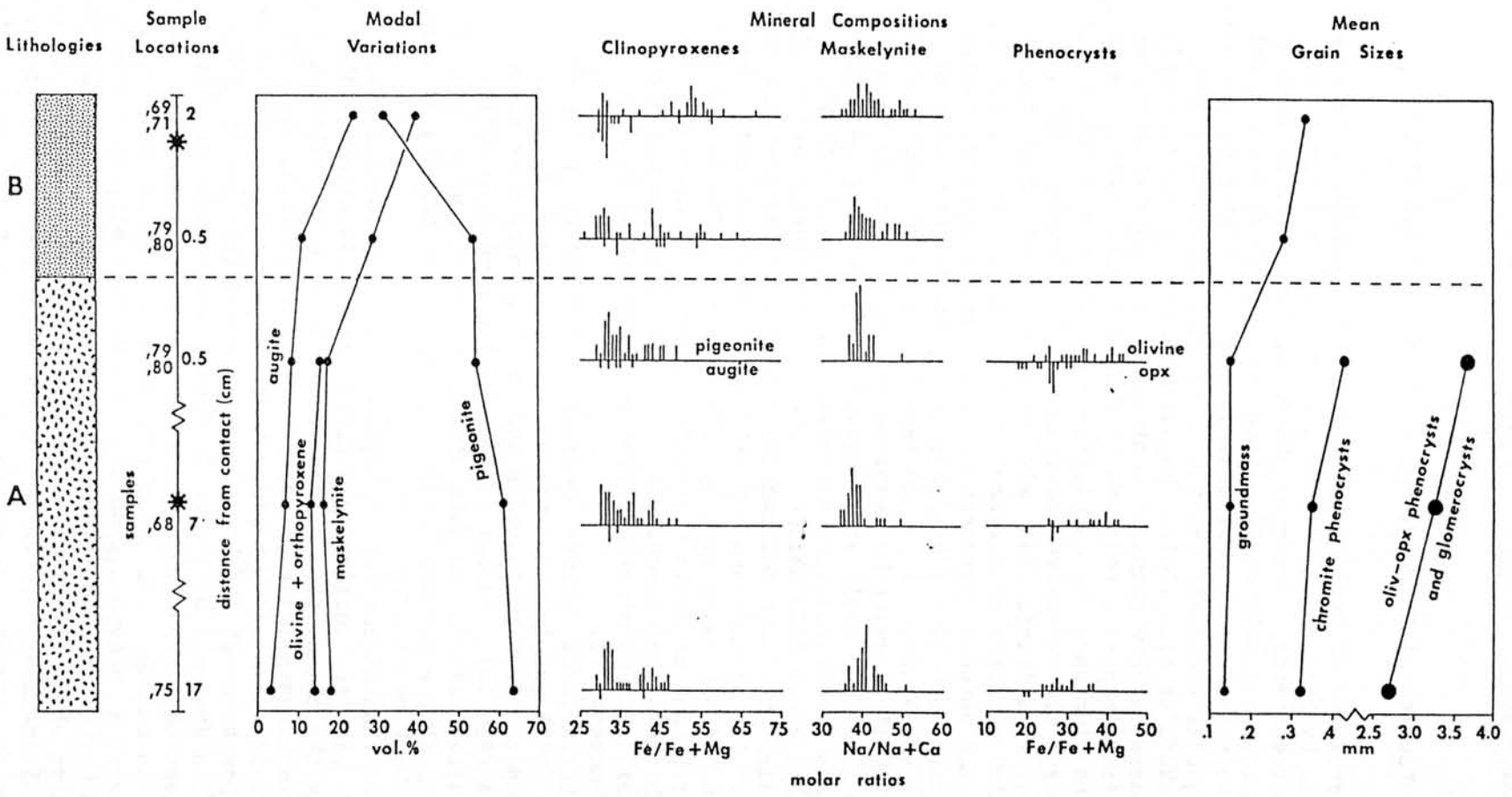


Figure 2. Petrographic variations in different portions of Elephant Moraine A79001 meteorite. Sample locations are approximate distances from the A-B contact; stars represent locations of bulk chemical analyses. Modal variations were determined from counts of > 1200 points; optically indistinguishable clinopyroxenes were counted together and augite/pigeonite ratios were calculated from microprobe surveys. The smallest vertical bars in mineral composition histograms represent one microprobe analysis. Mean grain sizes for groundmass were calculated from the number of grain contacts encountered during traverses of fixed distance and different orientations; phenocryst sizes are averages of measured diameters in two perpendicular directions.

# 16－1

## ANALYTICAL ELECTRON MICROSCOPIC STUDIES OF PIGEONITES IN EUCRITES

H. MORI and H. TAKEDA
Mineralogical Inst., Faculty of Science, Univ. of Tokyo, Tokyo 113.

The combined techniques of optical and electron petrography with localized chemical analysis by EPMA and ATEM have been applied to a lithic clast in the Yamato polymict eucrites. Pyroxene phases in most eucrites show no chemical zoning and are chemically equilibrated, regardless of their basaltic textures. Of these non-cumulate eucrites, Juvinas and Y74356 were studied using ATEM technique to elucidate their exsolution microtextures and thermal histories (Takeda et al., 1981). Basaltic clasts in the Antarctic polymict eucrites generally show chemical zoning. Y75011 is rich in large crystalline clasts with subophitic textures (Takeda & Yanai, 1981). It will be very interesting to elucidate the exsolution microtextures of the Y75011 pyroxenes which preserve the extensive chemical zoning. Sample Y75011,50 examined in this study is a lithic clast with medium-grained subophitic texture (Fig.1a), which consists of pyroxene, plagioclase, olivine, silica, ilmenite and other minor phases. Pyroxenes show extensive chemical zoning from colorless pigeonite core ($Ca_{5.1}Mg_{65.3}Fe_{29.6}$) to brown-gray subcalcic ferroaugite rim ($Ca_{25.3}Mg_{18.5}Fe_{56.2}$) as was reported by Takeda and Yanai (1981). Exsolution lamellae cannot be resolved optically, but two sets of lamellar twinning on (100) and (001) are observed. The twinning is extensive in sheared regions associated with microfaults running through the clast and attributed to shock deformation. Irregular fracturing and undulatory extinction are also prominent deformation textures in the pyroxene and plagioclase crystals. The plagioclase crystals are lath-shaped and range up to 0.4 mm in width and 3.0 mm in length. Olivine (Fa 72-78) occurs as veinlets within interior and at grain boundaries of pyroxene crystals, and in mesostasis. Fig.1b shows the pigeonite core traversed by the olivine veinlets (up to 10 μm). Silica minerals occur as interstitial patches associated with dark mesostasis.

The dominant substructural feature observed in TEM for the pyroxene phases is fine-scale (001) exsolution lamellae. In the pigeonite core, augite lamellae are up to 0.06 μm in width and the pigeonite host shows (100) stacking faults (Fig.1c). Subcalcic ferroaugite rims show (001) exsolution lamellae alternatly 0.2 μm wide of augite and pigeonite (Fig.1d). In the sheared regions of the pyroxene crystals, exsolution texture is disrupted by the later shock event (Fig.1e,f).

It has been known that Al content of pigeonite and plagioclase size empirically correlate with the cooling rate during crystallization (Walker et al., 1978). Using the calculation procedure illustrated by Walker et al., the cooling rate during crystallization recorded by the Y75011,50 clast is inferred to be 0.1°C/hr. However, pyroxene phases show extensive exsolution and the chemical compositions of the host-lamella pair determined by ATEM show as wide separation as those of the Moore County and Juvinas eucrites. These evidences suggest that Y75011,50 pyroxenes have reequilibrated during prolonged subsolidus annealing. The subsolidus annealing event must have predated the shock event as previously noted. The Fe-rich olivine veinlets could have developed by the decomposition of Fe-rich rim pyroxene to fayalite and silica or remelting of Fe-rich immiscible liquid in mesostasis developed during initial crystallization by reheating of short duration at high temperature (~1100°C). The temperature was estimated from a phase diagram present-

ed by Huebner and Turnock (1980). The reheating event must have postdated the shock event because the olivine veinlets show no evidence of shock-induced disruption. Moreover, the temperature rise which is induced by the shock compression is expected to be only limited because the peak pressure deduced from the deformation fabric observed in the clast may have reached up to 100-200 kb. The pressure estimate is based on a classification scheme of shock grade calibrated by the shock recovery experiments on terrestrial and lunar basalts by Kieffer et al. (1976) and Schaal and Hörz (1977). So the shock-induced local melting will be unprobable. Later impact events would have produced the polymict breccia composed of variable eucritic rock fragments on the surface of the howardite (eucrite) parent body (Takeda et al., 1979). In summary, five major events in the history of the Y75011 clast are outlined in Table 1. It is to be mentioned that such detail thermal and deformational histories as were revealed by the Y75011 clast can not be unravelled for ordinary eucrites because of later thermal event obstruction.

We thank Prof. Y. Matsumoto and his JARE party and National Inst. of Polar Res. for the meteorite sample.

References

Huebner, J.S. and Turnock, A.C.(1980): Am. Mineral., 65, 225-271.
Kieffer, S.W. et al.(1976): Proc. Lunar Sci. Conf. 7th, p. 1391-1412.
Schaal, R.B. and Hörz, F. (1977): Proc. Lunar Sci. Conf. 8th, p. 1697-1729.
Takeda, H. et al. (1979): Mem. Natn'l Inst. Polar Res., Spec. Issue 12, 82-108.
Takeda, H. and Yanai, K. (1981): Lunar and Planet. Sci. XII, p. 1071-1073.
Takeda, H. et al. (1981): Proc. Lunar planet. Sci. Conf. 12th, in press.
Takeda, H. et al. (1982): Lunar Planet. Sci. XIII, in press 1982.
Walker, D. et al. (1978): Proc. Lunar Planet. Sci. Conf. 9th p. 1369-1391.

Table 1. Thermal and deformational history.

| Stage | Nature of events | Results |
|---|---|---|
| I | Initial crystallization, rapid cooling (~0.1°C/hr.) | Subophitic texture |
| II | Prolonged subsolidus annealing | Exsolution in pyroxene phase |
| III | Shock deformation (100-200 kb) | Deformation texture |
| IV | Reheating of short duration at high temperature (~1100°C) | Olivine veinlets |
| V | Excavation and brecciation | Polymict breccia |

Note: Yamato 75011,50 is a part of the large crystalline clast, which was found when the whole meteorite was cut into halves at NASA Johnson Space Center by Dr. K. Yanai of the National Institute of Polar Research. The photograph of the cut surface is given in "Photographic Catalog of the Selected Antarctic Meteorites" compiled by K. Yanai, p. 41, 1981. The sample is a chip of upper right portion of the largest clast (2.7x0.9 cm) seen upper part of the photograph.

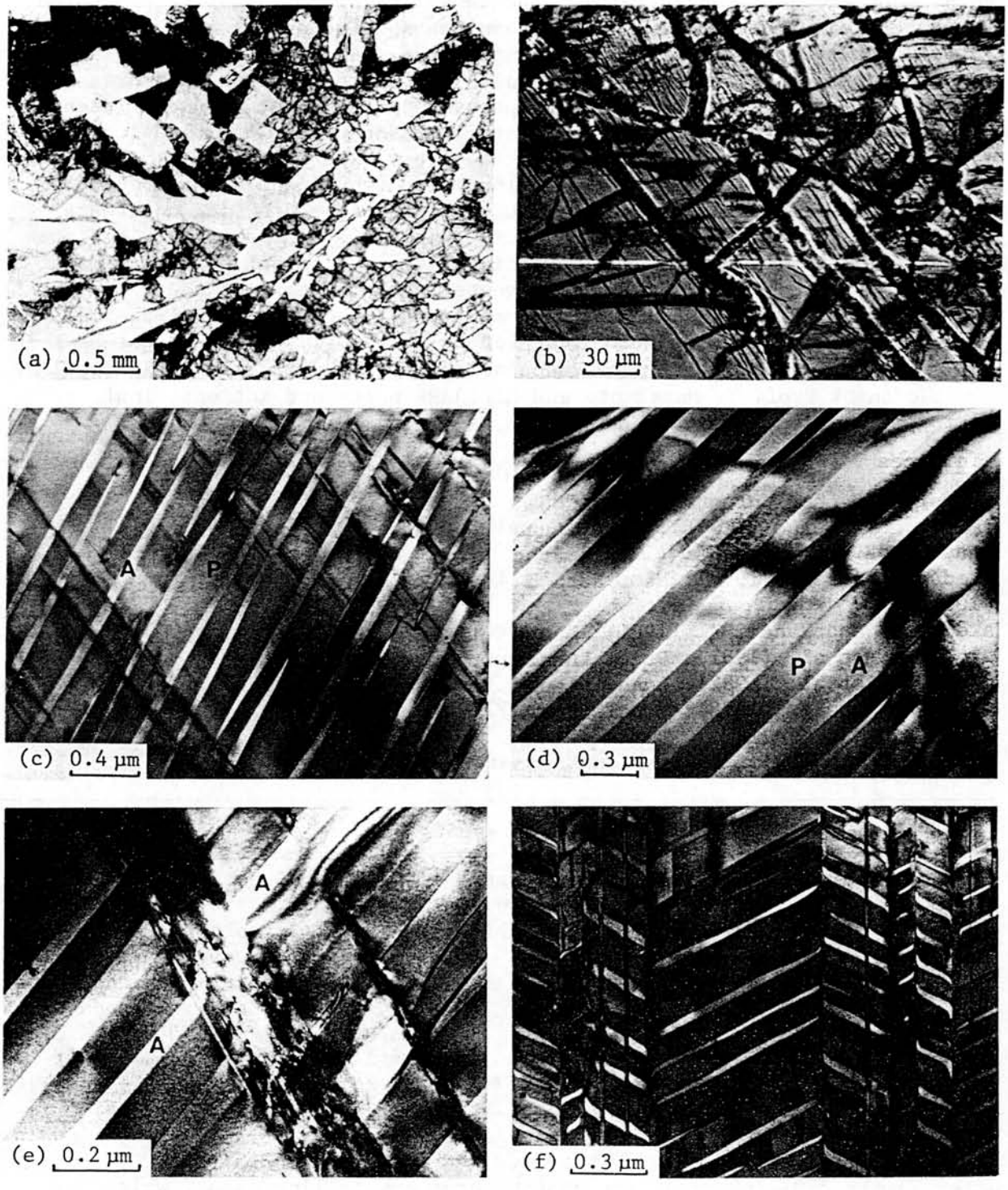


Fig. 1. Microstructures of Y75011,50. (a) is an optical micrograph(plane light). Note a large mesostasis segregation in upper left; (b) is an optical micrograph(crossed nicols) showing Fe-rich olivine veinlets in core pigeonite; (c)-(f) are bright field electron micrographs of the same grain in (b). Fine-scale lamellar intergrowths of augite(A) and pigeonite(P) are observed. (e) and (f) show the disruption of the exsolution texture by shock deformation.

# A MAJOR AND TRACE ELEMENT COMPARISON OF ANTARCTIC POLYMICT EUCRITES AND COMMON EUCRITES

M. B. Duke
NASA/Johnson Space Center, Houston, TX 77058

A computational model has been constructed for eucrites which allows consideration of major element variations based on phase relationships in the projection of the Ol-An-$SiO_2$ system onto the En-Fs-An plane, distributing Fe/Mg, calcium pyroxene and albite feldspar between liquid and solid phases according to coefficients reported by Stolper (1) and using distribution coefficients reported in the literature to model trace element variations. (E.G. ref. 2). Based on this model, several distinct groupings of eucrites are separable, including common eucrites (3), Antarctic polymict eucrite matrix, and polymict eucrite fragments reported by Wooden, et. al. (4). Stannern is also separable from ordinary eucrites in this model, in contrast to the interpretation by Consolmagno and Drake (2) among others that Stannern represents a smaller degree of partial melting of the same parent material from which the common eucrites such as Juvinas were derived. The groupings suggest derivation of suites of eucrites by partial melting of parental sources which had different plagioclase/(olivine + pyroxene) ratios and different albite/anorthite ratios. Fractional crystallization of wholly melted parent was necessary to produce the pyroxenes of howardites and diogenites. Derivation of eucrites and howardites either requires several parent bodies or multistage fractionation in a single body.

References:

1. Stolper, E. (1977) Experimental petrology of eucritic meteorites. Geochim. Cosmochim. Acta 41, 587-611.
2. Consolmagno, G. J. and Drake, M. J. (1977) Composition and evolution of the eucrite parent body: evidence from rare earth elements. Geochim. Cosmochim. Acta 41, 1271-1282.
3. Basaltic Volcanism Study Project (1981) The Basaltic Meteorites. Basaltic Volcanism on the Terrestrial Planets. Pergamon Press, Inc., New York, 236-265.
4. Wooden, et al (1981) Chemical and Isotopic Studies of the Allan Hills polymict eucrites in Lunar and Planetary Science XII, Lunar and Planetary Institute, Houston, 1203-1205.

# 18－1

## COMPOSITIONAL VARIATIONS OF PLAGIOCLASE, APATITE AND CHROMITE IN YAMATO-75135, 93 CHONDRITE

Miura, Y. and Matsumoto, Y.
Department of Mineralogical Sciences and Geology, Faculty of Science, Yamaguchi University, 1677-1, Yoshida, Yamaguchi 753, Japan

A Yamato-75135,93 meteorite is L4-5 chondrite determined by Miura and Matsumoto (1981). This chondrite contains oligoclase feldspar which shows higher An-content than that of L-chondrite reported by Van Schmus and Ribbe (1968). The detailed study was carried out in this research.

Chemical compositions of constituent minerals of the Yamato-75135,93 chondrite were determined by using JXA-50A electron microprobe at the Department of Mineralogical Sciences, Yamaguchi University. The instrument was operated at 15 kV and $2.0 \times 10^{-8}$ A specimen current. An expanded electron beam of 5 μm diameter was used to obtain reliable data.

This chondritic meteorite contains olivine ($Fo_{75.6}Fa_{24.4}$ in average), opx ($En_{78.1}Fs_{20.8}Wo_{1.1}$ in average), cpx ($En_{45.8}Fs_{9.8}Wo_{44.4}$ in average), plagioclase, phosphate, chromite, troilite and metal phases.

The following compositional variations are observed in the plagioclase, apatite and chromite in the Yamato-75135,93 chondrite:

(1) Various grain-sizes of plagioclase ( from 30 to 300 μm in length) have an average composition of oligoclase $An_{19.7}Or_{7.2}$. This average value is higher than that of L-chondrite reported by Van Schmus and Ribbe (1968).

(2) Plagioclases in chondrule change from $An_{12}Or_6$ (in core) to $An_{17}Or_7$ (in rim) in composition, whereas those in matrix show An-rich composition ($An_{23}Or_8$) as listed in Table 1.

(3) Table 2 shows that the dispersions of average contents of oxides in matrix are larger than those in chondrule, especially in glassy plagioclase. Glassy plagioclase in matrix shows compositional variation from $An_{9.9}Or_0$ to $An_{49}Or_{21}$, whereas compositions of crystalline plagioclases around the glassy those are ranging from $An_{10}Or_1$ to $An_{13}Or_8$. It is found that a relatively rapid ordering of M-site ions (K, Na, Ca) resulted in An-rich plagioclase, compared with that of T site ions (Si, Al), might be considered to be characteristic of impact metamorphosed plagioclase.

(4) Chlorapatite is almost found in matrix, whereas fluorapatite, in chondrule. Fluorine component was concentrated to whitlockite in matrix. The apatite in the Yamato-75135,93 chondrite is chlor-fluorapatite different from the previous reports on halides in meteorites by Fachs (1968) and Van Schmus and Ribbe (1969). That is, contents of chlorapatite are 67 to 72 % in matrix, those of fluorapatite, 51 % in matrix and 58 % in chondrule as listed in Table 3. The content of halogen, F and Cl, in matrix is more than that in chondrule. It is found that chemical environments of formation-stage between chondrule and matrix are considerably different.

(5) Chromite crystals (ca. 50 μm in diameter) in matrix coexisted with whitlockite show compositional zoning and grain to grain variation. The result that the dispersions of oxides in matrix are much larger than those in chondrule as listed in Table 4, also indicates quite different stages of formation between chondrule and matrix.

Therefore, the formation process of the Yamato-75135 chondrite could be estimated by compositional variations of plagioclase, chromite and F/Cl ratio in apatite. At least four major events of formation process are considered to be occurred in the Yamato-75135 chondrite.

First, formation of chondrule (less F,Cl-content; high P and low T).

Second, recrystallization of chondrule (high T).

Third, attachment of rim of chondrule.
Fourth, formation of chondritic meteorite (at high P and low T) induced by multiple-impact metamorphism.

The final major event of formation is supported by the glassy plagioclase showing An-rich content (up to ca. $An_{50}$) and considerable content of movable halogen.

Table 1. Average compositions of plagioclases in Yamato-75135,93 chondrite.

| No. / Oxides | Chondrule [5]* | Rim of Chondrule [1] | Matrix [10] |
|---|---|---|---|
| $SiO_2$ | 64.02(100)** | 64.29 | 65.32(146) |
| $TiO_2$ | 0.06(3) | 0.11 | 0.06(3) |
| $Al_2O_3$ | 25.07(121) | 23.17 | 25.98(229) |
| FeO*** | 0.50(13) | 0.51 | 0.30(21) |
| MgO | 0.11(2) | 0.15 | 0.07(3) |
| CaO | 1.97(84) | 2.91 | 2.10(28) |
| $Na_2O$ | 7.12(135) | 6.96 | 5.07(275) |
| $K_2O$ | 0.73(32) | 1.04 | 0.48(35) |
| Total | 99.58(54) | 99.14 | 99.38(217) |
| Or(mol%) | 5.9(30) | 7.4 | 7.8(72) |
| Ab(mol%) | 81.4(78) | 75.2 | 69.0(215) |
| An(mol%) | 12.7(57) | 17.4 | 23.2(149) |

* *Numbers of crystals analyzed are shown in square brackets.*
** *Numbers in parentheses are standard deviation referring to the last decimal place.*
*** *Total iron oxide as FeO.*

Table 2. Average compositions of glassy and crystalline plagioclases in Yamato-75135,93 chondrite.

| No. / Oxides | *Glass plagioclase* [8] | *Dispersion(%)* | *Crystalline plagioclase* [3] | *Dispersion(%)* |
|---|---|---|---|---|
| $SiO_2$ | 64.85(299) | *4.6* | 65.50(106) | *1.6* |
| $TiO_2$ | 0.03(3) | *100.0* | 0.03(2) | *66.7* |
| $Al_2O_3$ | 27.31(231) | *8.5* | 23.21(44) | *1.9* |
| FeO | 0.41(25) | *61.0* | 0.33(24) | *72.7* |
| MgO | 0.03(3) | *100.0* | 0.04(2) | *50.0* |
| CaO | 1.98(11) | *5.6* | 2.01(14) | *7.0* |
| $Na_2O$ | 5.67(328) | *57.8* | 8.00(122) | *15.3* |
| $K_2O$ | 0.49(36) | *73.5* | 0.55(31) | *56.4* |
| Total | 100.77(94) | *0.9* | 99.67(30) | *0.3* |
| Or(mol%) | 7.4(71) | *95.9* | 4.1(26) | *63.4* |
| Ab(mol%) | 71.5(200) | *28.0* | 84.1(34) | *4.0* |
| An(mol%) | 21.2(136) | *64.5* | 11.8(10) | *8.5* |

Table 3. Average compositions of apatites.

| No. Oxides | Matrix [3]** | Chondrule [2] | H6 chondrite# [15] | Lunar apatite ## [11] |
|---|---|---|---|---|
| $SiO_2$ | 0.12(8)*** | 0.30(1) | - | 1.07(80) |
| $Al_2O_3$ | 0.16(16) | 0.31(10) | - | 0.06(14) |
| FeO* | 0.26(25) | 0.47(1) | 0.3 | 0.75(72) |
| MgO | 0.41(47) | 0.06(2) | <0.1 | 0.08(9) |
| MnO | 0.01(1) | 0.02(0) | trace | - |
| $Cr_2O_3$ | - | 0.02(1) | - | - |
| CaO | 57.76(56) | 53.84(131) | 53.0 | 52.66(92) |
| $Na_2O$ | 0.27(14) | 0.18(15) | 0.5 | 0.04(7) |
| $K_2O$ | - | - | - | 0.03(5) |
| $P_2O_5$ | 41.26(14) | 40.69(23) | 41.8 | 39.66(98) |
| Cl | 4.53(36) | 3.94(34) | 4.8 | 0.49(64) |
| F | 1.52(53) | 2.90(24) | - | 3.13(40) |
| Subtotal | 102.30(52) | 102.73(45) | 99.3 | 99.87(114) |
| F,Cl≡O | 1.66(15) | 2.11(18) | - | 1.43(15) |
| Total | 100.64(14) | 100.62(63) | 99.3 | 98.44(117) |
| Cl/(F+Cl) (%) | 61.8(115) | 42.0(1) | 100.0 | 7.5(95) |

* *Total iron oxide as FeO.*
** *Numbers of crystals analyzed are shown in square brackets.*
*** *Numbers in parentheses are standard deviation referring to the last decimal place.*
\# From New Concord (Fuchs,1968).
\#\# Data from "Lunar Mineralogy"(ed. by Frondel,1976), pp.150-151.

Table 4. Average composition of chromite in Yamato-75135, 93 chondrite.

| wt.% of oxides | Matrix [9]* | Chondrule [6] | Nos. of ions in formula | Matrix [9] | Chondrule [6] | In (rim) | Matrix (core) | (core) |
|---|---|---|---|---|---|---|---|---|
| $SiO_2$ | 1.03(196)** | 0.19(3) | Si | 0.3(7) | 0.1(0) | 2.3 | 0.3 | 1.0 |
| $Cr_2O_3$ | 56.19(284) | 58.47(143) | Cr | 12.3(11) | 13.0(5) | 13.3 | 9.6 | 4.4 |
| $TiO_2$ | 2.40(91) | 2.32(105) | Ti | 0.5(2) | 0.5(2) | 0.4 | 0.6 | 0.2 |
| $Al_2O_3$ | 8.15(484) | 6.48(189) | Al | 2.6(14) | 2.1(6) | 0.9 | 5.9 | 13.1 |
| FeO | 28.35(246) | 29.90(85) | Fe | 6.6(8) | 7.0(3) | 6.7 | 4.7 | 2.4 |
| MgO | 2.27(45) | 2.10(11) | Mg | 1.2(8) | 0.9(4) | 3.3 | 0.8 | 0.5 |
| MnO | 0.69(50) | 0.41(13) | Mn | 0.2(1) | 0.1(0) | - | 0.1 | - |
| ZnO | 0.11(4) | 0.11(3) | Zn | 0.02(1) | 0.02(1) | - | - | - |
| CaO | 0.10(11) | 0.02(1) | Ca | 0.03(3) | 0.01(0) | - | 0.1 | 0.1 |
| $P_2O_5$ | 0.88(114) | 0.35(22) | P | 0.20(25) | 0.08(5) | 0.1 | 0.5 | - |
| Total | 100.07(94) | 100.35(47) | | | | | | |

* *Numbers of crystals analyzed are shown in square brackets.*
** *Numbers in parentheses are standard deviation referring to the last decimal place.*

# FIRST DESCRIPTION OF WHITLOCKITE IN YAMATO-75 CHONDRITES

Miura, Y. and Matsumoto, Y.

Department of Mineralogical Sciences and Geology, Faculty of Science, Yamaguchi University, 1677-1, Yoshida, Yamaguchi 753, Japan

The Yamato-75135,93 chondritic meteorite is a typical L4-5 chondrite of one hundred-fifty meteorites ( *i.e.* from Yamato-75108 to -75257 chondrites) reported by Miura and Matsumoto (1981). This chondrite contains phosphate minerals, such as whitlockite, chlorapatite and fluorapatite.

The whitlockite mineral is significant phase in meteorites for the following reasons:

(1) It is a minor in abundance but almost ubiquitous in occurrence in meteorite. In fact, the percentage of the previous EPMA studies on meteoritic whitlockite (*cf.* Fuchs, 1968; Buseck and Holdsworth, 1977) is 63.4 % in chondrite. In chondrite, it is widespread in all subgroup; that is, 3.6 and 10.7 % in L4 and L5 groups, respectively.

(2) It plays a cosmogenic and petrologic importance because it often contains relatively large amounts of some geochemically important trace elements, such as rare earths, uranium and thorium, and of the alkalis, such as Na and K, which are not accommodated within the major minerals. Thus, the composition of whitlockite may give some information about the abundance of certain components in the environment of formation.

Optically, it is very difficult to confirm the presence of the whitlockite, because the whitlockite is commonly plastered onto the surfaces of olivines and/or orthopyroxenes. By using the electron microprobe it is possible to immediately check for the existence of the phase.

Various sizes of whitlockite (up to 750 μm in length) occurred as irregular-shaped grains are found first in the Yamato-75 chondrites. In this study, whitlockite is found only in matrix of the chondrite, coexisted to olivine, orthopyroxene, chromite, metal phases and/or plagioclase.

Compositions of several grains of whitlockite have been determined by using JXA-50A electron microprobe at the Department of Mineralogical Sciences, Yamaguchi University.

Tables 1 and 2 show that slight compositional variation within crystal and grain to grain variation are observed in whitlockites of the Yamato-75135, 93 chondrite. The compositional variation is larger than that of H6 chondrite reported by Adib and Liou (1979), but is smaller than that of Lunar rock.

Large amount of fluorine (F), 1.73 wt.% in average, is obtained in the Yamato-75135,93 chondrite. It is found that the F-content depends on the grain-size of whitlockite. That is, the most F-content, 2.51 wt.%, is found in the smallest grain ( 20x40 μm), whereas the least F-content, 0.95 wt.%, in the largest grain (250x750 μm). The latter grain shows the compositional zoning; that is, 0.51 wt.%F in the rim and 0.95 wt.%F in the core. The relatively smaller grain (160x340 μm) shows also the same compositional zoning that F-content in the core is more than that in the rim. Trace amounts of chlorine and rare earths were obtained in the Yamato-75135,93 chondrite.

EPMA analytical data and textural evidence, therefore, indicate that the whitlockite was initially present as molten droplets, interstitial to the olivine, pyroxene, chromite and/or plagioclase clusters at the stage of matrix-formation probably induced by multiple-impact metamorphic event.

References

(1) Miura and Matsumoto (1982): Mem. Natl Inst. Polar Res., Spec. Issue, **20**,

pp.53-68.
(2) Adib and Liou (1979): Meteoritics, **14**, p.267.
(3) Fucks (1968): Meteoritic Res., Proc. Sympo., pp.683-695.

Table 1. Chemical compositions of whitlockite in Yamato-75135,93 chondrite.

| No. / Oxides | 01 | 50 | 10 | 11 | 12 | 51 | Average [6]** | Lunar rock# [10] | H6 chondrite## [4] |
|---|---|---|---|---|---|---|---|---|---|
| F | 1.00 | 1.61 | 0.95 | 2.20 | 2.51 | 2.13 | *1.73(60)* | *0.01(1)* | - |
| Cl | 0.03 | 0.03 | 0.02 | 0.02 | 0.02 | - | *0.02(1)* | - | - |
| $SiO_2$ | 0.16 | 0.07 | 0.18 | - | - | 0.07 | *0.08(7)* | *0.66(110)* | *0.09(2)* |
| $TiO_2$ | - | - | - | - | 0.01 | - | - | *0.03(4)* | - |
| $Al_2O_3$ | 0.15 | 0.05 | 0.03 | - | 0.07 | 0.05 | *0.06(5)* | *0.04(8)* | - |
| FeO* | 0.42 | 0.69 | 0.35 | 0.18 | 0.46 | 0.69 | *0.47(18)* | *2.49(171)* | *0.45(12)* |
| MgO | 3.65 | 3.53 | 3.54 | 3.68 | 3.82 | 3.64 | *3.64(10)* | *2.60(120)* | *3.35(7)* |
| $Cr_2O_3$ | 0.03 | 0.07 | 0.04 | 0.02 | 0.04 | 0.07 | *0.05(2)* | - | - |
| MnO | - | 0.02 | 0.01 | 0.01 | 0.01 | 0.02 | *0.01(1)* | *0.01(3)* | - |
| $Na_2O$ | 2.87 | 2.90 | 3.04 | 2.99 | 2.87 | 2.91 | *2.93(6)* | *0.38(71)* | *2.78(2)* |
| CaO | 45.39 | 45.67 | 44.14 | 44.10 | 44.42 | 45.69 | *44.90(70)* | *41.02(334)* | *46.7(3)* |
| $K_2O$ | 0.05 | 0.03 | 0.03 | 0.02 | 0.06 | 0.03 | *0.04(1)* | *0.02(3)* | - |
| $P_2O_5$ | 46.84 | 46.78 | 48.84 | 47.82 | 47.39 | 46.81 | *47.41(74)* | *43.42(255)* | *46.5(1)* |
| Subtotal | 100.59 | 101.45 | 101.17 | 101.04 | 101.68 | 102.11 | *101.34(50)* | *99.27* | *99.87* |
| F,Cl≡O | 0.43 | 0.69 | 0.41 | 0.93 | 1.06 | 0.90 | *0.74(25)* | - | - |
| Total | 100.16 | 100.76 | 100.76 | 100.11 | 100.62 | 101.21 | *100.60(38)* | *99.27(103)* | *99.87* |

* *Total iron oxide as FeO.*
** *Numbers of crystals analyzed are shown in square brackets.*
*** *Numbers in parentheses are standard deviation referring to the last decimal place.*
\# *Statistical analyses of data listed in "Lunar Mineralogy"(ed. by J.W.Frondel; pp. 156-157.*
\#\# *D. Adib and J.G. Liou (1979): Meteoritics, vol.14, No.3, p.267.*

Table 2. Chemical formulae of whitlockite.

| Sample | Chemical formula |
|---|---|
| Lunar whitlockite | $Ca_{16}(Y,RE)_2(Mg, Fe)_2(PO_4)_{14}$ |
| Pallastic whitlockite#[37]* | $Ca_{18.4(5)}Mg_{2.0(2)}Fe_{0.3(3)}Na_{0.8(8)}P_{14.0(1)}O_{56}$** |
| Achondrite ## | $Ca_{19}(Mg, Fe)_2(PO_4)_{14}$ |
| Chondrites | $Ca_{18}(Mg, Fe)_2Na_2(PO_4)_{14}$ |
| In this study: | |
| Yamato-75135,93 chondrite [6] | $Ca_{17.1(3)}Mg_{1.9(1)}Fe_{0.1(1)}Na_{2.0(1)}F_{2.0(7)}$ · $P_{14.3(2)}O_{56}$ |
| Core: | $Ca_{17.5}Mg_{1.9}Fe_{0.2}Na_{2.0}F_{1.8}Cl_{0.02}P_{14.1}O_{56}$ |
| Rim: | $Ca_{17.4}Mg_{1.9}Fe_{0.2}Na_{2.0}F_{2.4}Cl_{0.001}P_{14.1}O_{56}$ |

* *Numbers of crystals analyzed are shown in square brackets.*
** *Numbers in parentheses are standard deviation referring to the last decimal place.*
\# *P.R.Busech and E. Holdsworth (1977): Mineral. Magazine, vol.41, pp.91-102.*
\#\# *E. Dowty (1977): Earth and Planetary Science Letters, vol.35, pp.347-351.*

# EXSOLUTION TEXTURE OF PLAGIOCLASE IN METEORITE

Miura, Y.

Department of Mineralogical Sciences and Geology, Faculty of Science, Yamaguchi University, 1677-1, Yoshida, Yamaguchi 753, Japan

The formation process of plagioclase have been discussed from the experimental results of compositional and structural differences between exsolution lamellae individuals in the order of submicron, by using TEM, EPMA, AEM and IMMA (*cf.* Miura, 1976; Miura and Tomisaka, 1978; Miura and Rucklidge, 1979). The conventional method to determine the composition of exsolution texture with near-parallel lamellar boundary has difficulty in application to wormy (or domain-like) exsolution texture and to compositional variation in the order of micrometer.

A new method to estimate formation process of host rock is based on bulk An and Or contents of plagioclase with and without exsolution features. This useful factors of bulk An and Or contents related to lamellar shape parameters were obtained from statistical analyses of five lamellar shape parameters and ten compositional parameters in terrestrial and extraterrestrial plagioclases by Miura *et al.* (1981).

The sample used in this study is L4 chondrite from Holbrook, Arizona, U.S.A. (designated as HM-1 in this study). The sample HM-1 polished finally with 0.25 μm diamond paste was slightly etched by etchant to observe the colored exsolution texture. Compositional data of the sample were obtained on the carbon coated, by using JXA-50A electron microprobe of Yamaguchi University.

Table 1 shows that average bulk An and Or contents of meteorite HM-1, together with three terrestrial and one lunar plagioclases in both areas with and without exsolution features. The following tentative conclusions are obtained in this study.

(1) The compositional difference in bulk An($\ell$) and Or($\ell$) with lamellae and An($n\ell$) and Or($n\ell$) without exsolution feature of chondritic meteorite HM-1 is almost similar to that of lunar plagioclase L2 and metamorphic plagioclase M1, as shown in Tables 1 and 2. Distance-parameter of these values of HM-1, 0.60, is quite similar to that of L2, 0.63, as shown in Table 1.

(2) The formation condition of meteorite HM-1 might have been a rapid cooling rate ( under relatively low temperature). It is found that this is characteristic of impact metamorphism under relatively low temperature, compared with that in lunar plagioclase L2.

A new sensitive indicator of formation process would be applied to discuss chemical environments of extraterrestrial materials. The same investigation in Antarctic meteorite is being planned.

References:

(1) Wegner and Christie (1976): Contrib. Mineral. Petrol.,**43**, pp.196-212.
(2) Miura and Rucklidge (1979): American Mineral., **64**, pp.1272-1279.

Table 1. Compositional data in bulk An and Or contents of lamellae(*l*) and non-lamellae (*nl*) areas in typical terrestrial and extraterrestrial plagioclases.

| Bulk Composition | HM-1 [4]* | L2# [5] | M1## [16] | P1### [39] | I2#### [37] |
|---|---|---|---|---|---|
| An(*l*) | 10.0(8)** | 76.8(59) | 72.3(22) | 50.9(29) | 78.3(40) |
| Or(*l*) | 5.2(6) | 3.6(11) | 0.3(1) | 2.9(5) | 0.5(2) |
| An(*nl*) | 10.4(10) | 78.8(115) | 73.5(26) | 49.1(57) | 59.0(56) |
| Or(*nl*) | 4.6(5) | 4.2(38) | 0.2(1) | 1.6(10) | 1.0(5) |
| Distance Parameter | 0.60 | 0.63 | 0.16 | 1.31 | 1.99 |

* *Numbers of crystals analyzed are shown in square brackets.*
** *Numbers in parentheses are standard deviation referring to the last decimal place.*
\# *Lunar coarse-grained mare basalt 70017,24 (cf. Wegner et al., 1978).*
\## *Metagabbro HDK-7 (Mitra et al., 1981).*
\### *Anorthosite LB-1 (Mitra et al., 1974).*
\#### *Kohyama gabbro KG-1.*

Table 2. Relationships among bulk An-Or contents, their slopes, Compositional difference and Rock type.

| Sample | Bulk An contents | Bulk Or contents | Slope | Comp. Diff. | Rock type |
|---|---|---|---|---|---|
| HM-1 | An(*l*)<An(*nl*) | Or(*l*)>Or(*nl*) | r < 0 | weak | Impact metamorphic |
| L2 | An(*l*)<An(*nl*) | Or(*l*)>Or(*nl*) | r<<0 | sharp | Impact metamorphic+Igneous |
| M1 | An(*l*)<An(*nl*) | Or(*l*)>Or(*nl*) | r < 0 | weak | Metamorphic |
| P1 | An(*l*)>>An(*nl*) | Or(*l*)>>Or(*nl*) | r>>0 | sharp | Plutonic |
| I2 | An(*l*)>An(*nl*) | Or(*l*)<Or(*nl*) | r<<0 | sharp | Igneous |

# High resolution electron microscopic investigation on matrix phyllosilicate of Yamato-74662 ( CM2)

Junji AKAI
Dept.Geology & Mineralogy, Fac. Science, Niigata Univ. Ikarashi Niigata

Carbonaceous chondrites are generally considered to be the most primitive materials from the early solar system . They show various textures in petrographic observations and are subdevided into 5 groups ( McSween,1979 ). However, the interrelation of them has not been established and the origin of them has not been confirmed. One of the remarkable features in CI1 and CM2 is that they have significant amount of phyllosilicates. The characterization of the phyllosilicates may give significant suggestions on the formation of the phyllosilicates and then on the origin of carbonaceous chondrite ( CI1,CM2)*. The principal objectives in the present study are to describe the phyllosilicate and characterize them mineralogically, and to consider the mechanism of phyllosilicate formation and possible origin of CM2.

Specimen of Y-74662 ( CM2) was prepared for HERM observation mainly by ion-thinning. EM used are JEM 100C and H-500.

Optical ( Microscopic) Observation :

The specimen is mostly composed of black matrix. Olivine-,enstatite-, diopside- and other mineral grains are scatterred in the matrix , except chondrules are present in the matrix. Very small amygdale cavities are also present inthe matrix. They are often rimmed by small diopside grains and are filled with relatively pure phyllosilicates. The compositions of phyllosilicates in the matrix and in the amygdales were reported preliminarily ( Akai, 1981).

HREM,ED,AEM Observations :

A) EM observation indicates that small grains of olivine ,enstatite and diopside in $\mu$-scale are contained in the matrix . Some enstatite grains show stacking disorder . Some diopside grains have exsolution lamellae of Ca-poor pyroxene . Other minerals found are carbonate ( $CaCO_3$), Fe/Ni sulfides and so on. Furthermore, amorphous materials or poorly characterized phases which show no distinct ED patterns are also present ( Fig.1).

B ) Phyllosilicates

Phyllosilicate found in the specimen could be devided into the following 5 types by HREM ( & AEM).

i) 7Å platy phyllosilicate. Characteristic feature of this type is that the phyllosilicates have frequent stacking disorder of 1/3 nb, displacements. (Fig.2) Such the feature is similar to that in Murchison (CM2) ( Akai,1980).

ii) 7Å-poorly organized tubular phyllosilicate. This may correspond to chrysotile structure. (Fig . 3)

iii) 17 Å platy phyllosilicate. This is the same as that found in Murchison meteorite (Mackinon and Buseck,1979; Akai,1979,1980). ( Fig.4). AEM experiment confirmed that it is extremely Fe-rich siliacte (Fig.5).

iv) Poorly characterized 7 Å layer structure with interlayering of 5 Å layer (Fig.6).

v) 11 Å platy phyllosiliacte. Frequent parallel intergrowth of this 11 Å phyllosilicate and 7 Å platy phyllosilicate( type i) was observed. This may be the same phyllosilciate found in the Murchison ( Akai,1980). (Fi.7)

Summerizing the results observed,the following points can be noted . 1) Textural relations between olivine and pyroxene ,and phyllosilciate by OM (but not by EM) suggests that the phyllosilicate was derived directly from olivine or pyroxene. 2) Phyllosilicates in the matrix are not composed of unique type in structure, morphology and composition but composed of various types. This suggest that the phyllosilicates were formed in nonequilibrium conditions. 3) Close similarity in structure , morphology and composition of the phyllosilicates between Y-74662 and Murchison strongly suggests the similar genetic relation between Y-74662 and Murchison meteorite.

References :

Akai,J (1979) 23 Anual Meet. Clay Sci. Soc. Japan Abstract , 69.

------ (1980) Mem.Nat. Inst. Polar Res. Sp. Issue 17, 299-310.

------ (1981) 6th Symp. Ant. Meteo. Abstract

*Barber,D.J.(1981) Geochim.Cosmochi.Acta,45,945-970.

Bunch T.E. and Chang S.(1980) Geochim. Cosmochim.Acta ,44,1543-1577.

Mackinnon,D.R. and Buseck,P.R. (1079) Nature,280,219-220.

McSween,H.Y.Jr. (1979) Rev. Geophys.Space Phys. 17,1059-1078.

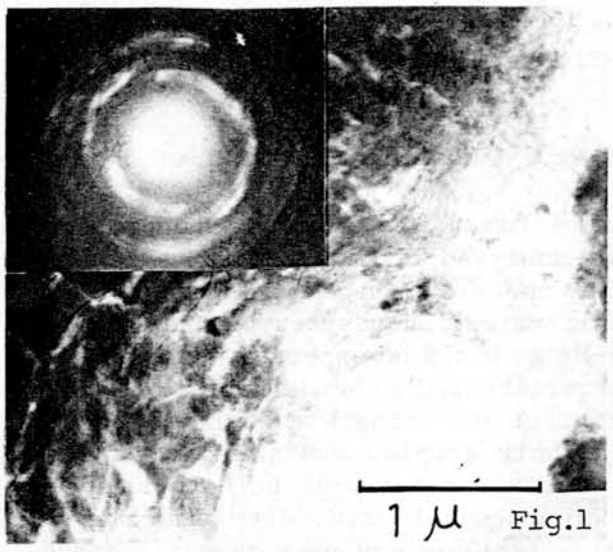


Fig.1

Fig.2

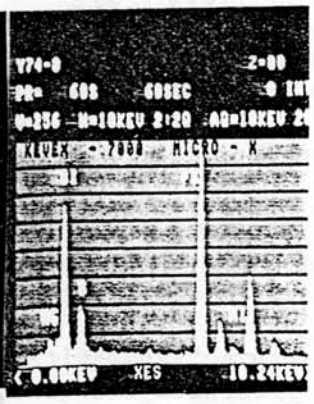

Fig.5

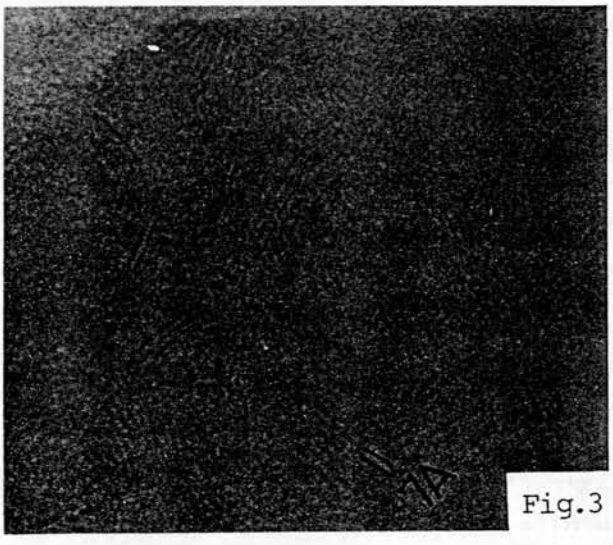


Fig.3

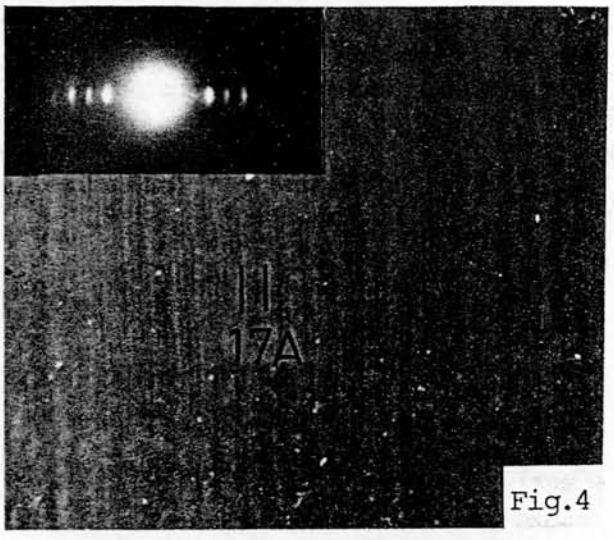


Fig.4

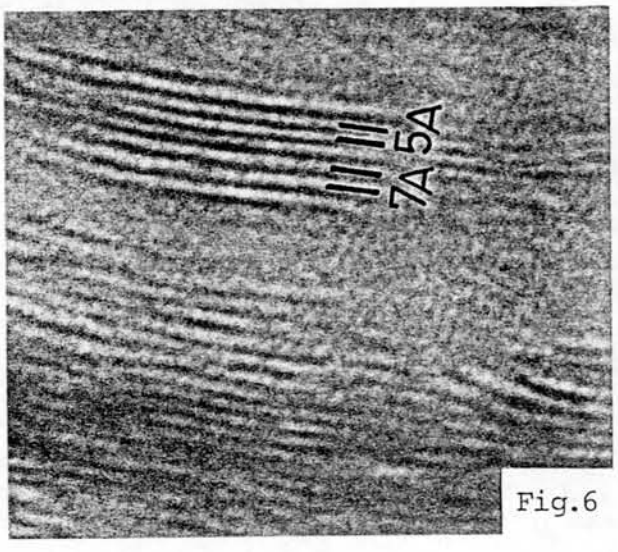


Fig.6

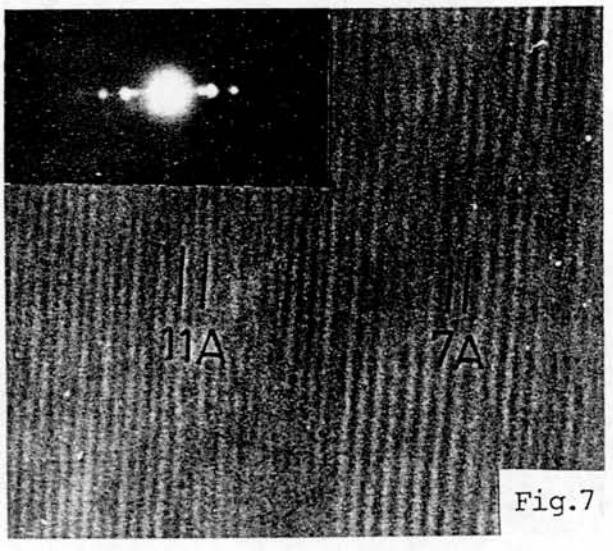


Fig.7

22

ELEMENTAL CORRELATION ANOMALIES IN INDIVIDUAL CHONDRULES FROM CHONDRITES OF DIFFERENT TYPES

Kurt Fredriksson
Dept. of Mineral Sciences, Smithsonian Inst., Washington, DC 20560

A large number of individual chondrules from H, L, and LL, chondrites of "petrographic grades" 3, 4, and 5 have been analyzed for major, and some minor elements using a micro technique employing the electron microprobe. A most striking result is that in so called "equilibrated" chondrites (grades >4) Al and Ca are negatively correlated while Fe-Mg as would be expected are strongly correlated; the reverse is true for "unequilibrated" (by definition) chondrites. Furthermore the average CaO content of chondrules from "equilibrated" chondrites is ∿30% higher than in bulk samples and the discrepancy increases with increasing $SiO_2$ content. These results will be discussed in conjunction with recently published data on unequilibrated "ultrafine primitive matrix" ("Holy Smoke", Rambaldi et al., 1981) in ordinary chondrites and the general controversy regarding "metamorphic equilibration" in chondrites.

REFERENCE

Rambaldi, E. R., Fredriksson, B. J., and Fredriksson, K. (1981). Primitive Ultrafine Matrix in Ordinary Chondrites. Earth and Planet. Sci. Let., 56, 107-126.

# STUDY OF THE RADIAL PYROXENE CHONDRULE IN YAMATO-74191 (L3) BY ANALYTICAL ELECTRON MICROSCOPY

Morimoto, N., Yasuda, M. and Kitamura, M.
Dept. Geology & Mineralogy, Fac. Science, Kyoto University, Sakyo, Kyoto, 606

Fine textures of pyroxenes in a radial pyroxene chondrule of Yamato-74191 (L3-chondrite) have been studied by an analytical transmission electron microscope (Hitachi-700H) to elucidate the cooling processes of this chondrule under the subsolidus conditions.

Yamato-74191 chondrite consists of various types of chondrules, mineral fragments and matrix (Ikeda and Takeda, 1979; Kimura and Yagi, 1980). The radial pyroxene chondrule consists of lath-shape clinopyroxene with polysynthetic twinning and cracks under the optical microscope (Figure 1). In the ion-thinned specimen, the pyroxene laths can be divided into three different regions in composition and texture : central, mantle and rim. The central region (Figure 2) is clinoenstatite with submicroscopic twinning in (100) and open cracks running almost perpendicular to the c-axis. The composition is almost constant with $En_{\sim 86}Fs_{\sim 14}$. The mantle region (Figure 3) with the composition of $En_{\sim 84}Fs_{\sim 12}Wo_{\sim 4}$ shows a characteristic exsolution texture with fine zig-zag lamellae of augite. The rim (Figure 4) has the composition increasing outward from $En_{\sim 80}Fs_{\sim 10}Wo_{\sim 10}$ to $En_{\sim 54}Fs_{\sim 10}Wo_{\sim 36}$ and shows the spinodal decomposition texture where the fine lamellae are in (001). In the groundmass between or the interstitial parts in the laths of clinopyroxene, glass, albite and iron sulfides were observed.

Microscopic and submicroscopic polysynthetic twinnings and cracks are considered to be formed during the inversion of protoenstatite to clinoenstatite as found in the synthetic and terrestrial clinoenstatites. The exsolution texture in the mantle and rim regions indicate the initial crystallization of C-clinopyroxene followed by the decomposition into P-clinopyroxene (pigeonite) and augite. The decomposition was considered to have taken place by nucleation-growth and spinodal decomposition in the mantle and rim regions, respectively. The experimental data on the spinodal decomposition of pyroxene (Nord and McCallister, 1979) indicate that the cooling rate of this chondritic pyroxene is in the order of a few tens °C/day at decomposition temperature (~1000°C). The rather slow rate in comparison with that previously estimated does not contradict with the existence of albite crystals in the groundmass of this chondrule.

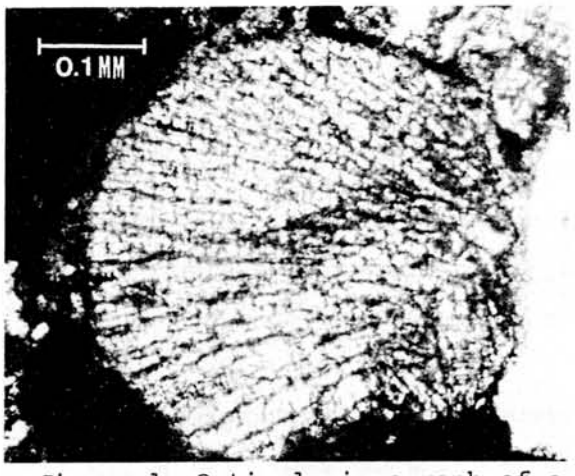


Figure 1. Optical micrograph of a radial pyroxene chondrule in Yamato-74191.

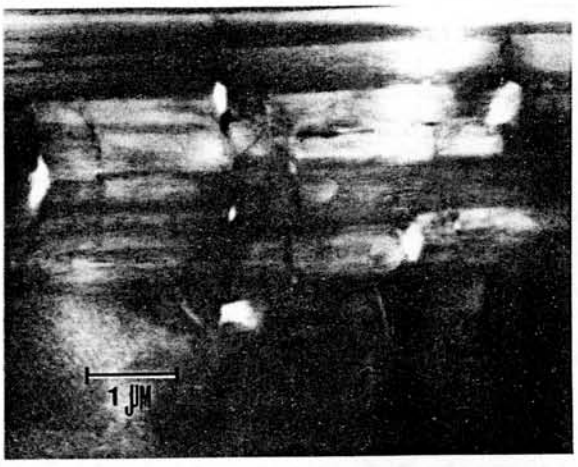


Figure 2. Electron micrograph of the central region of the pyroxene. Submicroscopic twinnings and open cracks are observed.

Figure 3. Electron micrograph of the mantle region. Fine zig-zag exsolution lamellae of augite in pigeonite which shows the anti-phase pattern are characteristic.

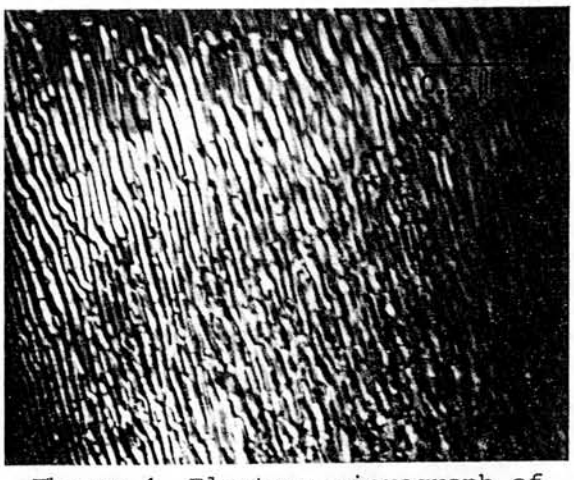

Figure 4. Electron micrograph of rim of the pyroxene. The spinodal decomposition texture with the lamellae of pigeonite (bright) and augite (dark) in (001) is observed.

[References]

Ikeda, Y. and Takeda, H. (1979) : Mem. Natl. Polar Res., Spec. Issue, 12, 38-58

Kimura, M. and Yagi, K. (1980) : Geochimica et Cosmochimica Acta, 44, 589-602.

Nord, G. L., Jr. and McCallister, R. H. (1979) : Geol. Soc. Am., Abstracts with Program, 11, 488.

# CHEMICAL COMPOSITIONS OF THE ALH-765 AND -77302 POLYMICT EUCRITES

Fukuoka, T., and Ishida, H.

Department of Chemistry, Gakushuin University, Mejiro, Toshima-ku, Tokyo 171

The ALH-765 and -77302 meteorites are polymict eucrites which were collected in the Allan Hills region by U.S.-Japan team during the 1976-77 and the 1977-78 Antarctic field seasons, respectively. A consortium study of these meteorites is now in progress. The study includes chemical, petrological, mineralogical, age determination, and stable isotope studies.

Previous report of the analytical results for the ALH-77302 meteorite (Fukuoka and Nakamura, 1982) showed that the chondritic normarized REE (rare earth elements) patterns of the matrices and igneous clasts were similar to those of known non-cumulative eucrites. The La abundances in the clasts ranged from the lowest La abundance in the known non-cumulative eucrites to the highest one. Nakamura and Masuda (1980) found the large Ce anomalies in the ALH-765 meteorite samples.

A block sample of the ALH-765 meteorite and sliced samples (about 6-7 mm thick) of the ALH-77302 meteorite were provided from National Institute of Polar Research. After mapping of the sample surfaces, igneous clasts, phenocrysts, and matrices were extracted from the sample specimens. The abundances of 16 major, minor, and trace elements (Fe, Na, Cr, Co, Sr, Ba, Sc, La, Nd, Sm, Eu, Tb, Yb, Lu, Hf, and Ta) in 7 clasts of the ALH-765 meteorite and in 6 clasts of the ALH-77302 meteorite have been determined by instrumental neutron activation analysis (INAA). We report the results as a part of the consortium study. The samples in synthesized quartz tubes were activated with thermal neutron in the JRR-2 or -4 nuclear reactor of the Japan Atomic Energy Research Institute. After 4-7 and more than 30 days cooling, the $\gamma$-ray spectroscopies of the activated samples were carried out on a $\gamma$-ray spectrometer with a Ge (Li) detector, respectively.

The results are similar to those of the previous report (Fukuoka and Nakamura, 1982). The Ce abundances in the igneous clasts could not be determined, because of the interference of the photo peak of $^{59}$Fe $\gamma$-ray to the photo peak of $^{141}$Ce $\gamma$-ray for Ce determination.

References

Fukuoka, T. and Nakamura, N. (1982) Mem. Natl. Inst. Polar Res., Spec. Issue (in press).

Nakamura, N. and Masuda, A. (1980) Mem. Natl. Inst. Polar Res., Spec. Issue 17, 159-167.

# 25

## MAJOR ELEMENT CHEMISTRY OF ANTARCTIC METEORITES I

Haramura, H. and Kushiro, I.
Geological Institute, University of Tokyo, Tokyo 113, Japan

Fifty four Yamato and Allan Hills meteorites including 40 chondrites (14 H, 21 L and LL, and 5 C) and 14 achondrites have been analyzed by the conventional wet chemical analysis method. Each specimen (1-10gm) was crushed and finely ground and separated into non-magnetic and magnetic fractions. The former fraction was analyzed by the established method for rock analysis. The latter fraction in which metallic phase is concentrated was analyzed for both metallic components and silicate components. The Antarctic meteorites are more or less oxidized. The effect of oxidation was, therefore, examined first. The effect of oxidation has extended into the center in relatively small specimens, but is limited in the outer portion of relatively large specimens. Two H chondrites were analyzed for both the outer oxidized portion and the relatively fresh inner portion. The results for ALH 768 are as follows. The fresh portion contains 16.75 wt.% Fe+Ni+Co and 13.04 % FeO with no $Fe_2O_3$, whereas the outer portion contains 8.08 % Fe+Ni+Co, 9.96 % FeO and 10.17 % $Fe_2O_3$ with 1.9 % $H_2O$ (+). Some other oxidized H chondrites contain large amounts of FeO with no $Fe_2O_3$. By the former type oxidation, even $Fe^{2+}$ in silicates as well as metallic iron was oxidized to $Fe^{3+}$ The normative olivine becomes magnesian in the former oxidation, while it becomes iron-rich in the latter oxidation. Next, heterogeneity of the specimens or sampling problem was examined. Three chondrites were analyzed in two different parts of the specimens. Except for the difference in the oxidation state, most of the elements show relatively small deviations (within the uncertainty of analysis); however, Fe, $Al_2O_3$ and $P_2O_5$ show relatively large variations.

The alkali (especially Na) contents in the H chondrites are systematically lower than those in the L and LL chondrites; however, when the silicate fractions (recalculated to 100%) are compared, there is no systematic difference. The $K_2O/Na_2O$ ratios of the chondrites as well as those of achondrites range from 0.06 to 0.15, except one chondrite (Y-74442). This range is the same as that of plagioclase in the equilibrated chondrites. The CaO and $Na_2O$ contents of the silicate fractions of most chondrites excluding C chondrites fall in relatively narrow ranges (CaO, 2.0±0.3 and $Na_2O$, 1.0±0.2 wt.%). The $Al_2O_3$ content, however, varies from 2.0 to 4.5 wt.%, which is beyond the uncertainty of analysis and variations due to sampling problem. The composition of normative plagioclase, therefore, varies considerably (An5 - An45) in contrast to the compositions of modal plagioclase (An10 - An13). The discrepancy in composition between normative and modal plagioclase suggests that some aluminous phase may be present in many of the relatively $Al_2O_3$-rich chondrites. The fact that CaO and $Na_2O$ in the silicate fractions are nearly constant, while $Al_2O_3$ varies considerably may have a significant meaning in the genesis of chondrites.

# SB Systematics on Meteorites

Naoki Onuma
Department of Earth Sciences, Ibaraki University,
Bunkyo, Mito, Ibaraki, JAPAN (310)

In the last Sixth Symposium on Antarctic Meteorites, we have proposed a new geochemical diagram, Sr/Ca-Ba/Ca(SB) diagram which can visualize origin and evolution of magmas in terms of partial melting process in source region and crystal fractionation process in magma reservior, and given a preliminary report on origin of several Antarctic eucrites (Onuma and Hirano,1981). In this presentation, we discuss about magma genesis occurred on a small eucrite parent body in the protosolar system, based on the SB diagram in detail.

There have been two different models on origin of the eucrites: (1) the eucrites were derived from a magnesian primary magma by extensive crystal fractionation process (Mason,1962; Schnetzler and Philpotts,1969; McCarthy et al., 1973; Shimizu and Allegre,1975; Takeda et al.,1976), and (2) the eucrites were produced by partial melting of a source material(Ol, Pxs, Pl, Sp and metal)with different degrees (Stolper,1975, 1977; Consolmagno and Drake,1977). The SB diagram shown in the figure supports the classical model, rather than the modern model, suggesting that a primary magma had generated on a small planetary body by a large scale partial melting( 60%) of a chondritic source material and various eucritic magmas had subsequently evolved from the primary magma through orthopyroxene-plagioclase-clino--pyroxene fractional crystallization.

The conclusions obtained in this work are summarized as follows:
(1) The source material of the planetary body shows chondritic composition in terms of Sr/Ca and Ba/Ca ratios.
(2) A primary magma had once generated on the planetary body by a large scale partial melting of the source material( 60%), leaving Ca, Sr and Ba poor phases behind as residual solids ( 40% as metal, Ol and Opx).
(3) Subsequently, a large volume of orthopyroxene( 25%) had crystallized from the primary magma.
(4) The mutant primary magma( 35%) had evolved and produced various eucritic magmas through crystal fractionation process, leaving plagioclase-clinopyroxene behind as cumulus solids.
(5) Thus, a small planetary body with layered structure had formed in the protosolar system. Iron meteorites, pallasites, and diogenites(in part) had situated in core, diogenites(in part) in intermediate layer, cumulus eucrites in lower crust, and normal eucrites in upper crust, respectively.

This model is similar to the classical model proposed by Mason(1967).

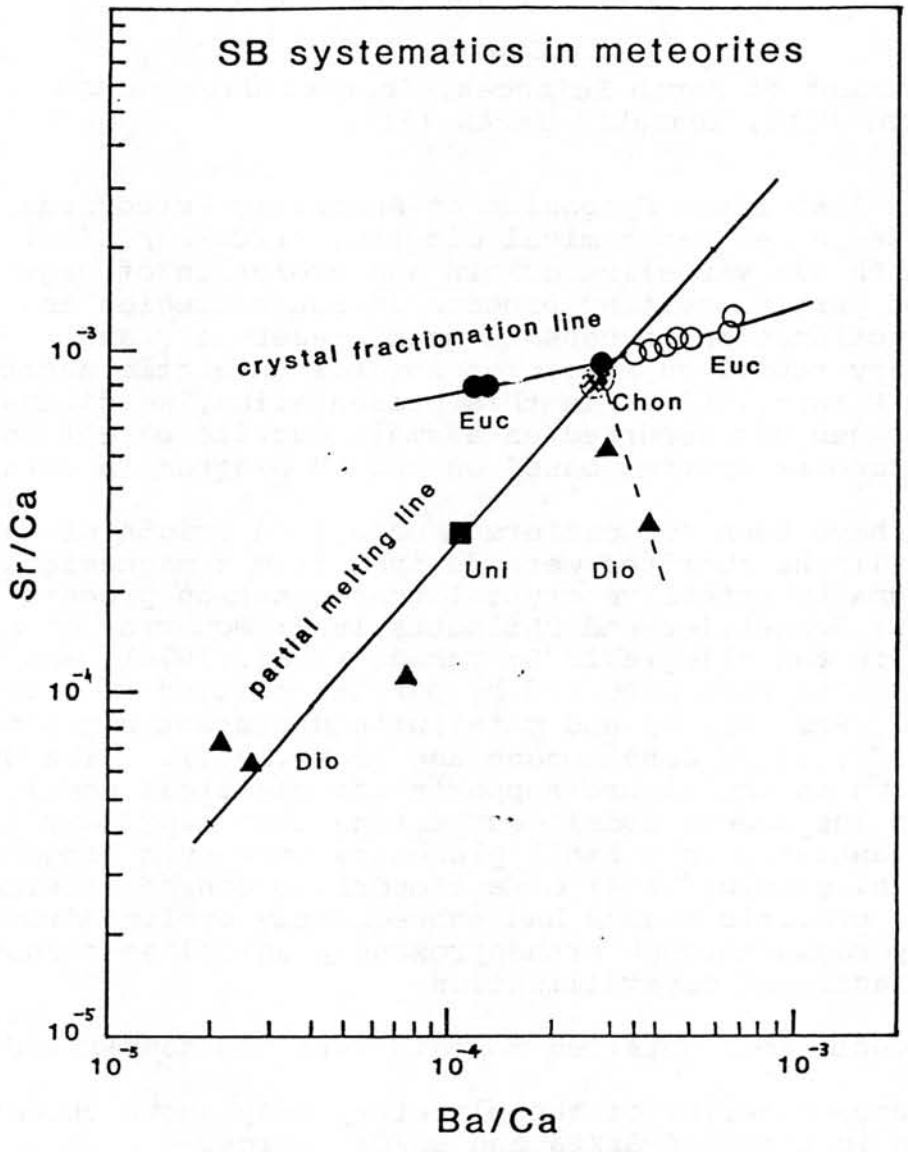


SB diagram for Meteorites

: Chondrites(E,H,L,LL,C)
: Normal Eucrites(from Haraiya to Stannern)
: Cumulus Eucrites(MC,SDM,ADR)
: Diogenites
: Unique(ALH77005)

The partial melting line is a line with slope of 45° through chondrites. The eucritic achondrites make a line with gentle slope which is established by plagioclase/ clinopyroxene fractional crystallization in magma reservior. The SB systematics represents a crystal fractionation line. The SB index defined by the intersection of the two lines corresponds to "degree" of partial melting on the source material, which is estimated to be appr. 60%.

# REE ABUNDANCES IN THE CHASSIGNY METEORITE

Noboru NAKAMURA, Hideto KOMI, Yoshiyuki NISHIKAWA and Paul PELLAS* (Dept. of Earth Sci., Faculty of Sci., Kobe University, Nada-ku, Kobe 657, Japan; * Lab. de Mineralogie, du Museum, 61 rue Buffon 75005, Paris, France

Chassigny is an olivine-rich achondrite, which has unique chemical and mineralogical features (Mason et al., 1976; Floran et al., 1978). In order to further clarify the chemical characteristics of the meteorite, we have undertaken precise determination of REE and other trace element abundances in the mineral phases of the meteorite, and report here the preliminary analytical results. Because of limited sample size of minor mineral components (10-500 micrograms), the "devised" technique of isotope dilution (Nakamura and Masuda,1980) was applyed to REE analyses for the mineral grains obtained by hand-picking. Concentrations of some major elements (Ca, Mg) were also measured by the isotope dilution method for the same samples.

The results are shown in Fig. 1. Blank corrections are not made at present stage. Our results for the whole rock is quite consistent with those obtained by Mason et al. (1976). Systematic difference between our results and theirs (Fig. 1) may be due to sample heterogenuity of this meteorite. The specimen Bx-1 and Bx-2 (Clinopyroxene) show marked REE fractionation from light to heavy REE with small Eu anomalies. The small, but significant negative Eu anomaly of the pyroxene suggests that the oxygen fugacity in Chassigny parent liquid may be much higher than that of eucritic magma but slightly lower than that of Nakhla. The olivine phase has a V-shape REE pattern but the pattern is much flatter than that of typical meteoritic olivine. This may be caused by inclusion of trapped liquid or impure mineral separation. It was found that contamination correction assuming a few per cents mixing of pyroxene yield the typical V-shape REE pattern for the "pure" olivine phase. G-1 (anorthic glass or feldspar) show large Eu (, Sr and Ba) anomaly(or anomalies), which is typical for feldspar. Because of extremely small sample size (13 micrograms), light REE in G-1 is considered to be contaminated from reagent impurities usded for chemical decomposition.

Using the solid/liquid partition coefficients, we have estimated REE patterns of the liquid in equilibrium with pyroxene, olivine and feldspar. The estimated REE pattern for the parent liquid (La 6-20, Eu 3-5, Lu 2-4 times chondrite)(Fig.2) is generally similar to that for Nakhla (Nakamura et al., 1982), except for Er Yb and Lu for olivine. Deviation of the heavier REE for olivine is significant but was not well-understood.

Acknowledgement: We are grateful to Prof. A. Masuda, University of Tokyo, who has enabled us to continue trace element analyses at Kobe University.

References:

Mason, B., Nelen, J.A., Muir, P. and Taylor, S.R. (1976) Meteoritics, 11, 21-28.

Floran, R.J., Prinz, M., Hlava, P.F., Keil, K., Nehru, C.E. and Hinthorne, C.E. (1978) Geochim. Cosmochim. Acta, 42, 1213-1229.

Nakamura, N. and Masuda, A. (1980) Abstract of the 1980-anual meeting of the Geochemical Society of Japan (in Japanese) 321-322.

Nakamura, N., Tatsumoto, M., Unruh, D.M. and Hutchison, R. (1982) Geochim. Cosmochim. Acta (in press).

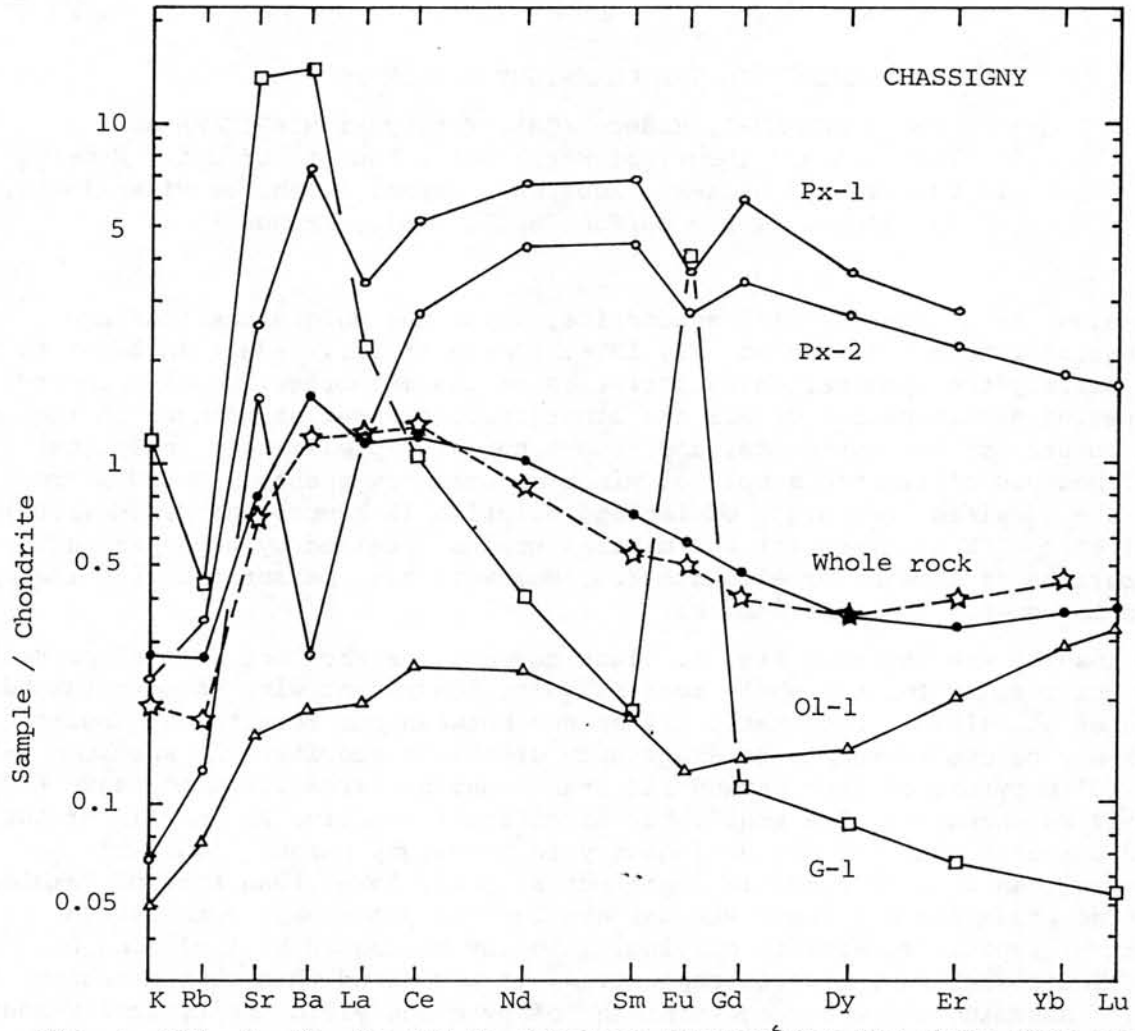


Fig. 1. REE, K, Rb, Sr and Ba abundace pattern[5] for the whole rock and mineral separate of the Chassigny meteorite. One of the whole rock patterns (dotted line) is from Mason et al. (1976)

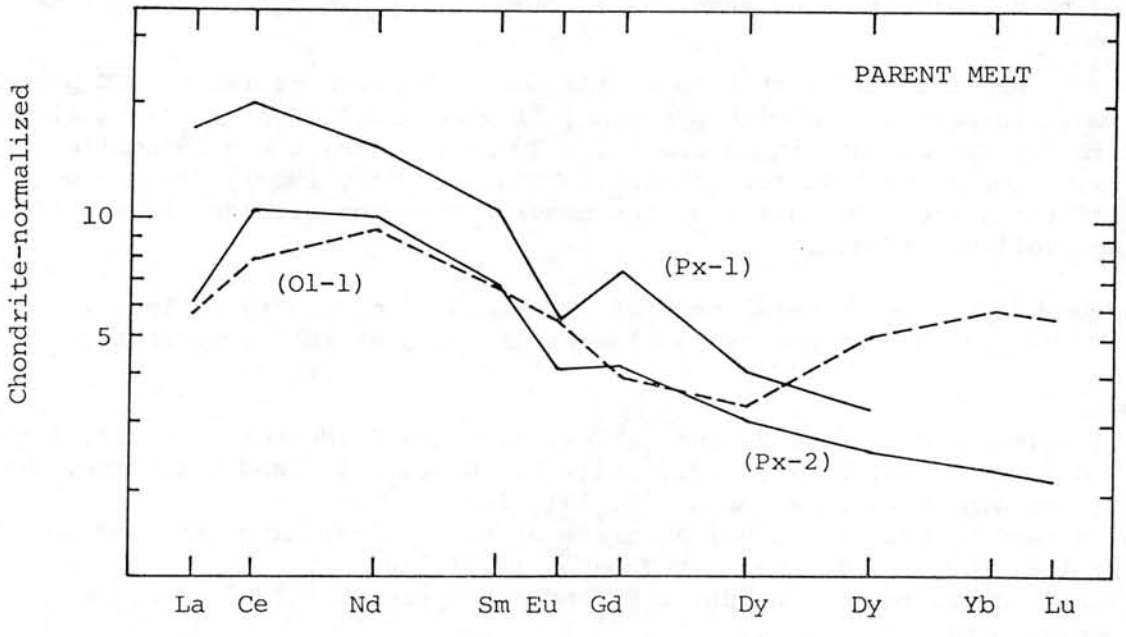


Fig. 2. Estimated REE abundance Pattern of Chassigny parent liquid.

A howardite model based on rare-earth and major elements in the Kapoeta meteorite and its mineral separates

Akimasa MASUDA, Yumi MAKOSHI*, Hiroshi SHIMIZU and Kazuya TAKAHASHI
Department of Chemistry, The Univ. of Tokyo, *Dept. of Earth Sci., Kobe Univ.

The whole-rock sample and mineral separates of the Kapoeta meteorite (howardite) were analysed for rare-earth and major elements. In addition, Y-7308 was investigated. The separation into mineral fractions was carried out by Clerici solution. The fraction M with intermediate density ($3.14 < d < 3.45$) is identical in FeO and MgO with Y-74010B diogenite (see Table 1) but quite different in REE concentrations from it (Fig. 1). Generally, it is seen that the fraction M under consideration is intermediate in major elements between Y-74010B and Y-75032. Takeda et al. (1979) observe that Y-75032 is an intermediate member between diogenite and cumulate eucrite. It is of much significance that the REE concentrations of the M fraction of Kapoeta is somewhat lower than but considerably close to those of Y-75032. It could be considered that a material

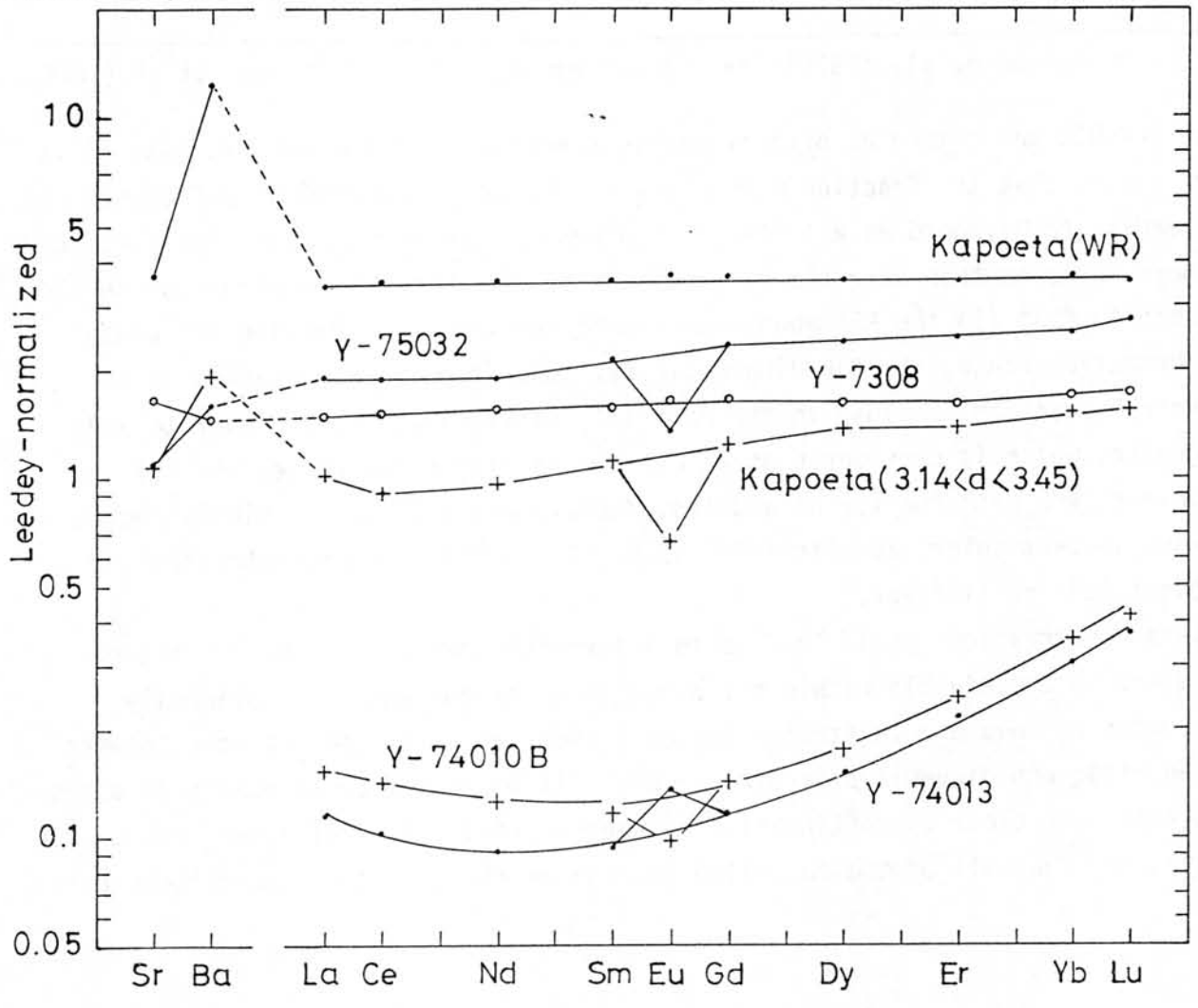

Table 1. Major element composition.

| | Kapoeta whole rock | Kapoeta [3.14<d<3.45] | Y-74010B* | Y-74013** | Y-75032** | Y-7308*** |
|---|---|---|---|---|---|---|
| $Al_2O_3$ | 7.5% | 1.7% | 0.54% | 0.89% | 2.28% | 3.64% |
| FeO | 18.5 | 15.2 | 15.4 | 16.35 | 18.85 | 16.00 |
| MgO | 14.5 | 23.2 | 23.7 | 26.04 | 20.99 | 22.02 |
| CaO | 5.9 | 2.0 | 1.06 | 1.10 | 3.31 | 3.50 |
| $Na_2O$ | 0.36 | 0.093 | 0.022 | 0.04 | 0.12 | 0.16 |
| $K_2O$ | 0.021 | 0.006 | —— | 0.02 | 0.04 | 0.06 |

* Masuda et al. (1979); ** Takeda et al. (1978); *** Yagi et al.(1978).

like Y-75032 was common as orthopyroxenic constituent of howardites. Also it is significant that the fraction M is close to Y-7308 (howardite) in REE abundances. [According to Miyamoto et al. (1978), the proportion of diogenite-like pyroxenes is more abundant than eucritic pyroxenes in Yamato-7308.] Keen attention should be paid to that (1) the REE abundances in diogenites vary covering the wide concentration range, (2) the diogenitic pyroxene fraction represented by the Kapoeta M fraction is close to the material intermediate between eucrite and diogenite, which is considered as an extreme of diogenitic range, and (3) the whole-rock REE patterns for howardites, Kapoeta and Y-7308, are highly rectilinear, in particular, for light REE span. [The REE pattern for eucrites is somewhat less rectilinear.]

These observations could lead us to inferences that (1) gradually layered structure is conceivable within the diogenitic stratum and (2) a primarily howarditic or *howarditoid* stratum can be present as an independent one between the eucritic and diogenitic strata. However, it would not be necessary to assume that there are clear discontinuities between eucritic, howarditic and diogenitic strata, and that all of the so-called howardites are from the"howarditic stratum."

Addendum:

Eucritic clast Y-790266,59 has been found to have a marked posive Ce anomaly (see below); the ratio of the observed value to the "normal" one is 2.2, the highest ever observed for eucrite. Our data on Juvinas whole-rock sample is also plotted.

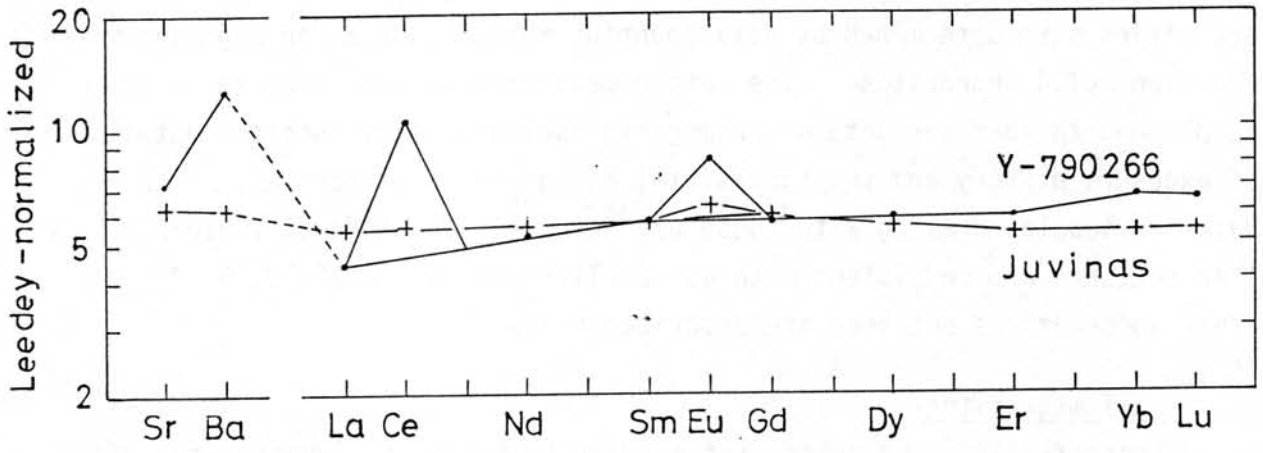

29－1

# COSMOGENIC RADIONUCLIDES IN ANTARCTIC METEORITES

K. Nishiizumi, J.R. Arnold, M. Imamura°, T. Inoue° and M. Honda
Dept. of Chem., B-017, Univ. of Calif., San Diego, La Jolla, CA 92093
° Inst. for Nuclear Study, Univ. of Tokyo, Tokyo 188

As part of program of $^{53}Mn$ survey of antarctic meteorites[1-6], we have measured cosmic ray produced $^{53}Mn(t_{1/2}=3.7x10^6y)$ activities in 23 meteorites including 12 chondrites, 10 irons and a pallasite using neutron activation analysis (Table 1.). Furthermore $^{10}Be(t_{1/2}=1.5x10^6y)$ activities were determined by beta counting method in the non-magnetic fractions of 4 chondrites. The latter measurements were made to complement the earlier data on cosmogenic nuclides to discuss the details of exposure history and the terrestrial age of these meteorites. $^{10}Be$ data are tabulated along with those of $^{36}Cl$, $^{26}Al$ and $^{53}Mn$ in Table 2. $^{10}Be$ contents are consistent with our earlier conclusions[2, 3, 5, 7]. Other informations obtained are described below.

Small meteorites

Except Y-74156, the chondrites studied here are small meteorites with fusion crusts, among which, Y-74065(paired with Y-74066),-74104, 74447, 74652 and 75270 are estimated to be complete individual specimens or nearly complete ones[8]. Since very small meteorites are hard to find in the other region of the world, small meteorites found in Antarctica are the very valuable collections. Some of them may be the survived residuals of really small objects in space, then they could provide new informations on cosmic ray effects in smaller meteoritic objects in space.

The $^{53}Mn$ contents found in the above samples are mostly consistent with rather small preatmospheric size. They could be simply as a result of undersaturation of $^{53}Mn$ radioactivity or near-surface sample of larger meteorite. We have to wait the analyses of rare gases and other radioactivities.

A small octahedrite, Y-75031, is described as a complete individual [8]. Based on the high $^{53}Mn$ content found in this work, Y-75031 is a residue or a fragment from a $\gtrsim$200kg sized body.

Table 1. Preliminary $^{53}Mn$ data

| | | Type(Class) | Rec. mass | $^{53}Mn$(dpm/kg Fe) |
|---|---|---|---|---|
| DRP | -78008 | Iron | 59.4 kg | 3.8 |
| | -78009 | Iron | 138.1 | 77 |
| Yamato- | 74044 | Pallasite | 0,0518 | 320 |
| | 74060 | H | 0.0171 | 294 |
| | 74065 | L3 | 0.0121 | 250 |
| | 74072 | H | 0.0290 | 329 |
| | 74074 | H | 0.0542 | 387 |
| | 74104 | H | 0.0218 | 365 |
| | 74138 | H | 0.0229 | 377 |
| | 74234 | (H) | 0.0259 | 205 |
| | 74372 | L | 0.0846 | 349 |
| | 74447 | H | 0.0143 | 220 |
| | 74652 | L | 0.0079 | 298 |
| | 75031 | Octahedrite | 0.0602 | 522 |
| | 75270 | L or LL | 0.0269 | 370 |
| | 74156 | H | 0.715 | 257±12 |
| ALH | -77250 | Og | 10.555 | 572 |
| | 77255 | Iron | 0.765 | 408 |
| | 77263 | Og | 1.669 | 589 |
| | 77283 | Og | 10.51 | 459 |
| | 77289 | Og | 2.186 | 561 |
| | 77290 | Og | 3.784 | 527 |
| | 78252 | IIIA | 2.789 | 405 |

Table 2. $^{10}Be$ data in some antarctic meteorites

| | Class | Recovered mass(kg) | dpm/kg# $^{36}Cl$ | $^{26}Al$ | $^{10}Be$## | $^{53}Mn$ | Ref. |
|---|---|---|---|---|---|---|---|
| ALH-768 | H6 | 1.15 | 9.4±1.0 | 11.4±0.4 | 3.9±0.5 | 22±3 | [2,7,9] |
| 77003 | C3 | 0.78 | 18.4±1.2 | 45 ±5 | 19 ±2 | 317±13 | [5,9] |
| 77214 | L3 | 2.10 | 17.0±0.8 | 55 ±6 | 15 ±1 | 151±6 | [5,9] |
| 77272 | L6 | 0.67 | 6.6±0.3 | 35 ±4 | 18 ±2 | 213±11 | [5,9] |

# $^{36}Cl$: dpm/kg(Fe+Co+Ni+6Ca), $^{53}Mn$: dpm/kg(Fe+1/3Ni) ## this work.

Irons

DRP-78008 has a very low $^{53}Mn$ content of several dpm/kg Fe. Other fragment, DRP 78009, has an order of magnitude higher $^{53}Mn$ content. These are interpretted as the result of shielding effect of cosmic rays due to a large preatmospheric size of the meteorite. These two are estimated to be broken fragments from the same meteorite of which size in space were as large as ~100 tons or more.

We will try a more detailed discussion on exposure and terrestrial histories of antarctic meteorites in the symposium.

[References]

[1] Nishiizumi, K. ,et al.(1978) Mem. Natl. Inst. Polar Res. Spec. Issue, 8, 209-219.
[2] Nishiizumi, K., et al.(1979) ibid, 12, 161-177.
[3] Imamura, M. et al. (1979) ibid, 15, 227-242.
[4] Nishiizumi, K., et al.(1980) ibid, 17, 202-209.
[5] Nishiizumi, K., et al.(1981)Earth Planet. Sci. Lett.,52, 31-38.
[6] Nishiizumi, K., et al.(1981) Abstract of 6th Symp. Antarctic Meteorites ,Natl. Inst. Polar Res., Tokyo, p.49-51.
[7] Nishiizumi, K., et al.(1979) Earth Planet. Sci. Lett.45, 285-292.
[8] Yanai, K.(1979) (compiled) Catalog of Yamato Meteorites.
[9] Evans, J. C., et al.(1979) Proc. Lunar Planet. Sci. Conf. 10, 1061-1072.

# Isotopic measurement of rare gases in antarctic meteorites

N. Takaoka and K. Saito, Department of Earth Sciences
Faculty of Science, Yamagata University, Yamagata 990.

Several important results have been reported on the basis of rare gas data for the antarctic meteorites. An ordinary chondrite Yamato-74035(L6) has the longest cosmic-ray exposure age among both antarctic and non-antarctic chondrites known to date.[1] An unequilibrated chondrite, Yamato-75028(H3 or L3(?)) contains solar-type rare gases. This meteorite is a so-called gas-rich meteorite, which was first found in the antarctic meteorite collection.[1] The Yamato-74191, unequilibrated hypersthen chondrite has been reported to contain appreciable amounts of $^{80}Kr$, $^{82}Kr$ and $^{128}Xe$ which had been produced by epithermal neutron capture on bromine and iodine, and the preatmospheric radius of this meteorite has been estimated to be R=32 cm with the neutron slowing-down density.[2] Rare gas data also give a clue for identifying fragments of a single fall. Two groups of paired meteorites have been reported.[1]

In continuing the rare gas study of antarctic meteorites, the isotopic compositions of five stable rare gases were determined in detail for the Yamato-74035 of the longest cosmic-ray exposure age.For the gas-rich chondrite Yamato-75028 and a carbonaceous chondrite Allan Hills 77003, the isotopic ratio of Xe is given in Table 1. The cosmic-ray exposure and K-Ar ages will be given for several tiny chondrites.

Table 1.

| meteorite | $^{124}Xe$ | $^{126}Xe$ | $^{128}Xe$ | $^{129}Xe$ | $^{130}Xe$ | $^{131}Xe$ | $^{132}Xe$ | $^{134}Xe$ | $^{136}Xe$ |
|---|---|---|---|---|---|---|---|---|---|
| Y-75028 | 0.481 ±.054 | 0.428 ±.051 | 8.40 ±.30 | 163.8 ±3.9 | 16.50 ±.47 | 82.8 ±2.7 | =100 | 37.8 ±.8 | 30.9 ±1.3 |
| A-77003 | 0.457 ±.005 | 0.408 ±.004 | 8.14 ±.03 | 111.6 ±.2 | 16.18 ±.08 | 81.6 ±.4 | =100 | 37.82 ±.14 | 31.30 ±.38 |
| AVCC-Xe | 0.459 | 0.410 | 8.20 | --- | 16.08 | 81.7 | =100 | 38.2 | 32.1 |

References: (1) N.Takaoka et al., Mem.Nat.Inst.Polar Res. to be published.
(2) N.Takaoka and K.Nagao, Z.Naturforsch. 35a, 29-36 (1980).

31－1

# Chemical Composition and Fission Track Age of of Some Muong Nong-Type Tektites

Kenzo YAGI*, Yoshimasu KURODA**, and Satoshi KOSHIMIZU***
*Hokusei Gakuen College,**Shinshu Univ. ***Hokkaido Univ.

Generally indochinites have characteristic forms, such as pear, dumbbell, tear drop, flask, etc, and have also sculptured surface, whereas Muong Nong-type tektites are commonly irregular in shape, with ragged surface. They are larger than the indochinites, and weigh sometimes more than 1 kg. We have studied some Muong Nong-type tektites from Laos (A,B,C,D,E,F), and also one indochinite fromViet Num with tear drop shape for comparison(G). Most of them are homogeneous under the microscope, but sample B has some fluidal structure, composed of fine pale brown streaks embedded within nearly colorless matrix, with slightly different index.

Major elements of these tektites were determined by EPMA. The composition is usually homogeneous within one sample, except in B, where it was noticed that the two parts mentioned above have slightly different composition as follows:

Pale brown streaks: $SiO_2$ 81.4, $Al_2O_3$ 9.4%
Colorless matrix: $SiO_2$ 79.4, $Al_2O_3$ 10.8%.

The reason for this difference is not clear. In Tables 1 and 2 overall average composition of B is given. It is remarkable that there is a wide range in chemical composition of Muong Nong-type tektites, ranging from 71 to 82% $SiO_2$.

The chemical composition of these tektites is compared with that of terrestrial and lunar granites, and a mixture of shale and quartz given by Taylor (1962). It is worthy of note that tektites are similar to the last in composition.

In order to determine the water content and $\delta D$, fine powder of the tektite was melted in a high frequency furnace in vacuum, and $H_2O$ was converted into $H_2$ by metallic uranium. $H_2O$ content was determined from the $H_2$ and $\delta D$ was measured by a mass spectrometer. The results are given in Table 3, and are shown in Fig.1, where $\delta D$ values are plotted against the$SiO_2$ contents. As seen from Fig.1, no definite relation is observed between the two. So far nothing can be mentioned from these results whether the water is terrestrial or lunar in origin.

For fission track age dating thin slice of tektite was first etched, and the spontaneous fission tracks were measured. Then the same slice was exposed to thermal neutron together with a standard glass of known U content, and the induced tracks were counted. U content of tektite can be obtained also. Thus, when spontaneous track density $\rho_s$ and induced track density $\rho_i$ are obtained, the fission track age A can be calculated from the following equation:

$$A = 6.01 \times 10^{-8} \frac{\rho_s}{\rho_i} \Phi$$

, where $\Phi$ represents thermal neutron per unit.

Table 1. Chemical Composition of Tektite

| | A | B | C | D | E | F | G |
|---|---|---|---|---|---|---|---|
| $SiO_2$ | 71.66 | 80.40 | 72.00 | 71.65 | 74.21 | 82.13 | 74.40 |
| $TiO_2$ | 0.85 | 0.71 | 0.76 | 0.72 | 0.66 | 0.51 | 0.73 |
| $Al_2O_3$ | 14.00 | 10.09 | 13.22 | 13.75 | 12.45 | 9.09 | 13.41 |
| FeO* | 4.55 | 3.48 | 4.45 | 4.51 | 4.30 | 3.08 | 4.38 |
| MnO | 0.02 | 0.07 | 0.06 | 0.06 | 0.01 | 0.03 | 0.05 |
| MgO | 2.50 | 1.66 | 2.33 | 2.32 | 2.28 | 1.23 | 2.15 |
| CaO | 2.72 | 1.00 | 2.87 | 2.70 | 2.13 | 0.99 | 1.99 |
| $Na_2O$ | 1.17 | 0.59 | 1.51 | 1.49 | 1.21 | 0.89 | 1.15 |
| $K_2O$ | 2.64 | 2.24 | 2.56 | 2.69 | 2.60 | 2.30 | 2.43 |
| Total | 100.11 | 100.17 | 99.76 | 99.89 | 99.85 | 100.25 | 100.69 |

Table 2. Comparison of Chemical Composition of Tektite and Various Rocks

| | Tektite | | | Terrest. Granite | Lunar Granite | Shale + Quartz |
|---|---|---|---|---|---|---|
| | A | B | F | | | |
| $SiO_2$ | 71.66 | 80.40 | 82.13 | 74.22 | 76.2 | 73.24 |
| $TiO_2$ | 0.85 | 0.71 | 0.51 | 0.20 | 0.5 | 0.54 |
| $Al_2O_3$ | 14.00 | 10.09 | 9.09 | 13.61 | 11.6 | 12.79 |
| FeO* | 4.55 | 3.48 | 3.08 | 1.83 | 2.6 | 5.04 |
| MnO | 0.02 | 0.07 | 0.03 | 0.05 | 0.0 | 0.08 |
| MgO | 2.50 | 1.66 | 1.23 | 0.27 | 0.3 | 2.62 |
| CaO | 2.72 | 1.00 | 0.99 | 0.71 | 1.8 | 2.57 |
| $Na_2O$ | 1.17 | 0.59 | 0.89 | 3.48 | 0.4 | 1.08 |
| $K_2O$ | 2.64 | 2.24 | 2.30 | 5.06 | 6.6 | 2.69 |
| $P_2O_5$ | 0.00 | 0.00 | 0.00 | 0.14 | 0.0 | 0.12 |
| Total | 100.11 | 100.17 | 100.25 | 99.57 | 100.0 | 100.77 |

The results are given in Table 4. U content is 1.6 ppm in average. The fission track age is about 0.67 million years for both Muong Nong tektites and indochinite. The age is in close agreement with that estimated by other methods.

Table 3. $H_2O$ and D of Tektite

| | $SiO_2$ | $H_2O$ wt% | D% |
|---|---|---|---|
| A | 71.66 | 0.104 | -59.3 |
| B | 80.40 | 0.085 | -69.3 |
| C | 72.00 | 0.084 | -59.4 |
| D | 71.65 | 0.106 | -56.4 |
| E | 74.21 | 0.086 | -71.4 |
| F | 82.13 | 0.075 | -69.4 |
| G | 74.40 | 0.102 | -79.2 |

Table 4. Fission Track Age Data of Tektite

| | $\rho_s$ Spon Fiss Track Dens x $10^2/cm^2$ | $\rho_i$ Induced Fiss Track Dens x $10^4/cm^2$ | $\Phi$ Neutron Fluence x $10^5$ $n/cm^2$ | Age $10^6$ y | U wt ppm |
|---|---|---|---|---|---|
| A | 3.49 | 8.71 | 2.81 | 0.68 | 1.6 |
| B | 3.68 | 5.84 | 1.73 | 0.65 | 1.7 |
| C | 3.97 | 9.25 | 2.71 | 0.70 | 1.7 |
| D | 3.50 | 8.48 | 2.69 | 0.67 | 1.6 |
| E | 3.59 | 5.55 | 1.74 | 0.68 | 1.6 |
| F | 3.47 | 6.10 | 1.91 | 0.65 | 1.6 |
| G | 3.38 | 7.97 | 2.63 | 0.67 | 1.6 |

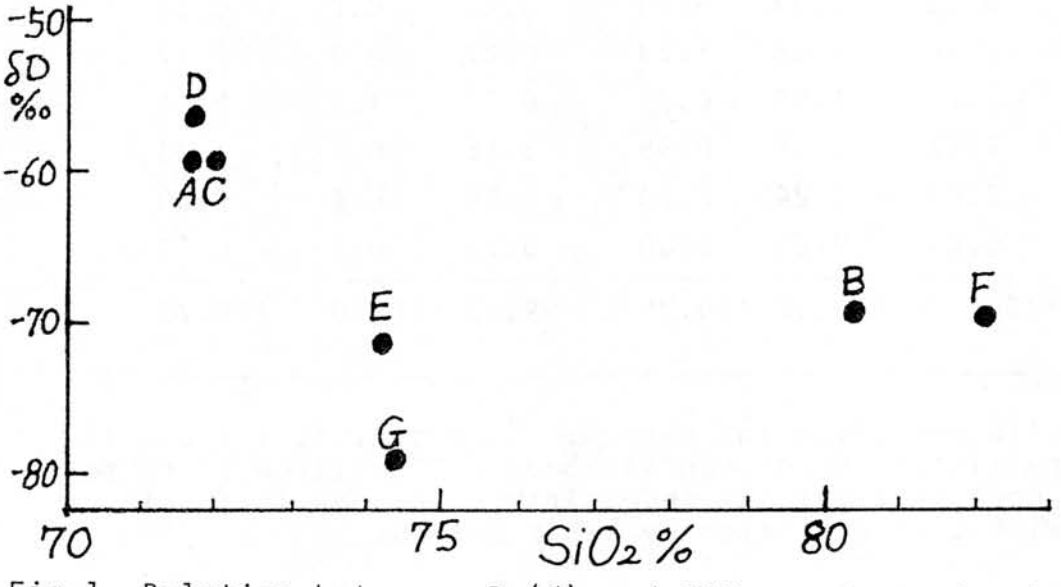


Fig.1. Relation between D (%) and SiO2 content of tektite

# SIMS MEASUREMENT OF MAGNESIUM ISOTOPIC RATIOS IN YAMATO-74191 AND -74662 METEORITES

Nishimura, H. and Okano, J.
College of General Education, Osaka University, Toyonaka, Osaka 560.

From the anomalies of $^{16}O$ (CLAYTON et al., 1973) and $^{26}Mg$ (LEE et al., 1976) in chondrites, the primordial solar nebula has been thought to be multi components. The excess $^{26}Mg$ is due to the decay of now extinct $^{26}Al$. This $^{26}Al$ and $^{16}O$ are both considered to be formed during an explosive carbon burning process at a supernova explosion. At the same time as the formation of these $^{16}O$ and $^{26}Al$, $^{24}Mg$ might have been synthesized.

Preliminary examination for searching the remnant of this kind of $^{24}Mg$ has been carried out for Al-poor and Mg-rich portions in a few Yamato and some other chondrites, and a preliminary result has been reported in 1981 (NISHIMURA and OKANO, 1981). Successive investigation gave us a relatively clear evidence that $^{24}Mg$ anomaly is kept in the Yamato-74191 (L3) chondrite.

A Hitachi IMA 2A ion microprobe mass analyzer was used for the magnesium isotopic analysis. The diameter of $O_2^+$ primary ion beam was 100 to 200 μm on the sample surface, and the current, 0.5 to 1.2 μA. The energy of the primary ions was 12 keV. Analysis was performed at Al-poor portion at which the concentration ratio of Al/Mg was less than 0.1. Mass scannings were controlled by a microcomputer and were repeated 20 times in one run over the mass range of 24 to 26. In order to avoid charge-up under the primary ion bombardment, electron spray was applied.

Interferences of doubly-charged ions and molecular ions with mass peaks of 24, 25 and 26 were carefully examined. A cold finger with liquid nitrogen was put aside the sample, in order to lower the interferences due to the molecular species that come from the enviromment of hydrocarbons and

water vapor. The maximum contribution of the interference was estimated to be less than $1 \times 10^{-3}$ of the subject peak.

Samples used were Yamato-74191 (L3) and Yamato-74662 (C2). Terrestrial forsterite from Ehime Pref., Japan, was analyzed as a laboratory standard. Polished and ultrasonically washed surfaces were used for the analyses. $^{25}Mg^{+}/^{24}Mg^{+}$ and $^{26}Mg^{+}/^{24}Mg^{+}$ were calculated from raw secondary ion intensities, and the deviations of $\Delta_{25}$ and $\Delta_{26}$ from the laboratory standard values were evaluated in permil. These calculations and statistical procedures were automatically done by a microcomputer. Data obtained for the sample of Yamato-74191 are shown in Fig. 1. In the figure, plotted points are grouped according to the difference of the concentration ratio of Mg/Si as shown in the lower right of the figure. The data for the portions at which Mg/Si ratios are between 1.5 and 2.5 are plotted well on a straight line with the slope of unity, although the data for the portions with lower Mg/Si ratios (0.7 to 1.3) comparatively scatter. The data for Yamato-74662 did not give a clear tendency.

The data shown in Fig. 1 points the direction to support a consideration of the addition of almost pure $^{24}Mg$.

REFERENCES

CLAYTON, R.N., GROSSMAN, L. and MAYEDA, T.K. (1973): Science, 182, 485-488.

LEE, T., PAPANASTASSIOU, D.A. and WASSERBURG, G.J. (1976): Geophys. Res. Lett., 3, 41-44.

NISHIMURA, H. and OKANO, J. (1981): Abstract of 6th Symposium on Antarctic Meteorites (Natl. Inst. Polar Res.), 46-48.

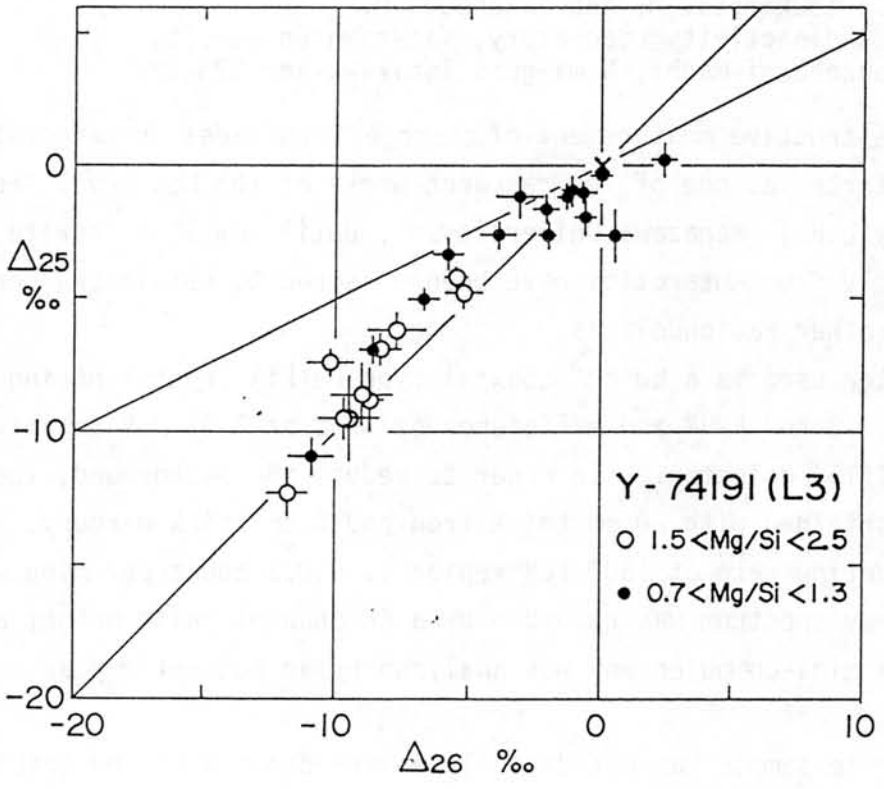


Fig. 1. Three isotope plot of magnesium for the sample of Yamato-74191 (L3) chondrite. Cross mark at the origin corresponds to the data for a forsterite (laboratory standard).

$$\Delta_m = \left[ \frac{(^mMg/^{24}Mg)_{met}}{(^mMg/^{24}Mg)_{std}} - 1 \right] \times 1000$$

33－1

# COSMOGENIC $^{26}Al$ OF YAMATO-METEORITES

Komura, K., Tsukamoto, M. and Sakanoue, M.
Low Level Radioactivity Laboratory, Kanazawa University
Wake, Tatsunokuchi-machi, Nomi-gun, Ishikawa-ken 923-12

The non-destructive measurement of cosmogenic nuclides in meteorite samples has started as one of the research works at the Low Level Radioactivity Laboratory(LLRL), Kanazawa University. Until now 15 meteorite samples collected mostly from Antarctica have been measured to obtain the contents of $^{26}Al$, $^{40}K$ and other radionuclides.

The detector used is a 80 $cm^3$ coaxial type Ge(Li) crystal having energy resolution of 1.8 keV FWHM and efficiency of 16 % at 1.33 MeV relative to 7.6 cm x 7.6cm NaI(Tl) detector. In order to reduce the background, the Ge(Li) detector was shielded with 20 cm thick iron and 5 cm thick mercury. A typical background counting rate at 1800 keV region is 0.003 count per minutes per keV. Gamma-ray spectrum was recorded by a 4K channel pulse height analyzer coupled with a mini-computer and was analyzed by an automatic peak search program.

The meteorite sample was put directly on the end-cap of the Ge(Li) detector and the gamma-ray spectrum was measured for 5500 to 12500 minutes each. An example of the Ge(Li) spectrum measured for Yamato-74191 is shown in Fig. 1. As seen from Fig. 1, 1808 keV peak due to $^{26}Al$ and 1461 keV peak due to $^{40}K$ are clearly observed in the spectrum. The 662 keV peak due to $^{137}Cs$ is the contamination of the meteorite with radioactive fallout derived from nuclear detonation in the atmosphere. Other peaks due to U- and Th-series nuclides are the background of our Ge(Li) system.

In order to obtain the absolute detection efficiencies for $^{26}Al$ and $^{40}K$ peaks, mock-up sources were prepared for each meteorite sample. Commercially available oily clay for moulding was used to make mock-up, not only because the mock-up can easily be prepared by handmaking but also because the clay contains rather high amounts of U, Th and K which can be applied as the standard sources for the calibration of detection efficiency. The only problem for using clay is the difference of density between mock-up and meteorite sample, which affects to the self-absorption of gamma-rays within the sample matrix, particularly for large one. The self-absorption effect was corrected by a simple Monte Carlo code developed by the authors. The absolute peak detection efficiency for 1808 keV gamma-ray of $^{26}Al$ ranges from 0.22 to 0.53 % depending on the size and shape of meteorite sample.

The results by Ge(Li) measurements are summarized in Table 1 together with that of $^{53}Mn$ data compiled by Honda. The contents of $^{26}Al$ is given by the unit dpm/kg-meteorite, while that of $^{40}K$ by %K. The $^{137}Cs$ data are also given in Table 1 as an indicator of surface contamination of meteorite with non-cosmogenic nuclides and/or terrestrial matters. As known from Table 1, while half of the meteorite samples (Yamato-74007, -74010, -74011, -74037 and -74191) show the saturated $^{26}Al$ activity (60-70 dpm/kg) for ordinary chondrite, the rest (Yamato-7305, =74001, 74035, -74036, -74156 and ALH-76006) show deficiency of $^{26}Al$ activity. This may be explained either by short exposure age or by long terrestrial age of the order of the half-life of $^{26}Al$. If we assume that the $^{26}Al$ defficiency is caused mainly due to long terrestrial age, the maximum age is calculated to be $7 \times 10^5$ y for Yamato-74036.

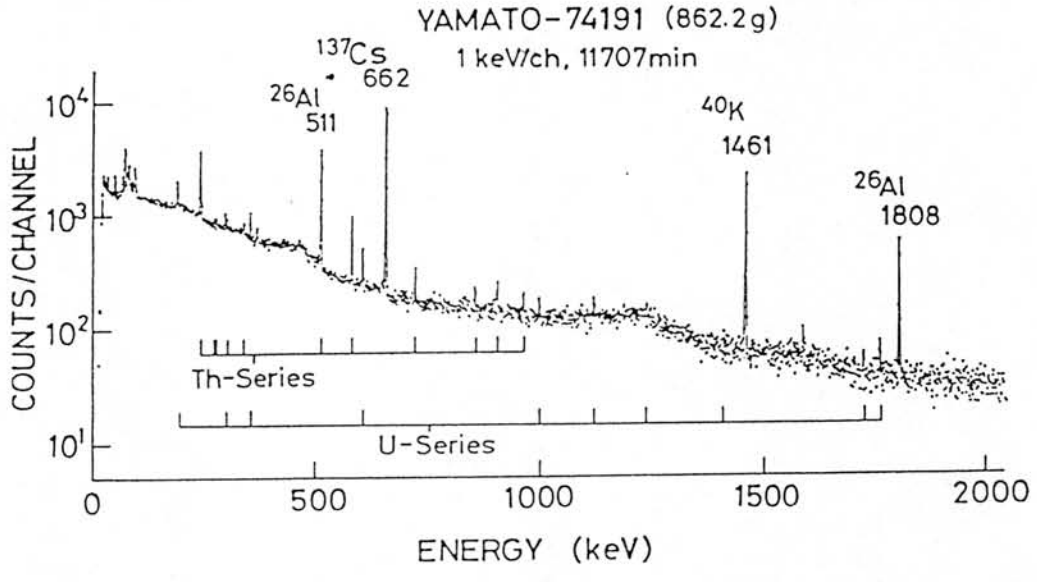


Fig. 1 Ge(Li) spectrum of Yamato-74191

Table 1. Radioactivity determined in Antarctica meteorites.

| Meteorite | Type | Weight [g] | Measuring time [min] | Measured radioactivity Al-26 [dpm/kg] | Mn-53# [dpm/kg] | K [%] | Cs-137 [cpm] |
|---|---|---|---|---|---|---|---|
| YAMATO- | | | | | | | |
| 7305 | L5 | 733.8 | 10161 | 48/4 | 352/18 | .084/5 | .415/12 |
| 74001 | H5 | 244.8 | 10772 | 38/3 | 351/16 | .072/4 | .440/7 |
| 74007 | L6 | 147.3 | 10830 | 62/5 | 433/19 | .086/5 | .267/67 |
| 74010 | D | 275.9 | 6228 | 72/5 | | .002/2 | .116/5 |
| 74011 | D | 197.7 | 12396 | 61/4 | 523/23 | .001/2 | .117/4 |
| 74035 | L6 | 101.0 | 12533 | 53/4 | 430 | .073/5 | .263/6 |
| 74036 | D | 195.0 | 10579 | 29/3 | | .091/4 | .598/9 |
| 74037 | D | 544.6 | 5497 | 66/4 | 432/16 | LTD | .140/5 |
| 74156 | H4 | 707.7 | 9833 | 35/3 | 255/15 | .061/4 | .551/10 |
| 74191 | L4-3 | 862.2 | 11707 | 71/5 | 450/23 | .104/6 | 1.774/3 |
| ALLAN-HILLS- | | | | | | | |
| 76006 | H6 | 562.8 | 12342 | 54/4 | | .080/5 | .469/8 |

# HONDA et al.

# Measurement of terrestrial age of meteorites by thermoluminescence technique

S. Miono, M. Yoshida : Osaka City University
N. Takaoka : Yamagata University
K. Ninagawa : Okayama University of Science

This report describes preliminary results of the thermoluminescence measurement of 8 "find" meteorites (Allan Hills) which have had their terrestrial age determined by the $^{36}Cl$ or $^{14}C$ methods.

Feasibility of new heating technique was performed using a $CO_2$ gas Laser is also refered to.

35－1

# REFLECTANCE SPECTROSCOPY AND MINERALOGY OF A CRYSTALLINE LL CHONDRITE

McFadden, L.A.[1], Gaffey, M.J.[1], and Takeda, H.[2]
[1] Planetary Sciences, Hawaii Institute of Geophysics, University of Hawaii Honolulu, Hawaii USA 96822
[2] Mineralogical Institute, Faculty of Science, Univ. of Tokyo, Hongo, Tokyo

A cooperative project among the authors at the University of Hawaii and University of Tokyo is in progress in which the spectral properties of meteorites from the Antarctic collection are studied and related to the spectral properties of asteroid surfaces. Our prime motivation to studying the spectral reflectance of meteorites is to relate these properties to those which we can also measure for the asteroids. The meteorites serve as an important calibration source to the interpretation of asteroid reflectance properties. It is also possible to address a number of meteoritics problems using reflectance spectroscopy as a simple, fast, non-destructive and safe method of investigation.

We are reporting measurements of Yamato recrystallized chondrites and it is compared with an unusual achondrite, Allan Hills ALHA77005. The mineralogy of a coarse-grained crystalline clast of Y-74160 is also given.

The measurements are made on a laboratory spectrometer consisting of two instruments (which are also used at the telescope for asteroids) mounted on a goniometer and optical bench. One instrument measures the reflectance from 0.33-1.13 μm with a Si phototube detector cooled by solid $CO_2$, a circular variable filter (CVF) and a choice of aperture sizes. The second instrument uses an indium-antimonide detector, a CVF which transmits light between 0.6-0.2 and apertures all of which are cooled by liquid $N_2$. Our standard, "perfect" reflector is Halon, a good standard for its long term stability and its inability to absorb water. The spectra are given in Fig. 1.

The Yamato meteorite samples we studied were kindly supplied by the National Institute of Polar Research, Tokyo. They include Yamato-74160, which is composed of fragments produced when the meteorite was chipped. The Allan Hills ALHA77005 was supplied to us by the Antarctic meteorite working group, NASA-Johnson Space Center, Houston, Texas, USA. The mineralogy of ALHA77005 is given in detail by Ishii et al. (1979), and preliminaly mineralogical examination of Y-74160 was done by Takeda et al. (1979).

Yamato-74160 is a nearly complete hemispherical stone covered with black fusion crust. The interior is pale olive yellow to greenish gray. The meteorite is brecciated and is composed of subangular recrystallized clasts. Fine-grained portions exhibiting granoblastic texture with rounded grain boundaries, consist of olivine (approximately 49%), orthopyroxene (29%), augite (9%), plagioclase (8%), chromite (3%), troilite (2%) and Ca phosphate (0.5%). Coarse-grained crystalline portions about 1cm in diameter consist of irregular interstices (more than 1mm) filled with a plagioclase, into which euhedral crystals of pyroxene and olivine up to 0.5mm in size have grown. Small amount of metal (Fe 50.0, Co 2.3, Ni 46.7 wt%) has been detected with troilite and chromite. Microprobe analyses show olivine ($Fa_{30}$) and pyroxenes of uniform compositions (Fig. 2). The orthopyroxene compositions are slightly more Fe and Ca rich than the LL6 chondrites. The plagioclase shows a small range of compositions from one interstices to another (Fig. 3). At one dead end of the interstice very small K-feldspar ($Ab_{17}An_{5}Or_{78}$) has been detected.

The bulk chemical composition of Yamato-74160 obtained by the standard wet chemical analysis by H. Haramura ($SiO_2$ 44.03, $TiO_2$ 0.14, $Al_2O_3$ 2.81, $Fe_2O_3$ 0.25, FeO 19.05, MnO 0.35, MgO 28.21, CaO 2.30, $Na_2O$ 1.06, $K_2O$ 0.08, $H_2O$ (-) 0.00, $H_2O$ (+) 0.17, $P_2O_5$ 0.20, $Cr_2O_3$ 0.60, Ni 0.09, FeS 0.34, total 99.68) and the reflectance spectra are suggestive of an extensively

crystallized LL chondrite (LL7). An evidence that euhedral pyroxene crystals grown into the interstice filled with plagioclase and minor K-feldspar suggests that at least a portion of the meteorite had been molten. The chemical variation of the plagioclases from one interstice to the other and nearly uniform composition within an interstice also supports the above hypothesis. Our new finding of shock molten LL chondrite (Sato et al., 1981) implies that if such partly molten LL chondrites are cooled relatively slowly, they may eventually become a Yamato-74160-like chondrite. Mineralogical examination of Yamato 791067 recovered by JARE in 1979 (Yanai and Kojima, private com.) revealed that this meteorite shows textural similarity to Y-74160 except that this meteorite is not as fragile as Y-74160. The microprobe analysis of the large olivine gave Fa30.4, the same value as that of the Y-74160 LL chondrite. Y791067 is more olivine-rich than Y74160.

Preliminary examination of the spectra of Yamato 74160 show prominent 0.9 and 2.0 μm absorption bands due to interelectronic transitions of d-orbital electrons in pyroxene minerals. The depth of the absorption is controlled by the abundance of the mineral and the optical depth of the components in the sample (Gaffey, 1976). Differences in these absorption bands are apparent upon examination and reflect differences in the pyroxene mineralogy in the meteorites and the presence of additional components, such as olivine and plagioclase. Y-74160 is spectrally similar to known LL6 chondrites (Fig. 1). It is interesting to note that in spite of extensive recrystallization, the spectral reflectance of Y-74160 is not much different from that of the LL6 chondrites.

The unusual achondrite ALHA77005 which is related to shergottite, (McSween et al., 1979), shows 0.9 and 2.0 μm absorption features due to the presence of pyroxene. This meteorite contains chemically three different pyroxenes; but crystallographically they are pigeonite and augite (Ishii et al., 1979). The depth to the bands is not characteristic of previously known achondrites. The bandwidth of the 0.9 μm feature, and inflection at 0.6 μm and the high infrared reflectances indicate the presence of a significant olivine component in agreement with the mineralogical observation (Ishii et al., 1979 and McSween et al., 1979). A 1.25 μm plagioclase band also contributes a significant spectral component. The visible charge transfer absorptions characteristic of silicates are also present. The suggestion by Feierberg et al. (1980) that this meteorite is the same type as the surface of the asteroid 349 Dembowska is not supported by these measurements.

In conclusion, in spite of similarity in their crystalline textures and mineral assemblages, the reflectance spectra of Y-74160 and ALHA77005 differ significantly. Both meteorites contain coarse crystals of olivine, pyroxene and plagioclase and minor opaque minerals. The difference we can find is that crystal structure of the low-Ca pyroxene in Y-74160 is orthopyroxene, but that in ALHA77005 has been transformed to low-Ca pigeonite by shock events.

We thank the National Inst. of Polar Res. of Japan and the Antarctic Meteorite Working Group of NASA Johnson Space Center, USA for supplying us with samples. Funding was in part by NASA grant number NSG-7462, and by a Fund for Sci. Res. of the Ministry of Education, in Japan.

References: Feierberg. M.A., Larson, H.P., Fink, U., Smith, H.A. (1980) Geochim. Cosmochim. Acta, 44, 513-524.
Gaffey, M.J. (1976) J. Geophys. Res. 81, 905-920.
Ishii, T., Takeda, H., and Yanai, K. (1979) Miner. Journ. 2, 460-481.
McSween, H.Y. Jr., Taylor, L.A., Stolper, E.M., Nuntaean, R.A., O'kelley, G. D. & Eldridge, J.S. (1979) Earth Planet. Sci. Lett. 45, 275-284.
Sato G., Takeda H., Yanai K., and Kojima H. (1981) Abstr. Workshop on Lunar Breccias and Soils and Their Meteoritic Analogs, Lunar and Planet. Inst.

# 35－3

Takeda, H., Duke, M.B., Ishii, T., Haramura, H., Yanai, K. (1979) Mem. Natl. Inst. Polar Res., Spec. Issue 15, 54-76.

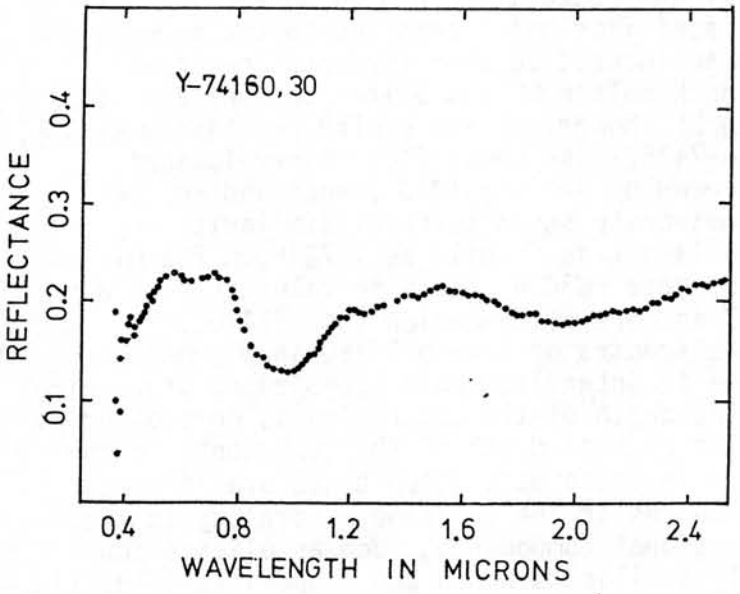


Fig. 1. Bidirectional reflectance spectra relative to Halon of Yamato 74160.

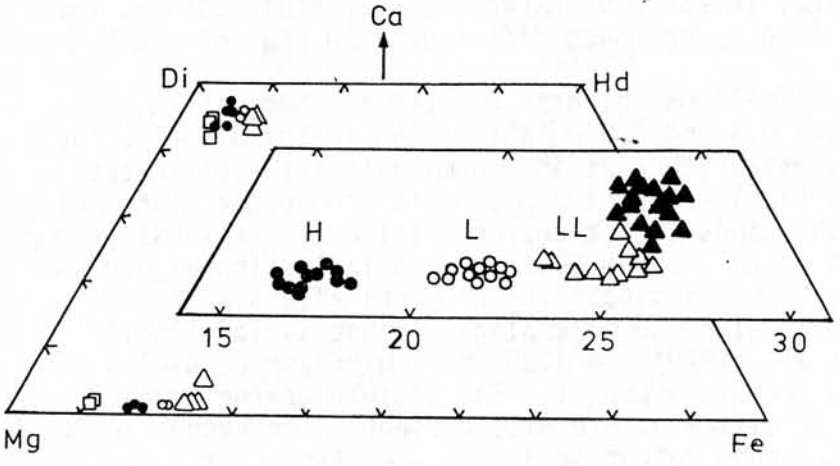


Fig. 2. Pyroxene quadrilateral of Yamato 74160. Solid triangle: Y74160, others: H, L, and LL chondrites.

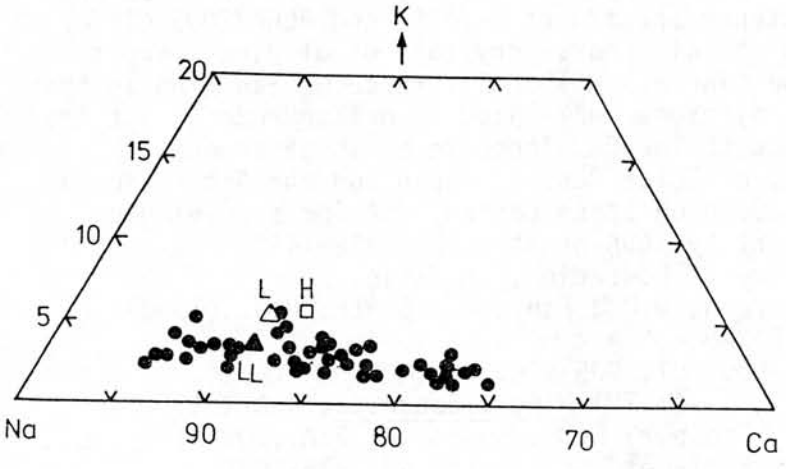


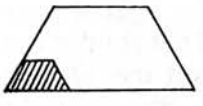

Fig. 3. Plagioclase compositions in Yamato 74160. Shaded portion above is enlarged. Solid circle: Y74160, H, L, and LL are chondrites.

# MAGNETIC CLASSIFICATION OF METEORITES
## - IRON METEORITES -

Takesi NAGATA
National Institute of Polar Research, Tokyo 173

A magnetic classification scheme for stony meteorites (i.e. chondrites and achondrites) has been proposed by the present author with reasonable success (Nagata 1979, 1980). The classification scheme is based on two magnetic parameters;i.e. the saturation magnetization($I_S(\alpha)$) and ratio of the $\alpha$-phase (kamacite) magnetization to the total magnetization ($I_S(\alpha)/I_S$). The two parameters chemically represent respectively the content of metallic Fe and the relative content of Ni in the metallic component in individual stony meteorites. This note is a supplementary report of an applicability of the classification scheme for newly examined chondrites and a modified magnetic classification scheme for iron meteorites.

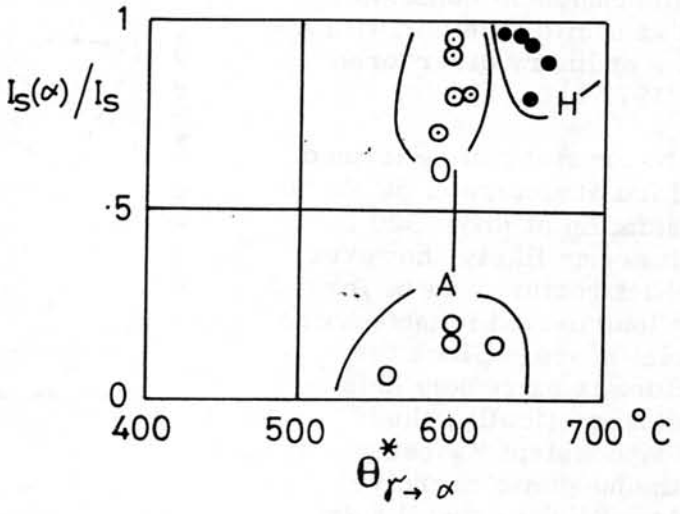


Fig. 1 $I_S(\alpha)/I_S$ versus $\textcircled{H}^*_{\gamma\to\alpha}$ diagram for iron meteorites
H: Hexahedrites and Ni-poor ataxite
O: Octahedrites
A: Ni-rich ataxite

(i) Chondrites The magnetic properties of 1 H-chondrite, 4 L-chondrites, 2 LL-chondrites are newly examined. These chondrites also can be well classified in respective domains on the $I_S(\alpha)/I_S$ versus $I_S$ diagram where the domains for E-, H-, L-, LL- and C-chondrites are separately designated.

(ii) Iron-meteorites In the case of iron meteorites, however, it seems better to take the $\gamma\to\alpha$ transition temperature of kamacite phase ($\textcircled{H}^*_{\gamma\to\alpha}$) which represents the Ni-content in kamacite phase and $I_S(\alpha)/I_S$ in order to separately group iron meteorites into 3 groups, namely, hexahedrites plus Ni-poor ataxites, octahedrites and Ni-rich ataxites. Fig. 1 illustrates the three separated domains for hexahedrites plus Ni-poor ataxites, octahedrites and Ni-rich ataxites on an $I_S(\alpha)/I_S$ versus $\textcircled{H}^*_{\gamma\to\alpha}$ diagram.

References:

Nagata T., (1979) Mem. Nat'l. Inst. Polar Res., Spec. Issue No.15, 273-279.

Nagata T., (1980) Mem. Nat'l. Inst. Polar Res., Spec. Issue No.18, 219-232.

37 – 1

# HIGH COERCIVE MAGNETIC PROPERTIES OF METEORITES CONTAINING ORDERED FeNi (TETRATAENITE)

Takesi NAGATA
National Institute of Polar Research, Tokyo 173.

The natural remanent magnetization (NRM) of ordinary chondrites is, in general, not stable for the AF-demagnetization test (e.g. Nagata 1979). However, some particular ordinary chondrites such as ALHA 77260 ($L_6$) and St. Séverin ($LL_6$) have NRM of unusually high stability, as shown in Fig. 1. The origin of the highly stable NRM of these chondrites was not reasonably well known. Recently, the presence of the ordered FeNi phase (tetratanite) has been found in a number of iron and stony meteorites, including Antarctic meteorites (e.g. Clarke and Scott, 1980). In St. Séverin ($LL_6$) chondrite, for example, its metallic component consists of ordered taenite and kamacite together with a smaller amount of the ordinary disordered taenite (Danon et al 1979 b).

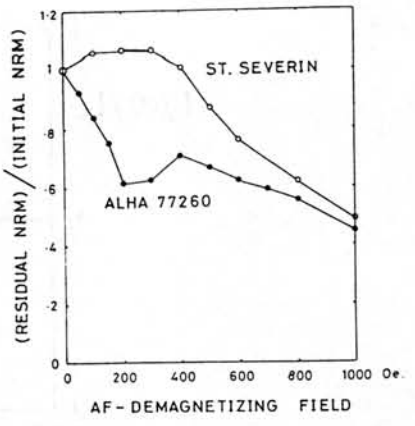


Fig. 1

The ordered FeNi crystal can be formed from the disordered fcc structure of 50 Fe 50 Ni by a neutron irradiation at about 320°C (Néel et al 1964). It seems likely, however, that the ordered FeNi structure can be formed during an extremely long period in meteorites in the extraterrestrial space. Since the ordered FeNi structure is extremely anisotropic, optically and magnetically, the crystalline anisotropy constant $K_1$ being $3.2 \times 10^6$ emu/cm$^3$, the magnetic coercive force ($H_c$) of an ordered FeNi crystal must be verly large (about $5 \times 10^3$ Oe). The $H_c$-value of meteorites containing the ordered FeNi grains as the major ferromagnetic constituent will therefore be very large and consequently their NRM must be very stable for the AF-demagnetization test. Both St. Séverin and ALHA 77260 contain the ordered FeNi phase as one of the major ferromagnetic constituents.

Figs. 2 and 3 show the thermomagnetic curves of the first and second runs for St. Séverin and ALHA 77260. In both cases, the magnetic transition at 550°C or 580°C in the first-run heating curve is identified to Curie point of the ordered FeNi phase, and $\alpha \rightarrow \gamma$ and $\gamma \rightarrow \alpha$ transitions of a kamacite phase of 5.2 – 5.5 wt%Ni are identified in the heating and cooling thermomagnetic curves respectively. After once heating up to 800°C, however, the ordered FeNi phase of St. Séverin is transformed to taenite phase of a wide spectral range of Ni-content (i.e. 30 – 55 wt%Ni), while that of ALHA 77260 is transformed mostly to a taenite phase of 50 – 55 wt%Ni.

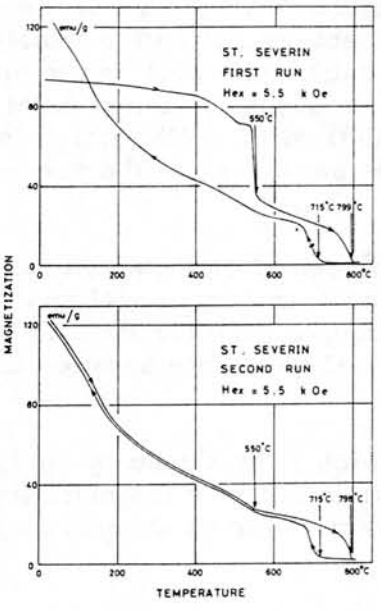


Fig. 2

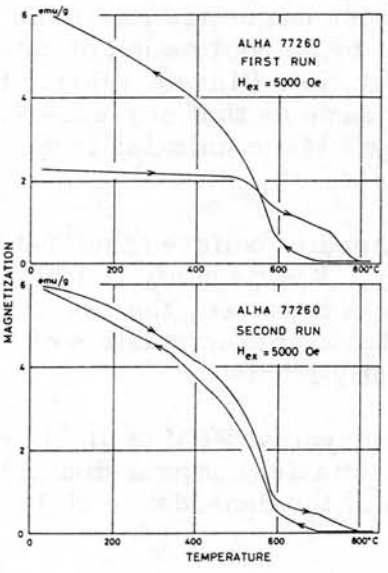


Fig. 3

The observed transformation of the ordered FeNi phase to taenite phases of a broad range of Ni-content in the case of St. Séverin may be interpreted as due to a remelting of small domains (1500-3000 Å) of the ordered FeNi phase, in varying ratios, with neighbouring taenite phase of less than 30 wt% in Ni-content into homogeneous taenite phases of various Ni-contents between 30 and 55 wt%. This interpretation can be supported by observed thermomagnetic characteristics of Santa Catherina ataxite which consists of small domains of the ordered FeNi phase and matrix of taenite of 28 wt%Ni (Danon et al 1979 a).

References:

Clarke R.S. Jr. and Scott E.R.D. (1980) Amer. Mineral. 65, 624-630.

Danon J. et al (1979 a) Nature. 277, 283-284.

Danon J. et al (1979 b) Nature. 281, 469-471.

Nagata T. (1979) Mem. Nat'l. Inst. Polar Res., Spe. Issue No.12, 238-249.

Néel L. et al (1964) J. Appl. Phys., 35, 73-76.

38－1

# PIEZO-REMANENT MAGNETIZATION OF ANTARCTIC METEORITES

Takesi NAGATA and Minoru FUNAKI
National Institute of Polar Research, Tokyo 173

Effects of mechanical stresses on the magnetization of terrestrial rocks have been studied in fair detail as summarized by Nagata (1970). One of the stress effects on rock magnetization is the shock remanent magnetization (SRM) which is produced by an application of compressional shock on a rock in the presence of a magnetic field (Nagata 1971). The mechanism of production of SRM is essentially same as that of piezo-remanent magnetization (PRM) which is produced by a static uniaxial compression on the same rock in the presence of a magnetic field.

It is generally believed that meteorites have been often impacted in their past history. If a magnetic field is present in the extraterrestrial space where a meteorite is impacted, the meteorite should acquire SRM (or PRM). In this work, the basic characteristics of PRM of selected meteorite samples are experimentally studied.

The most typical PRM is $J_R''(H+P+PoHo)$, which is produced by applying and removing a uniaxial compression (P) along the direction of a magnetic field (H). An example of the dependence of $J_R''(H+P+PoHo)$ on H for an achondrite is shown in Fig. 1.

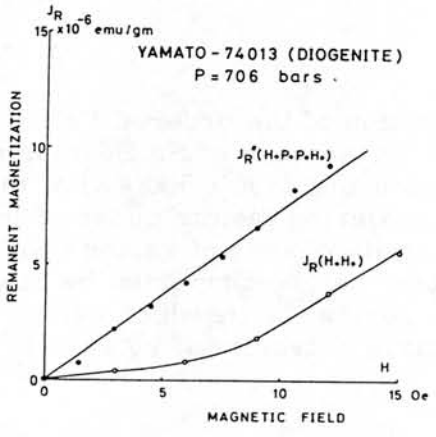


Fig. 1

Nagata-Carleton theory of PRM (1969) gives that

$$J_R''(H+P+PoHo) \simeq \frac{16}{5\pi} B\, H H_c \qquad (H \ll H_c), \qquad (1)$$

with $H_c \equiv 3|\lambda|P/\sqrt{2}\, J_S$,

and

$$J_R(H+Ho) = IRM = BH^2 , \qquad (2)$$

where $\lambda$ and $J_S$ denote respectively the isotropic magnetostrictron coefficient and the spontaneous magnetization of ferromagnetic grains, while B is the coefficient of a parabolic dependence of IRM on H for a bulk rock sample. The

observed curves of $J_R''(H+P+PoHo)$ versus H and $J_R(H+Ho)$ versus H are well presented by equations (1) and (2) respectively.

Equation (1) leads to

$$J_R''(H+P+PoHo) = CHP \quad \text{and} \quad C \equiv 48|\lambda|B/5\sqrt{2}\pi J_S. \qquad (3)$$

In Table 1, observed values of B and C for 3 meteorites, Mt. Boldr 2 ($H_{6-5}$), ALHA 76009 ($L_6$) and Yamato 74013 (Diogenite) are summarized together with their natural remanent magnetization (NRM=$I_n$), saturation magnetization ($I_S$), saturated IRM ($I_R$), and coercive force ($H_c$). These results suggest that the observed intensity of NRM can be acquired as PRM or SRM by a mechanical impact of several kilo-bars in the presence of a magnetic field smaller than 1 Oe.

| Magnetic Parameters | Mt. Boldr-2 ($H_{6-5}$) | ALHA76009 ($L_6$) | Yamato74013 (Diogenite) | unit |
|---|---|---|---|---|
| B | $8.6 \times 10^{-5}$ | $2.5 \times 10^{-5}$ | $2.4 \times 10^{-8}$ | emu/g/Oe$^2$ |
| C | $3.1 \times 10^{-6}$ | $1.6 \times 10^{-6}$ | $1.1 \times 10^{-9}$ | emu/g/Oe. par |
| B/C | $3.6 \times 10^{-2}$ | $6.4 \times 10^{-2}$ | $4.6 \times 10^{-2}$ | |
| $I_n$ | $1.1 \times 10^{-4}$ | $2.0 \times 10^{-3}$ | $3.4 \times 10^{-6}$ | emu/g |
| $I_s$ | 27.4 | 8.4 | 0.17 | " |
| $I_R$ | 0.14 | 0.52 | 0.0012 | " |
| $H_c$ | 12 | 160 | 10 | Oe |

Table 1.

References:

Nagata T. (1970) Tectonophys. 9, 167-195.

Nagata T. (1971) Pure Appl. Geophys. 89, 159-177.

Nagata T. and Carleton B.J., (1969) J. Geomag. Geoele., 21, 623-645.

39－1

# MAGNETIC SUSCEPTIBILITY ANISOTROPIES OF SOME ANTARCTIC CHONDRITES

Hamano, Y. and Yomogida, K.
Geophys. Inst., Univ. of Tokyo, Tokyo 113

Stacey et al. (1961), Weaving (1962), and Brecher and Arrhenius (1974) measured the magnetic anisotropy of meteorites. Their observations indicate that most of the meteorites have large magnetic anisotropy. Although Stacey et al. (1961) proposed a metamorphic origin of the magnetic anisotropy, high magnetic anisotropy in carbonaceous chondrites observed by Brecher and Arrhenius (1974) is not compatible with their conclusion. Preferred orientation of chondrules in unequilibrated chondrites (Dodd, 1965; Martin, Mills and Walker, 1975) also indicates the different origin of the anisotropy.

In order to investigate the origin of the anisotropy, we measured the magnetic susceptibility and the porosity in eleven Antarctic chondrites. These samples are ordinary chondrites (H and L) in various metamorphic stages. Full susceptibility matrix was determined by using a Schonstedt SSM-1A spinner magnetometer and a Bison susceptibility bridge, and three principal values and the directions of the principal axes were calculated. The porosity of each sample was estimated from the intrinsic density observed by a helium pycnometer and the bulk volume obtained by an immersion technique. Table 1 summarizes the above observations, where $\bar{K}$ is the mean susceptibility, anisotropy parameters are defined by $a = K_{max}/K_{int}$, $b = K_{int}/K_{min}$ and $c = K_{max}/K_{min}$, and $K_{max}$, $K_{int}$ and $K_{min}$ are the maximum, the intermediate and the minimum susceptibilities respectively.

Table 1.

| Sample | Type | $\bar{K}$ ($10^{-3}$G/Oe) | a | b | c | porosity (%) |
|---|---|---|---|---|---|---|
| Y74156 | H4 | 46.09 | 1.032 | 1.527 | 1.576 | 9.2 |
| Y74647 | H45 | 69.23 | 1.060 | 1.368 | 1.450 | 9.1 |
| ALH77294 | H5 | 44.18 | 1.049 | 1.491 | 1.564 | 12.9 |
| ALH77288 | H6 | 46.02 | 1.011 | 1.022 | 1.034 | 2.0 |
| Y74191 | L3 | 14.12 | 1.038 | 1.425 | 1.480 | 10.3 |
| Y75097 | L4 | 19.22 | 1.035 | 1.346 | 1.393 | 10.3 |
| MET78003 | L6 | 18.95 | 1.043 | 1.443 | 1.505 | 7.8 |
| ALH78251 | L6 | 14.12 | 1.019 | 1.280 | 1.304 | 13.2 |
| ALH78103 | L6 | 14.30 | 1.047 | 1.288 | 1.342 | 13.4 |
| ALH769 | L6 | 12.78 | 1.011 | 1.306 | 1.320 | 19.4 |
| ALH77231 | L6 | 17.34 | 1.059 | 1.260 | 1.335 | 14.3 |

The results are summarized as follows. (1) Most of the chondrites (10 out of 11) show large anisotropy ($c > 1.3$). (2) The shape of the susceptibility ellipsoid is an oblate type. (3) Low metamorphosed chondrites are highly anisotropic. (4) The porosity is not related to the metamorphic type.

Followings are the inferrences derived from the above results. (a) The observed high anisotropy precludes the possibility of the shock origin after

the chondrites were solidified, because a large deformation in a short time would cause a destruction of the shocked parts. (b) The metamorphic origin is also inappropriate because of no correlation between the metamorphic type and the degree of the anisotropy. (c) The above two evidences suggest a large deformation at a low temperature as a cause of the anisotropy. This type of deformation is possible only when the material is non cohesive. (d) This stage can be realized near the surface of the accumulating parent body of the chondrites, where the meteoritic material had not been solidified yet. (e) Compaction of the powder-like material, due to a collisional shock or a static compression, causes an anisotropic distribution of elongated magnetic particles and the magnetic anisotropy arises. (f) Uni-axial compression type of deformation, inferred from the type of the anisotropy (foliation), is compatible with the above interpretation. (g) Although the anisotropy and the porosity are apparently independent to the metamorphic type, the two properties show some correlation as shown in Fig. 1. An evolution of the two properties during a uni-axial compaction was calculated and the two curves correspond to the initial porosity of 30% and 35% are shown in Fig. 1. Comparison of the curves with the observed data support the above interpretation of the origin of the anisotropy. (h) Fig. 1 also suggests that the porosity of the chondrites was also determined by the initial compaction stage. Various porosity observed in L6 chondrites supports the above conclusion.

In summary, the present observations indicate that surface phenomena on the accumulation planetesimals are responsible for the determination of the magnetic anisotropy and the porosity. If this is the case, the degree of the anisotropy and the porosity can be used to infer the accumulating process of the chondrite parent body. Since it is not unreasonable to assume that the high susceptibility plane is parallel to the surface of the parent body, the above interpretation opens the possibility to reconstruct the paleo-orientation of the chondrites within their parent body.

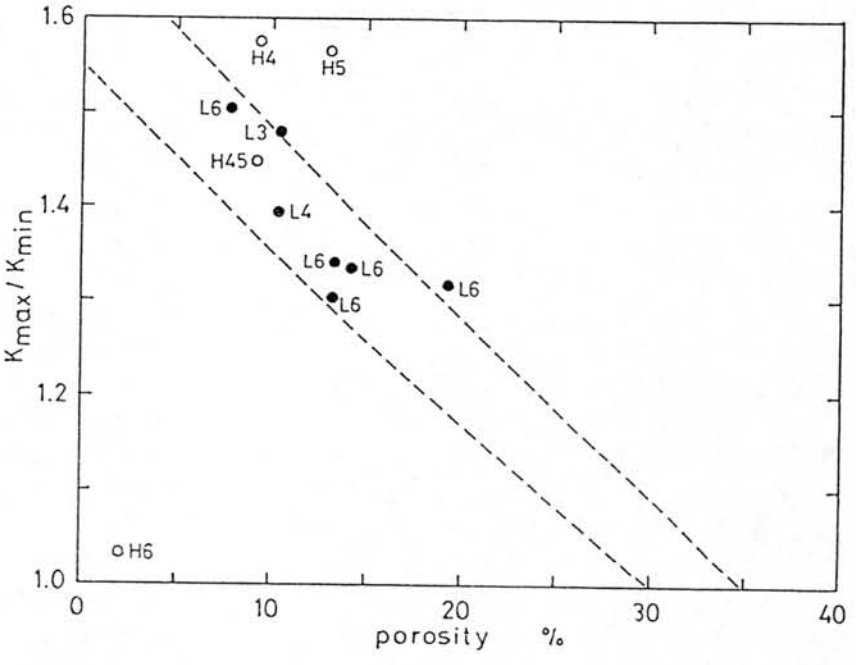


Fig. 1

References

Brecher, A. and Arrhenius, G., J. Geophys. Res., 79, 2081-2106, 1974.
Dodd, R.T., Icarus, 4, 308-316, 1965.
Martin, P.M., Mills, A.A. and Walker, E., Nature, 257, 37-38, 1975.
Stacey, F.D., Lovering, J.F. and Parry, L.G., J. Geophys. Res., 66, 1523-1534, 1961.
Weaving, B., Geochim. Cosmochim. Acta, 26, 451-455, 1962.

# THE SPECTRAL REFLECTANCE OF BLACK METEORITES.

Masamichi Miyamoto, Akihiro Mito and Yukio Takano

Dept. of Pure and Applied Sciences, College of General Education
Univ. of Tokyo, Komaba, Meguro-ku, Tokyo 153.

The comparison between the spectral reflectances of asteroids and those of meteorites enabled us to interpret the mineral assemblages of asteroidal surface materials(1). Their works revealed that most of asteroids show very low reflectivity and relatively flat spectra. These features make it difficult to estimate their mineral assemblages of the surface material.

In order to examine the effects of low reflectance materials on the spectral reflectance of meteorites or asteroids, we carried out the spectral reflectance measurements of meteorite samples in which various amounts of low reflectance materials were mixed. We mixed powders of LL6 chondrite(Yamato-75258) with various amounts of carbon black(0,2,5 wt%) or magnetite(0,1,2,3,5 wt%)(2,3). The effects of carbon on the spectral reflectance are as follows: 1) ∿1 wt% of carbon lowers the reflectance to half. 2) The peak at ∿0.5 μm is suppressed. 3) The UV drop-off position apparently shifts toward longer wavelength. These effects can also be found in the spectral changes by magnetite.

On the basis of these spectral reflectance data, we developed a method to enhance the spectral contrast which are suppressed by the effects of the low reflectance materials in the spectral reflectance of black meteorites such as C-chondrites(2). We use Kubelka-Munk function(4) and construct the spectral reflectance curve from that of the black meteorite(Murchison(C2)) by reducing the effects of the black material contained in the meteorite, and make the spectral contrast of the meteorite clear. Although the reflectance around 0.55μm in the constructed curve is enhanced by reducing the effects of carbon or magnetite and the shape of the constructed curve resembles the reflectance of Ceres, the small peak at ∿0.45 μm found in the spectral reflectance of Ceres can not be explained.

Fig. 1 shows the preliminary results of the spectral reflectance measurements of shock-melted LL-chondrites in the Yamato-79 collection(5) and ureilite ALH-77257. Heavily shocked LL-chondrites show very low reflectance compared with usual ordinary chondrites. This result is probably due to the glassy materials contained in these LL-chondrite produced by impact processes. The reflectance of these meteorites is as low as that of Allende(∿7 %). One of the differences in the reflectances between these meteorite and Allende is that the reflectance of these meteorites increases remarkably by pulverization(∿15 %), whereas that of powdered sample of Allende shows little increase.

We thank Natl Inst. Polar Res. for meteorite samples, Prof. C. B. Moore for Murchison, and Miss L. McFadden for Halon.

References: (1) Gaffey M.J. & McCord T.B.(1977) Proc. Lunar Sci. Conf. 8th 113. (2) Mito A., Miyamoto M. & Takano Y.(1981) Proc. 14th ISAS Lunar Planet. Symp. 141. (3) Miyamoto M., Mito A., Takano Y. & Fujii N.(1981) Mem. Natl Polar Res. Spec. Issue(in press). (4) Wendlandt W.W. & Hecht H.G. (1966) Reflectance spectroscopy. (5) Yanai K. Takeda H., Sato G. & Kojima H.(1981) Abstr. Meteor. Soc. 44th Ann. Meet. Bern, 138.

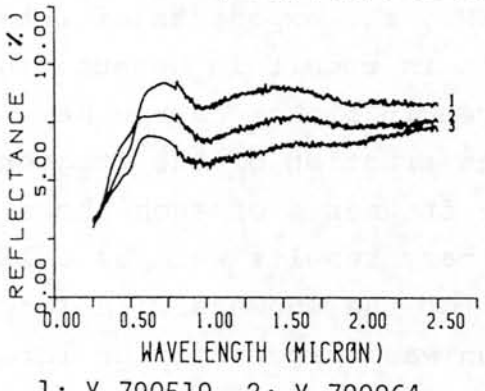


1: Y-790519, 2: Y-790964
3: ALH-77257

41－1

# DESTRUCTION OF METEORITES

Hasegawa, H.
Kyoto University, Kyoto, 606

Destruction phenomena of meteorites were studied as to (i) the shape of the fragments and (ii) the mass spectra of the showers. The data of the Yamato79 meteorites in addition to those of the Yamato73-75 meteorites were used.

(i) The shape of the fragments was described by the axial ratios (b/a) and (c/a) of the approximated ellipsoid of each fragment (Fig.1). The a, b and c are the longest, intermediate and the shortest axis respectively. The average $\langle b/a \rangle$ is 0.77 and the average $\langle c/a \rangle$ is 0.55. These are slightly larger than those for the basaltic fragments of Fujiwara's. The fragments with the axial ratio (c/a) less than 0.3 were rare, which means the plate or the needle shape fragments are scaresly produced.

(ii) In the Yamato79 series, 7 showers were found among about 990 meteorites. The total number of showers are 13, one is diogenite shower and the remainder are the ordinary chondrite showers. (Table 1)

It seems that the correlations exist among the total moss $\Sigma M$, average mass of the fragments $\langle M \rangle$ and the ratio of the largest fragmental mass to the total mass ($M_a/\Sigma M$). The mass spectrum expressed by the commulative number $N(>M)$ can be represented by power law. The exponent is correlated with $\Sigma M$, $\langle M \rangle$ and ($M_a/\Sigma M$) and the value of the exponent deereases with increasing these mass parameters. (Fig.2) For the showers with small $\langle M \rangle$, the exponents of integral mass spectra were large. But this is uncertain because the mass spectra of these showers are given in rather narrow mass range.

The fraction of the fragments having fusion crust among all the fragments of each shower is an interesting quantity. Preliminary results were as follows; (1) The above fraction was larger for the showers with larger $\Sigma M$ or larger $\langle M \rangle$ and (2) the fraction was larger for the larger fragments of each showers (Fig.3). It is suggested from (2) that the larger fragments

come from the surface part of an original meteorite. But for the result (1) the clear-cut interpletation was not of tained.

Table 1

| Shower | No. of fragments | Total mass Mt (g) | Mass of max. frag. Ma (g) | (Ma/Mt) (%) | Equivalent E/Mt (erg/g) | Av. mass ⟨M⟩ | α | Mass range (g) |
|---|---|---|---|---|---|---|---|---|
| 7 | 22 | 42.88 | 7.18 | 16.7 | 1.8 (7) | 1.95 | 2.4±0.2 | 1.5-3 |
| 2-L | 38 | 64.2 | 6.3 | 9.8 | 2.8 (7) | 1.69 | 3.0±0.4 | 2-4 |
| 4-L | 57 | 110.8 | 8.1 | 7.3 | 3.5 (7) | 1.94 | 2.5±0.1 | 2.5-8 |
| 9 | 20 | 251.36 | 104.34 | 41.5 | 0.86 (7) | 12.6 | 1.1±0.2 | 5-20 |
| 10 | 24 | 495.33 | 130.98 | 26.4 | 1.2 (7) | 20.6 | 1.2±0.2 | 10-30 |
| 6 | 64 | 620.25 | 50.90 | 8.2 | 3.2 (7) | 9.69 | 1.75±0.15 | 10-30 |
| 1 | 149 | 715 | 25.9 | 3.6 | 6.2 (7) | 4.80 | 3.5±0.3 | 5-15 |
| 8 | 62 | 2,274.19 | 1,269.2 | 55.8 | 0.68 (7) | 36.7 | 0.65±0.06 | 10-100 |
| 12 | 162 | 2,989.73 | 938.8 | 31.4 | 1.1 (7) | 14.0 | 0.82±0.07 | 3-200 |
| 5-L | 150 | 3,199.5 | 706.9 | 18.0 | 1.7 (7) | 26.1 | 0.60±0.05 | 5-100 |
| 3-H | 169 | 5,273.8 | 1,719.7 | 32.6 | 1.05 (7) | 31.2 | 0.95±0.05<br>1.4±0.1 | 6-100<br>80-300 |
| D | 29 | 6,775.8 | 2,193.9 | 32.4 | 1.06 (7) | 233.6 | 0.35±0.02 | 25-700 |
| 11 | 204 | 10,011.65 | 1,338.4 | 13.4 | 2.1 (7) | 49.1 | 0.60±0.07<br>1.4±0.2 | 5-150<br>150-1000 |

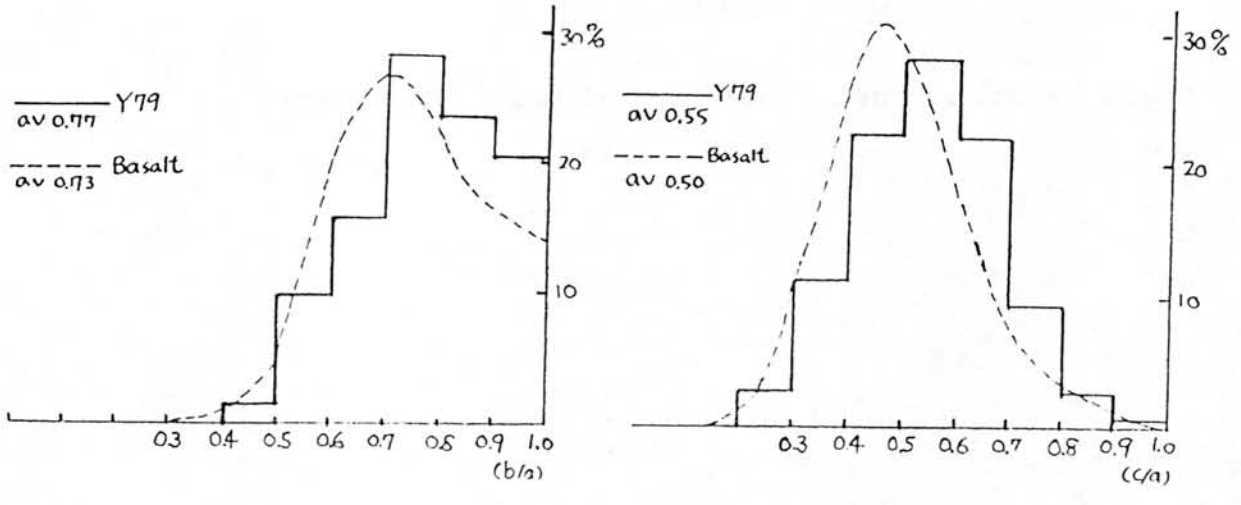


Fig.1 Axial ratio distributions

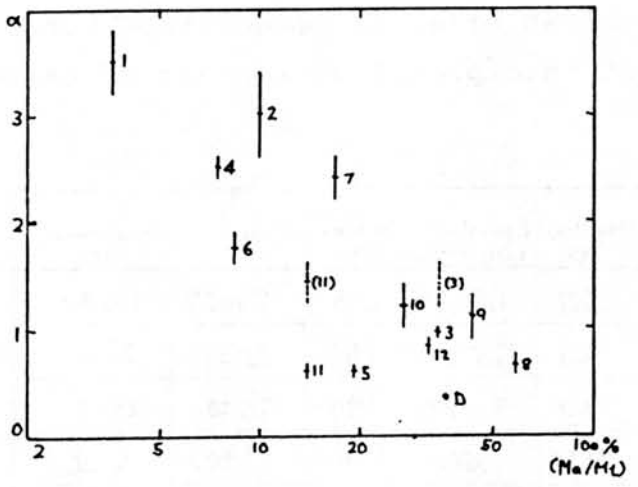


Fig.2 Relation between the exponent and ($M_a/\Sigma M$).

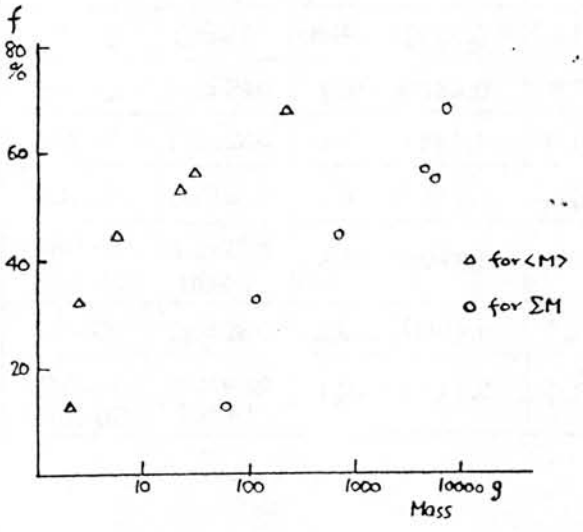


Fig.3 Fusion crust fraction and mass parameters.

# PHYSICAL PROPERTIES OF ANTARCTIC CHONDRITES, II

Kiyoshi YOMOGIDA and Takafumi MATSUI
Geophysical Institute, Faculty of Science, University of Tokyo

In order to obtain informations on the consolidation process of chondrites and also to reveal a nature of chondrite parent bodies, we measured the intrinsic and bulk densities, porosity, elastic wave velocity and thermal diffusivity of the four unequilibriated antarctic chondrites; Y-74156(H4), Y-74191(L3), Y-74647(H4-5) and Y-75097(L4). Thermal diffusivity of the five samples (ALH-77288(H6), -77294(H5), -78103(L6), -78251(L6) and MET-78003(L6)), whose elastic properties have already reported (3), was also measured. Please refer the previous(1, 2, 3) papers for more details of the method of the measurement. The newly distributed four samples are the unequilibriated chondrites. Therefore, the physical properties of all petrologic types of ordinary chondrites have been measured in our laboratory. Then, it is now possible to grasp the general characteristics of physical properties of chondrites by comparing the physical property data of each prtrologic type of chondrite with those of other types of chondrite. The unequilibriated chondrites have included several tiny cracks. However, the measured values were shown not to be disturbed by the existence of such a few distinguishable tiny cracks.

The results on densities, porosity and elastic properties are summarized in Table 1, 2 and 3. In Fig. 1 are shown the relationships between the porosity and the petrologic type in each chemical group. Since all of the data in this figure were obtained from the apparently fresh samples by using the same measurement techniques, it can be said that there is no bias in these data. Therefore, we may see characteristics between the porosity and the petrologic type from this figure if they exist. Consolidation states of the composite materials of chondrites have been considered to be determined by the sintering process such as the low-tempearature creep. If so, the porosity of chondrites is expected to decrease with increase in petrologic type. Because, the petrologic type represents the maximum metamorphic temperature which the chondrites have experienced. However, it is difficult to find such a clear tendency in Fig. 1. Most of the L6 chondrites have a fairly wide range of porosity values. On the other hands, for the H chondrites there seems to be a correlation between the porosity and the petrologic type. Anyway, we can say that the metamorphic temperature may have very few effect on proceeding the consolidation state of chondrites.

The porosity seems to be correlated with the elastic wave velocity as shown in Fig. 2. The elastic wave velocity is greatly affected by the number and aspect ratio of cracks, while the porosity is primarily determined by the volume of pores. Therefore, such a correlation may exibit that there is a proportional relation between the crack and pore volumes. The elastic wave velocities of the chondrites are lower than those of the terrestrial rocks with the same porosity, which means that the chondrites have more cracks compared with the terrestrial rocks. The thermal diffusivity of the samples in this study is comparable with that in the previous studies, except for ALH-77288. ALH-77288 shows much higher values of thermal diffusivity (e.g. $15 \times 10^{-7} m^2/sec$ at 200 K, while for other samples $3 \sim 7 \times 10^{-7} m^2/sec$), which may depend on its low porosity (2.0 %).

REFERENCES (1) Matsui, T. and Osako, M. (1979) Mem. Natl Inst. Polar Res., Spec. Issue, No. 15. (2) Matsui, T., Hamano, Y. and Honda, M. (1980) Mem. Natl Inst. Polar Res., Spec. Issue, No. 17. (3) Yomogida, K. and Matsui, T. (1981) Mem. Natl Inst. Polar Res., Spec. Issue, No. 20.

Table 1. Intrinsic and bulk densities and porosity.

| Sample | Type | Volume ($cm^3$) | Mass (g) | Density ($g/cm^3$) Bulk | Intrinsic | Porosity (%) |
|---|---|---|---|---|---|---|
| Y-74156 | H4 | 4.05 | 13.98 | 3.45 | 3.80 | 9.2 |
| Y-74191 | L3 | 2.39 | 7.72 | 3.23 | 3.60 | 10.3 |
| Y-74647 | H4-5 | 2.63 | 9.17 | 3.49 | 3.83 | 9.1 |
| Y-75097 | L4 | 2.40 | 7.85 | 3.28 | 3.65 | 10.3 |

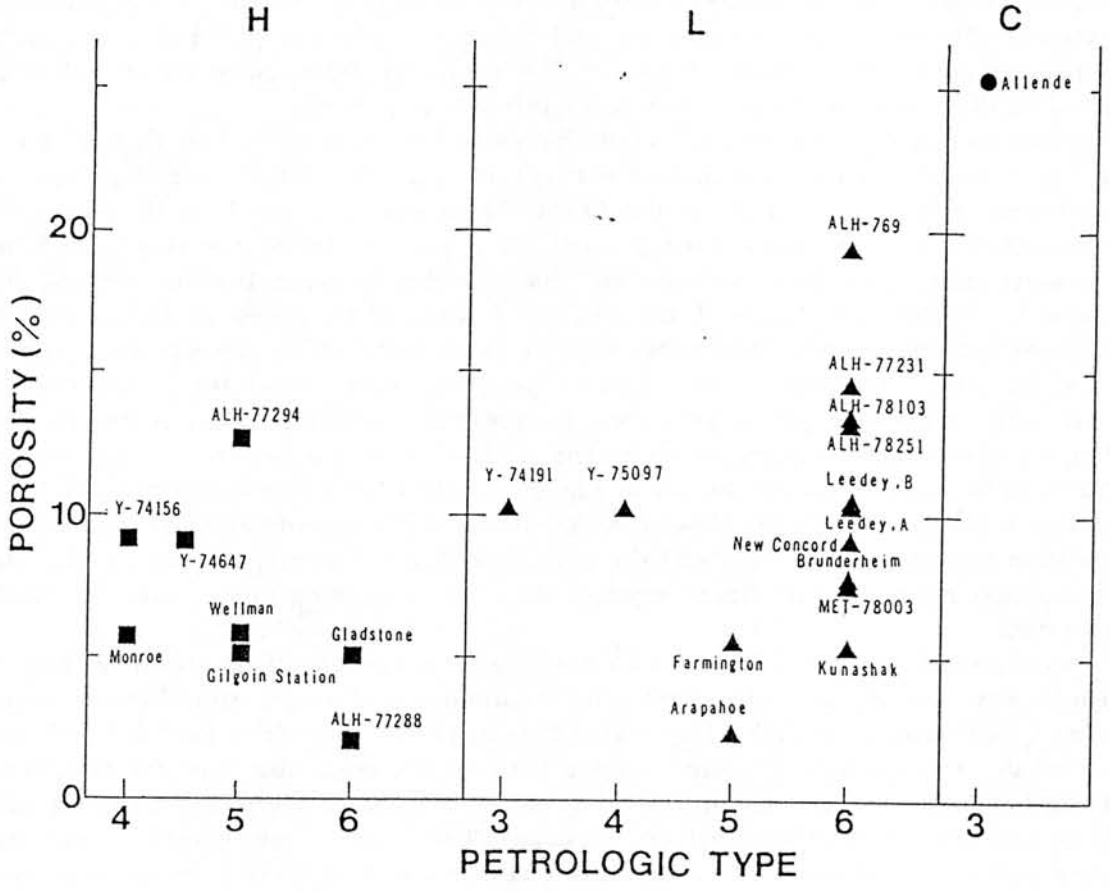


Fig. 1. Porosity versus petrologic-type systematics of each chondrite group.

Table 2. Elastic wave velocity.

| Sample | Direction | Length (mm) | Velocity $V_p$ (km/s) | Velocity $V_s$ (km/s) |
|---|---|---|---|---|
| Y-74156 | L1 | 14.98 | 3.23 | 1.87 |
| | L2 | 15.76 | 3.38 | 1.77 |
| | L3 | 17.16 | 3.29 | 2.01 |
| Y-74191 | L1 | 11.08 | 3.36 | 1.97 |
| | L2 | 13.76 | 3.74 | 2.08 |
| | L3 | 15.65 | 3.38 | 2.05 |
| Y-74647 | L1 | 12.03 | 2.74 | 1.65 |
| | L2 | 14.45 | 3.09 | 1.92 |
| | L3 | 15.14 | 2.98 | 1.87 |
| Y-75097 | L1 | 12.73 | 2.64 | 1.68 |
| | L2 | 12.77 | 2.29 | 1.49 |
| | L3 | 14.74 | 2.90 | 1.54 |

Table 3. Elastic properties of stony meteorites.

| Sample | Type | $\rho_{bulk}$ ($g/cm^3$) | $\rho_0$ ($g/cm^3$) | $\phi$ (%) | $V_p$ (km/s) | $V_s$ (km/s) | $\lambda$ (kbar) | $\mu$ (kbar) | K (kbar) | E (kbar) | $\nu$ |
|---|---|---|---|---|---|---|---|---|---|---|---|
| Y-74156 | H4 | 3.45 | 3.80 | 9.2 | 3.30 | 1.88 | 132 | 122 | 213 | 308 | 0.26 |
| Y-74191 | L3 | 3.23 | 3.60 | 10.3 | 3.49 | 2.03 | 127 | 134 | 216 | 332 | 0.24 |
| Y-74647 | H4-5 | 3.49 | 3.83 | 9.1 | 2.93 | 1.81 | 70.8 | 115 | 147 | 273 | 0.19 |
| Y-75097 | L4 | 3.28 | 3.65 | 10.3 | 2.61 | 1.57 | 61.8 | 80.6 | 116 | 196 | 0.22 |

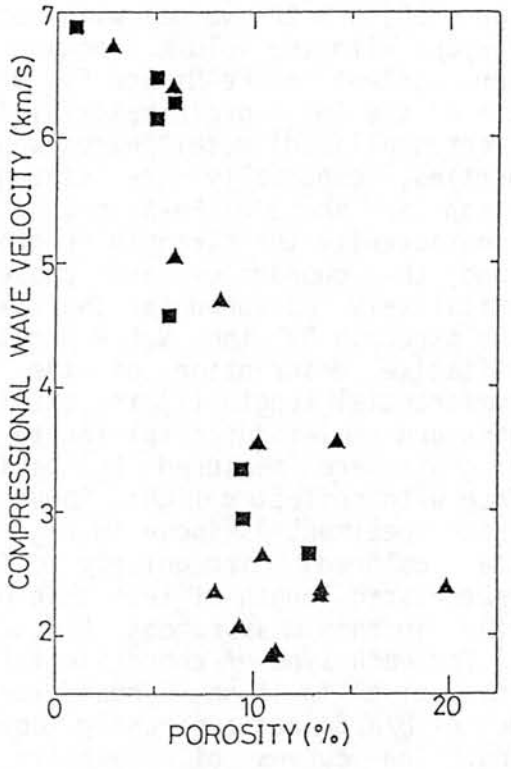


Fig. 2. Mean compressional-wave velocity versus petrologic-type systematics. ▲ and ■ represent L and H chondrites, respectively.

43－1

# ON THE SHAPE OF Fe-Ni GRAINS AMONG ORDINARY CHONDRITES

Naoyuki Fujii (1), Masamichi Miyamoto (2), Yoji Kobayashi and Keisuke Ito (1):

(1) Dept. Earth Sci., Kobe Univ., Kobe 657, (2) Dept. Pure & Appl. Sci., Tokyo Univ., Tokyo 153.

Chondrites have not experienced intense remelting processes in parent bodies, which have evolved through the accretion of mutually colliding planetesimals. Metal grains and rock-forming minerals in chondrites are more or less deformed or recrystallized and bonded together to some extent. As planetesimals are loosely consolidated aggregates of silicate and metal grains in the early stage of their growth process, the degree of lithification has increased in the evolutional history of chondrites. From the low-velocity impact experiments on loosely consolidated aggregates, significant increases of consolidation are observed when minor components with sticking properties between grains exist. Such minor components are once melted and successively frozen low melting-temperature material (e.g. ice) and easily deformed or recrystallized amorphous materials (e.g. fine grain and glassy matrix). Thus, the lithification of chondrites has been attributed to static heating or shock-induced metamorphism in parent bodies or their fragmentation process. The degree of lithification is closely related with the fracture strength of chondrites. Differences of the strength of chondrites have quantitatively been demonstrated by using the vibrational fracturing rate (V.F.R.) method, in which a ground surface of the chondrite was excavated by an ultrasonically vibrating 2 mm-diameter steel rod and the excavation rate was measured under an appropriate normal load and mechanical impedance condition. Chondrites are classified into two groups from the ratio -log (V/Vo), where V and Vo respectively denote the value of V.F.R. for a chondrite sample and calcite single crystal with the excavation direction perpendicular to r{10$\bar{1}$1}. One (H4, H5, H6, L3, L4 and L5) has the values between 0.8 and 1.2 and the other (L6 and LL6) has the values with less than 0.1. This classification appears to correspond with the volume fraction of metal phase, i.e. the former group has higher content of Fe-Ni and FeS grains than the latter. So, the presence and nature of the inter-grain materials such as pore-filling matrix and deformed (or recrystallized) metal phases would have strong influence on the mechanical properties, especially the strength, of chondritic aggregates. The volume fraction and shape of Fe-Ni grains in ordinary chondrites are of importance to characterize the strength or grain-to-grain adhesion. In this respect, H-, L- and LL- chondrites are chosen and the shape of Fe-Ni grains is quantitatively measured for the same specimen as used in the the measurements of the strength by the V.F.R. method. In the first step toward a quantitative description of the nature and shape of Fe-Ni grains, the circumferectial length (1) the axial ratio (b/a), where a and b are the longest and semi-major axial length respectively, and the area fraction (S) of each grain were measured by taking a photograph (X100) for polished sample surface with reflected light. About 2.7mm x 3.5 mm of the surface was surveyed for each specimen. As shown in Fig. 1, the shape and size of Fe-Ni grains (white colored) irregularly differ among chondrites. The grains with characteristic length of less than 0.05mm and FeS grains were tentatively omitted in this measurement. Fig. 2 shows the distribution of the axial ratio (b/a) for each type of chondrites. It appears likely that more rounded Fe-Ni grains exist in type 6 chondrites, especially in Y-75258 (LL6). The larger values of b/a do not apparently correspond to the smaller area of Fe-Ni grains. The curves of cumulative number versus the area of Fe-Ni grains are

shown in Fig. 3. Three H-chondrites have relatively continuous distribution of the area fraction, whereas Y-74191 (L3) has one large Fe-Ni grains and Y-75258 (LL6) has no large ones (Fig. 1 and 3). The ratio 1/S is used to represent irregularity of the shape of Fe-Ni grains. This ratio is hereafter called the shape parameter and is independent of the units of measurement but depends on a divider opening. Although it needs to consider a fractal dimension in such a measurement for generalization, we tentatively used a divider opening of 0.01 mm. Distribution of the shape parameter for each chondrite is shown in Fig. 4. It is noticed that the mean value of shape parameter decreases from type 4 to 6 in H- and L- chondrites. It appears likely that the irregularity of the Fe-Ni grain-surface decreases as thermal metamorphism advances. Fig. 5. shows the shape parameter versus the area of Fe-Ni grains for H-chondrites. It is evident that the grains with larger values of shape parameter tend to have larger area. Similar relation is also found among L- chondrites. As the number and size of Fe-Ni grains differ for each sample, circumferential length and area are summed and the ratio is normalized by square root of the number (n), i.e. $1 / ( S \times n )$ . This extent can be considered as an average shape parameter (S.P.), which is likely to represent an averaged irregularity in the shape of Fe-Ni grains for each sample. Volume fraction of Fe-Ni grains is assumed to be equal to the area fraction, and listed in Table 1 together with S.P. and average values of b/a. It is noticed that Fe-Ni grains in ALH-77231 (L6) and Y-75258 (LL6) have the value of S.P. similar to those of a circle (3.545). Whereas for ALH-77182 (H5), ALH-77115 (H6), and Y-74191 (L3), the shape of Fe-Ni grains are in average similar to that of a regular triangle (4.560). Though the number of sample is limited, the values of S.P. appear to decrease with the increase of petrologic types from 4 to 6 for each chemical group of chondrites. This tendency may represent that the shape of Fe-Ni grains becomes rounded as the thermal metamorphism advances. In spite of the limited number of chondrites studied, the value of S.P. and the volume fraction of Fe-Ni grains correspond well with the strength represented by the V.F.R. measurement except for ALH-78105 (L6). It is, however, noticed that the volume fraction of Fe-Ni grains does not always correspond to total Fe content, because we only investigated large Fe-Ni grains and limited area of the samples.

Table 1. Volume fraction, average shape parameter (S.P.) and axial ratio (b/a) of Fe-Ni grains, logalithmic ratios of V.F.R., and porosity.

| Sample | Fe-Ni grains | | | -log(V/Vo) | Porosity | Remark |
|---|---|---|---|---|---|---|
| | (vol.%) | S.P. | b/a | | (%) | |
| ALH-77233 | 6.3 | 6.0 | .41 | 1.13 | 5 | H4 |
| ALH-77182 | 4.1 | 4.7 | .52 | 1.11 | 15 | H5 |
| ALH-77115 | 4.9 | 4.6 | .59 | 1.05 | (8) | H6 |
| Y-74191 | 7.1 | 4.6 | .58(.72) | 1.09 | - | L3 |
| ALH-77230 | 8.8 | 6.3 | .44 | 0.98 | 1 | L4 |
| ALH-77254 | 4.0 | 5.2 | .59 | 0.81 | 18 | L5 |
| ALH-78105 | 2.3 | 5.0 | .61 | 0.09 | 4 | L6 |
| ALH-77231 | 1.4 | 3.6 | .55 | -0.22 | (3) | L6 |
| Y-75258 | 0.9 | 3.7 | .74 | -0.23 | (33) | LL6 |

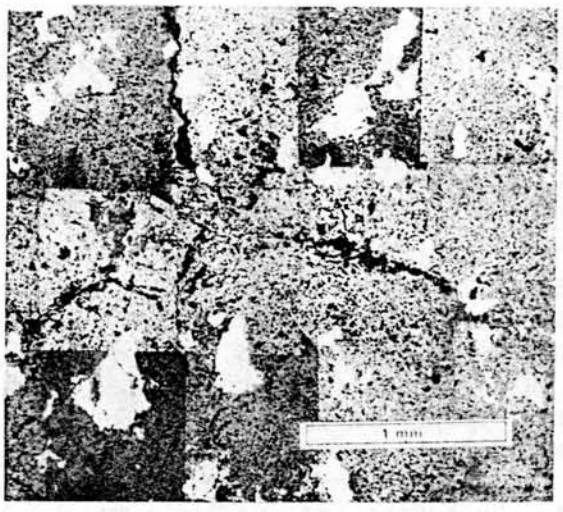

a) ALH-77233 (H4)

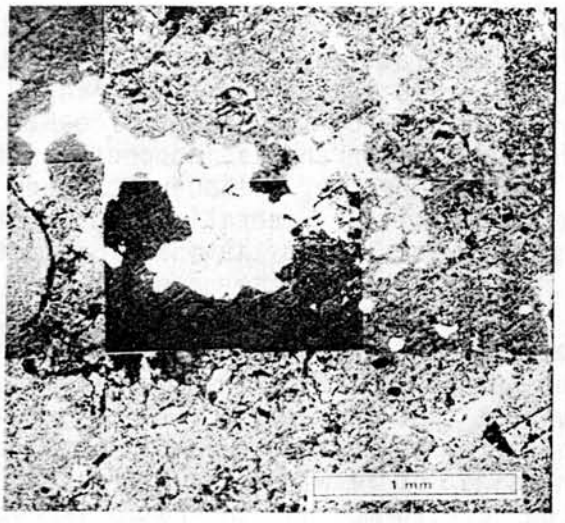

d) Y-74191 (L3)

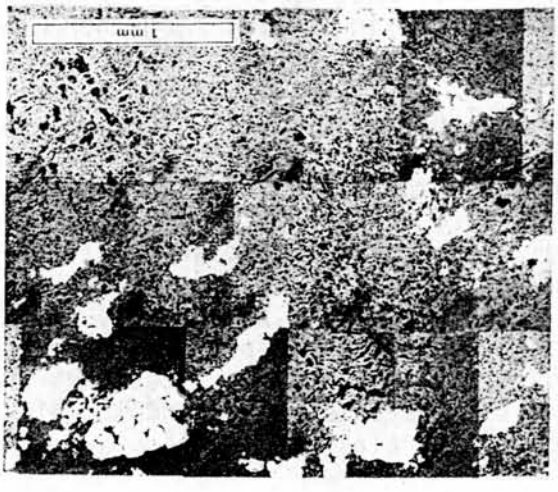

b) ALH-77182 (H5)

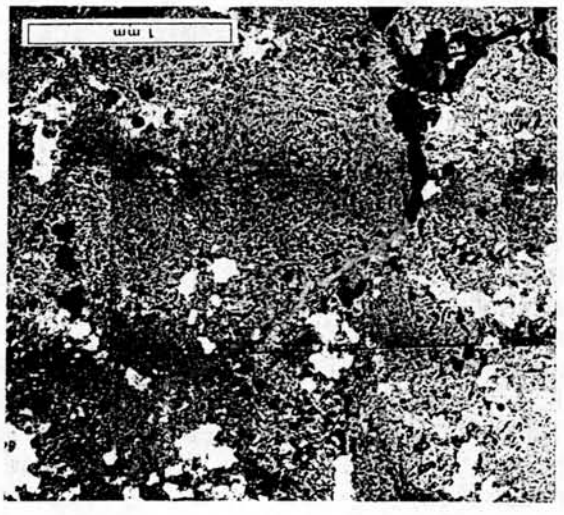

e) ALH-77230 (L4)

c) ALH-77115 (H6)

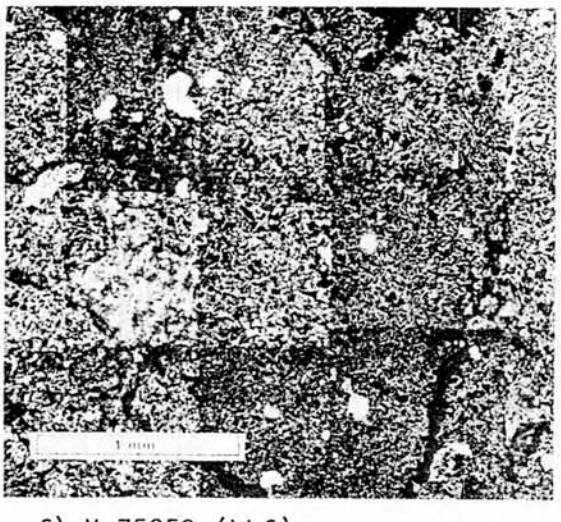

f) Y-75258 (LL6)

Fig.1. Examples of surveyed area. White grains are Fe-Ni grains.

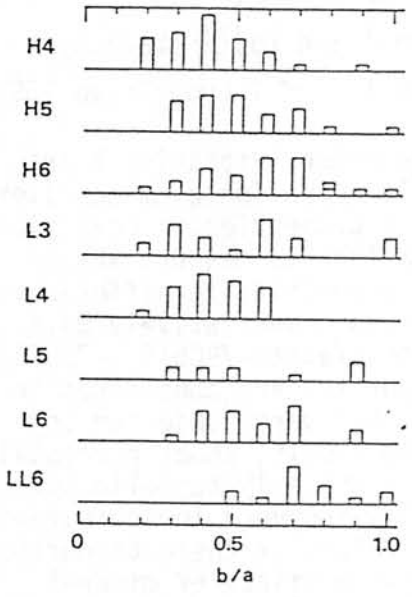


Fig.2. Distribution of the axial ratio (b/a).

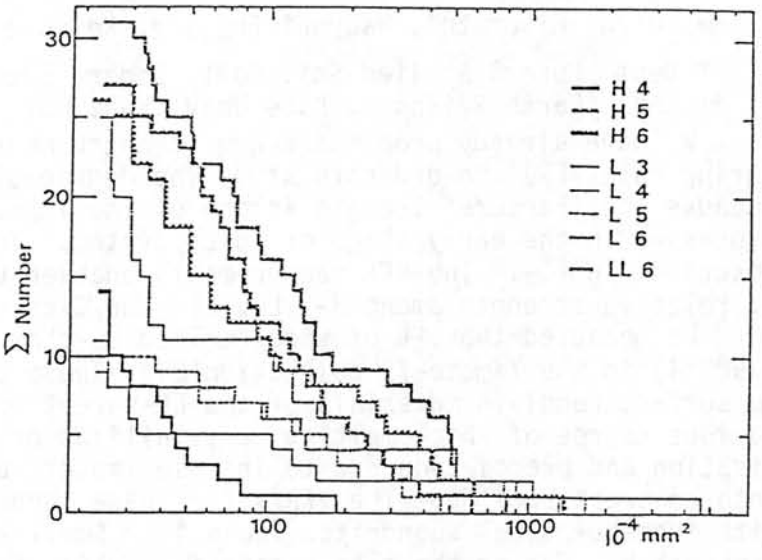


Fig.3. Cumulative number versus area of Fe-Ni grains.

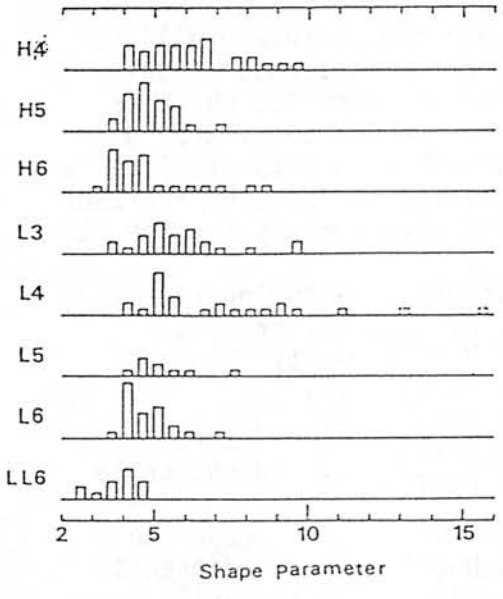


Fig.4. Distribution of the shape parameter.

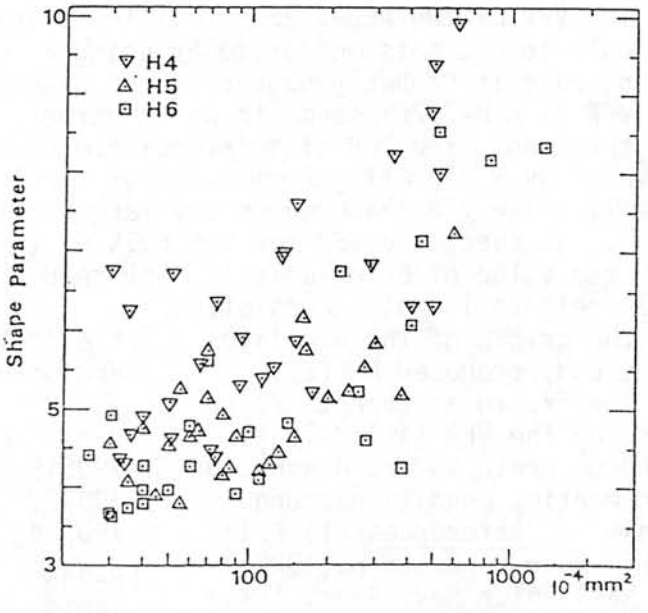


Fig.5. Shape parameter versus area of Fe-Ni grains for H-chondrites.

44

# THE VIBRATIONAL FRACTURING RATE OF SHOCK-MELTED CHONDRITES.

Masamichi Miyamoto*, Naoyuki Fujii**, Keisuke Ito** and Yoji Kobayashi**

* Dept. Pure & Applied Sci. Coll. Gener. Educ. Univ. of Tokyo, Tokyo 153
** Dept. Earth Sciences, Kobe Univ. Kobe 657.

We have already proposed a new strength measure named 'vibrational fracturing rate(VFR)' in order to study the degree of lithification of meteorites because the fracture strength is one of the important properties in collision processes in the early stage of solar system. The method to measure VFR is described in (1). The VFR measurements enabled us to demonstrate differences of relative strength among H-, L-, LL- and C-chondrites quantitatively(2).

We measured the VFR of shock-melted LL-chondrites(Yamato-790519, -790723, -790964) in the Yamato-79 collection(3). These chondrites are considered to be surface regolith materials of the LL-parent body that were subjected to various degree of shock melting, crystallization from a melt, shock recrystallization and brecciation due to intense impacts and eventually consolidated into coherent rock(3). The VFR's for these chondrites are very low compared with those of usual chondrites(Table 1). Small VFR values of these chondrites are probably due to the glassy materials which fill interstices of mineral fragments, produced by impact processes. Although Y-790964 is the most porous among these LL-chondrites, the VFR value is the smallest.

Polymict eucrite ALH-765 which is considered to be the product of the brecciation processes on the surface of a howardite parent body shows high VFR compared with that of the Y-74013 diogenite(Table 1). The Y-74013 diogenite shows a recrystallized granoblastic texture unlike that of common diogenites(4).

The VFR of the ALH-77257 ureilite is relatively high, whereas it is very difficult to cut this meteorite by using a rotating diamond blade. Very slow cutting rate is probably caused by the diamond contained in this ureilite. High VFR of ALH-77257 seems to be in harmony with the brittleness of this hand specimen. The VFR of this ureilite depends on the location which is excavated by a vibrating 2 mm-diameter steel rod to measure the VFR(B, G in Table 1). The VFR measured on the large grain contained in this ureilite is low(G). However, the VFR for the bulk of this ureilite seems to be represented by the value of B in Table 1. Our result of VFR measurements for the ALH-77257 ureilite is not inconsistent with the origin of the ureilite-parent body proposed by (5).

Table 1. Vibrational fracturing rate(VFR) and porosity of some meteorites.

| | VFR (mm/min) | Porosity (%) | Remarks |
|---|---|---|---|
| Y-790519 | 0.0023 | 7 | LL-chondrite |
| Y-790723 | 0.0023 | 8 | LL-chondrite |
| Y-790964 | 0.0017 | 16 | LL-chondrite |
| ALH-765 | 0.0050 | 7 | eucrite |
| Y-74013 | 0.00081 | 1 | diogenite |
| ALH-77257(B) | 0.011 | 6 | ureilite |
| ALH-77257(G) | 0.0013 | | |
| Y-75258 | 0.230 | (33) | LL6 |
| Y-74191 | 0.011 | - | L3 |
| Calcite | 0.135 | - | |

The fracture strength represented by the VFR is likely to depend on grain to grain adhesion and cementing condition among grains.

References:(1) Fujii N., Miyamoto M. & Ito K.(1980) Mem. Natl Polar Res. Spec. Issue 17,258. (2) Fujii N., Miyamoto M. Kobayashi Y. & Ito K.(1981) Mem. Natl Polar Res. Spec. Issue(in press). (3) Yanai K., Takeda H., Sato G. & Kojima H.(1981) Abstr. Meteor. Soc.44th Ann. Meet. Bern 138, (4) Takeda H., Duke M.B., Ishii T., Haramura H. & Yanai K.(1979) Mem. Natl Polar Res. Spec. Issue 15,54 (5) Takeda H., Mori H., Yanai K. & Shiraishi K. (1980) Mem. Natl Polar Res. Spec. Issue 17, 119.

# MAGNETIC AND THERMAL HISTORY OF THE BRECCIATED CHONDRITE ABEE

N. Sugiura and D.W. Strangway

Department of Geology

University of Toronto

Toronto, Ontario

Canada

The meteorite Abee is a type 4 enstatite chondrite with many cm-cize clasts. The paleomagnetic conglomerate test was applied to these clasts, to study the thermal and magnetic history of the meteorite. The directions of magnetization in mutually oriented clasts are significantly different, suggesting that the meteorite was not reheated to temperatures much above 100 C during or after accretion. The matrix seems to be homogeneously magnetized. The matrix magnetization was acquired either during the accretionary process at low temperature or during a brief shock reheating process.

The above thermal history inferred from the magnetic study is consistent with the results of a metallographic study by Herndon and Rudee (1978) and the fact that Abee is highly enriched in volatile elements (Ganapathy and Larimer, 1980).

The strength of the magnetic field was estimated to be 7 Oe using the Thellier method.

References

J.M. Herndon and M.L. Rudee, Earth Planet. Sci. Lett. 41 (1978) 101

R. Ganapathy and J.W. Larimer, Science 207 (1980) 57.

# MAGNETIC PROPERTIES OF PRIMITIVE NON-CARBONACEOUS CHONDRITES

N. Sugiura and D.W. Strangway
Department of Geology
University of Toronto

Magnetic properties of primitive (low petrologic grade) non-carbonaceous chondrites are of particular interest because 1) their metallic grains are relatively fine-grained and could possess stable remanence. (This is important because most ordinary chondrites have very unstable remanence whose origin is not well known); 2) they are supposed to contain a relatively small amount of plessite, an intergrowth of kamacite and taenite, which changes its structure when heated to 550°C and therefore its presence is troublesome for paleointensity determinations; 3) they are likely to preserve the record of the matnetic field in the early solar system as recorded in carbonaceous chondrites, because they were not reheated to high temperatures.

In this study we describe the magnetic properties of Chainpur (LL3), ALHA77304 (LL3), Mezo Madaras (L3), Bjurbole (L4) and Indarch (E4) in detail. Three chondrites (Yamato 74191 (L3), Yamato-a (E3), Abee (E4)), which were previously studied, are also included in the discussion. Some petrological and magnetic properties of these chondrites are summarized in Table 1.

The NRM intensity of E chondrites is by far larger than that of L and LL chondrites. The difference is only partly explained as due to the difference in the amount of ferromagnetic materials (which is measured as saturation magnetization: Js). The bulk coercive force (Hc) of L and LL chondrites is mainly determined by the amount of plessite. Cohenite and schreibersite and their grain sizes are important factors determining the Hc of E chondrites.

NRM in primitive chondrites are generally more stable than those in metamorphosed chondrites. The difference in NRM stability seems to be due to the presence of coarse, well-annealed kamacite in metamorphosed chondrites.

Indarch, Yamato-a and Yamato-74191 have a single component NRM. NRM in Indarch and Yamato-a is less stable than ARM and interpreted as a partial thermoremanence (pTRM) acquired after a shock event. The NRM in Yamato-74191 was probably acquired during slow cooling.

Chainpur and ALHA77304 have a two-component NRM, which could be interpreted as a primary TRM (or depositional remanence: DRM) plus a pTRM.

Abee has random NRM components and Bjurbole has partially random NRM components. The former can be interpreted as a typical DRM, while it is probably not possible to interpret the latter as a DRM plus a pTRM, because the metamorphic temperature for type $ chondrites exceeds 700°C. An alternative explanation, random NRM due to anisotropy is proposed, but not yet confirmed experimentally.

NRM in Mezo Madras is similar to that in Bjurbole, i.e. partially random NRM.

Paleointensities were estimated with the ARM method or Thellier's method. The paleointensities for E chondrites are definitely larger than those for L and LL chondrites. Because in one meteorite the components are random (i.e. conglomerate test) and in others there is evidence of primitive components we conclude that these do record primitive solar system fields. The very high fields recorded by the enstatite chondrites suggest that these were formed in strong magnetic fields.

TABLE 1

| | Bj | Ch | 74191 | MM | 77304 | Y-a | Ab | In |
|---|---|---|---|---|---|---|---|---|
| type | L4 | LL3 | L3 | L3 | LL3 | E3 | E4 | E4 |
| friable | o | o | x | x | x | x | x | x |
| chondrule rich | o | o | o | o | o | m | x | m |
| breccia | x | o | x | o | o | x | o | x |
| plessite | o | o | o | o | x | x | x | x |
| slow cooling | o | o | o | o | m | - | x | m |
| shock | x | x | x | m | x | m | x | m |
| age (b.y.) | 4.5 | - | - | - | 4.5 | - | 4.5 | - |
| NRM (10-4emu/g) | 1.5 | 4.3 | 1.5 | 3.7 | 4.3 | 133 | 800 | 579 |
| Js (emu/g) | 13 | 11 | 21 | 17 | 13 | 48 | 82 | 66 |
| Hc (Oe) | 630 | 89 | 30 | 42 | 12 | 12 | 14 | 15 |
| Hp (Oe) | .25 | .74 | .13 | .15 | .45 | 10? | 7 | 15.7 |
| | .60 | | | | | | | |

m: moderate; -: unknown; Hp: paleointensity.

# LUNAR MAGNETISM

D.W. Strangway and N. Sugiura
Department of Geology
University of Toronto

It has been very difficult to conduct suitable paleointensity determinations on lunar samples since a) they frequently have a large soft component of magnetism and b) the magnetic minerals change during heating experiments making Thellier tests very difficult. As a result there are only a few samples that have been useful for paleointensity tests. In general, these have been breccias which contain fine-grained metallic iron and frequetnly are glass rich. Perhaps the glass protects the magnetic minerals during heating.

To date there have been five fully successful tests. These samples range in age from a) the last phase of intense lunar bombardment at or about 4.0 billion years, b) breccias younger than the 3.3 billion year-old basalts from Apollo 15 to c) a glass sample from a very fresh small crater wall probably less than 10-20 million years in age.

One sample has a very high value of about 1.0 oersted while all others record ancient fields of only a few thousand gammas. These samples suggest that the ancient lunar field was small, although the high field found in one sample remains to be explained. Nevertheless, the discovery of magnetic anomalies from surface and orbital experiments show that there was an ancient lunar field but the geometry and time dependence is still unknown.

Various explanations for the origin of this field include a) internal ancient dynamo, b) relation to major impact events and c) a moon magnetized during its accretion process.